Analysis of the effect of leaf-on and leaf-off forest canopy conditions on LiDAR derived estimations of forest structural diversity

SOPHIE TANITH DAVISON

Analysis of the effect of leaf-on and leaf-off forest canopy conditions on LiDAR derived estimations of forest structural diversity

Sophie Tanith Davison

Master of Science by Research

Durham University

2017

Analysis of the effect of leaf-on and leaf-off forest canopy conditions on LiDAR derived estimations of forest structural diversity

Sophie Tanith Davison

ABSTRACT

UK legislation aims to conserve and enhance biological diversity within the UK and so accurate measurements of forest biodiversity are important to assess efficacy of management activities in this context. Forest structural diversity metrics can be used as indicators of biodiversity and airborne LiDAR data provide a means of producing these metrics. Forest structure metrics derived from LiDAR can be significantly affected by the canopy conditions the datasets are collected under. Existing studies have combined and compared leaf-on and leaf-off LiDAR datasets in existing analyses, however the majority of these utilise field sites where climate, species and terrain are very different to those found in the UK. Additionally, studies comparing leaf-on and leaf-off LiDAR over forested areas assess the changes in pulse penetration through the canopy and how this effects forest structure metrics and not the effect on modelled forest structure diversity. The novel aim of this research is to assess and compare the accuracy of forest structural diversity modelled from two LiDAR surveys collected under leaf-on and leaf-off conditions, and do so in a UK forest environment.

A robust methodology for correcting the absolute and relative accuracy between datasets was adopted and comparative analysis of ground detection and return height metrics (maximum, mean and percentiles of return height) and return height diversity (L-CV, CV, kurtosis, standard deviation, skewness and variance) was undertaken. Regression models describing the field tree size diversity measurements were constructed using diversity metrics from each LiDAR dataset in isolation and, where appropriate, a mixture of the two.

Both surveys were consistently effected by growth and differing survey parameters making the isolation and assessment of the effects of seasonal change difficult. Despite this, models created using diversity variables from both LiDAR datasets were generally very similar. Both leaf-on and leaf-off LiDAR dataset models described 65% of the variance in tree height diversity (R^2 0.65, RMSE 0.05, $p < 0.0001$), however models utilising leaf-off LiDAR diversity variables described DBH diversity, crown length diversity and crown width diversity more successfully than leaf-on (leaf-on models resulted in R^2 values of 0.68, 0.41 and 0.19 respectively and leaf-off models 0.71, 0.62 and 0.26 respectively). When diversity variables calculated from both LiDAR datasets were combined into one model to describe tree height diversity and DBH diversity their efficacy was increased (R^2 of 0.77 for tree height diversity and 0.72 for DBH diversity).

The results suggest strongly that tree height diversity models derived from airborne LiDAR collected (and where appropriate combined) under any seasonal conditions can be used to differentiate between single and multiple storey UK forest structure with confidence. However, leaf-off LiDAR acquisitions can generate models with the ability to better explain the diversity of crown shapes in a forest stand than leaf-on, with no improvement in model performance when the two are combined.

CONTENTS

LIST OF FIGURES

LIST OF TABLES

NOTATION

SI units include the metre (m) and the hectare (ha). An additional unit used is degrees (°). Symbols and abbreviations are defined when they first appear however the following are used frequently:

Field notation

Variable	Name	Description
DBH	Diameter at breast height	Tree diameter 1.5m above the ground
L-CV	Coefficient of L-variation	Analogous to the coefficient of variation, but based on L-moments. Identical to the Gini Coefficient. Measures the inequality among values of a frequency distribution.
THdiv	Tree height Diversity	Coefficient of L-variation of Tree height (across a plot)
DBHdiv	DBH Diversity	Coefficient of L-variation of DBH (across a plot)
CLdiv	Crown length Diversity	Coefficient of L-variation of Crown length (across a plot)
CWdiv	Crown width diversity	Coefficient of L-variation of Crown width (across a plot)

LiDAR notation

Variable	Name	Description
x	Easting	
y	Northing	
z	Height	
CV	Coefficient of variation	Relative dispersion of a frequency distribution. The ratio of standard deviation and mean and is expressed as a percentage.
skew	Skewness	A measure of the asymmetry of a frequency distribution

kurt	Kurtosis	The sharpness of the peak of a frequency distribution.
var	Variance	A measure of the spread from the mean. The average of the squared differences from the mean.
SD / σ	Standard deviation	A measure of the variation or dispersion of a distribution. The square root of the variance.
L-CV	Coefficient of L-variation	Analogous to the coefficient of variation, but based on L-moments. Identical to the Gini Coefficient. Measures the inequality among values of a frequency distribution.
P99	99th percentile of return height	
P90	90th percentile of return height	
P75	75th percentile of return height	
P50	50th percentile of return height	
P25	25th percentile of return height	
P99/90	Ratio of the 99th and 90th percentile of return height	
P99/75	Ratio of the 99th and 75th percentile of return height	
P99/50	Ratio of the 99th and 50th percentile of return height	
P99/25	Ratio of the 99th and 25th percentile of return height	
x_{lon}		The 'lon' denotation indicates a variable has been calculated from the leaf-on LiDAR dataset
x_{loff}		The 'loff' denotation indicates a variable has been calculated from the leaf-off LiDAR dataset

Abbreviations

BAP	Biodiversity Action Plan
MODIS	MOderate-resolution Imaging Spectroradiometer
SAR	Synthetic Aperture Radar
InSAR	Interferometric Synthetic Aperture Radar
LiDAR	Light Detection and Ranging
GPS	Global Positioning System
IMU	Inertial Measuring Unit
LVIS	Land Vegetation and Ice Scanner
SLICER	Scanning LiDAR Imager of Canopies by Echo Recovery
CHM / CSM	Canopy Height Model / Canopy Surface Model
DTM	Digital Terrain Model
AVIRIS	Airborne Visible Infrared Imaging Spectrometer
GLAS	Geoscience laser altimeter system
ICESat	Ice, Cloud and land Elevation Satellite
DSM	Digital Surface Model
PAWS	Plantation on Ancient Woodland Site
A.g.l.	Above ground level
ppm^2	Points per square metre
NERC	National environmental research council
ARSF	Airborne Research Facility
TIN	Triangulated Irregular Network
CI	Confidence Interval
VIF	Variance Inflation Factor

DECLARATION AND STATEMENT OF COPYRIGHT

I hereby certify that the work described in this thesis is my own, except where otherwise acknowledged, and has not been submitted previously for a degree at this or any other University.

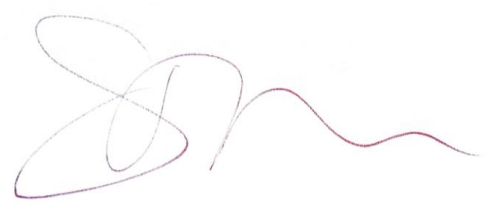

ACKNOWLEDGEMENTS

I would like to first and foremost extend my thanks to my supervisors, Prof. Danny Donoghue and Dr. Niko Galiatsatos, for their valuable help, advice, guidance and, of course, patience. I would further like to acknowledge the Forestry Commission for granting access to Chopwell Woodland Park to enable field data collection and allowing me to spend time shadowing a forest harvester at Kielder Water and Forest Park. Further thanks go to friends and family, especially my dad Chris and friend Lauren, who lent a hand during a cold fieldwork campaign.

1. INTRODUCTION

Biodiversity, or variability within nature, allows species to adapt to changing conditions. The very rapid changing conditions observed in forests due to human interference and climate change (such as habitat fragmentation, species extinctions and spread of invasive species) all have a detrimental effect on biodiversity (Butchart et al., 2010). Forest regrowth following disturbance can restore habitat to some extent, but the success of this depends on sufficient conservation management knowledge for species habitat requirements and their relationships to vegetation vertical structure and biomass (Martinuzzi et al., 2009). A better understanding of the vulnerability of vegetation and forest dwelling animal species to climate change and changes to the structure and extent of forests is essential to facilitate conservation and management efforts that can counter any decline forest biodiversity (Hall et al., 2011).

Many countries now have some form of plan or policies in place to safeguard and promote biodiversity. The national Biodiversity Action Plan (BAP) is the UK government's manifestation of such a plan, instigated in response to the convention on Biodiversity (signed at the Rio Earth Summit (1992)). The BAP has the overall goal of conserving and enhancing biological diversity within the UK and contributing to the conservation of global biodiversity. This is to be undertaken through all appropriate mechanisms, such as preserving and where practical enhancing species, habitats and natural and managed ecosystems.

Within the UK BAP it is recognised that sensitive management of existing forests and woodlands through restructuring of even-aged plantations can enhance biodiversity. Introducing species and age diversity can enhance the structural diversity of a forest stand and in general the more diverse the vertical structure of a forest the more diverse its biota (Brokaw and Lent, 1999). For example vegetation structure has been observed to influence bird habitat selection in a variety of ways: it may impede the movement of foraging birds (Brodmann et al., 1997) and may influence foraging

proficiency through its effects on birds' ability to find and reach food items (Whittingham and Markland, 2002). Jansson and Andrén (2003) found that in Boreal Swedish forests the number of bird species increased as the proportion of older mixed trees and tree heights increased and the bird species numbers decreased as forest fragmentation increased. Beier and Drennan (1997) found that Northern Goshawks (*Accipiter gentilis*) selected foraging sites based on forest structure rather than prey abundance and preferred areas with higher canopy closure (>40%), high tree densities and higher tree heights regardless of more open stands displaying higher prey abundance. Vertical positioning, mixture and age distribution of vegetation elements have also been shown to affect insect and herbaceous plant diversity (Berger and Puettmann, 2000; Recher et al., 1996).

Although the assessment of vegetation structure is critical to managing forested ecosystems, conventional methods remain unable to facilitate all management goals (Jones et al., 2012). In lieu of destructive methods (less than ideal when trying to conserve the biodiversity present) forest structure can be reliably estimated in the field using allometry with much less damage, but considerable labour. Allometry uses measures (for example tree height and diameter) with which biomass or structural characteristics can be calculated. The data is then typically aggregated from sample plots over spatially and structurally continuous groups of trees growing under similar soil and climatic conditions, also known as stands (Oliver and Larson, 1990) within (Bergen et al., 2009). These measurements are scaled up in this way as complete censuses of every tree are too costly, both in time and resources (Bergen et al., 2009). Because of this, when relying on field measurements alone, a trade-off always exists between amount of vertical detail measured and the horizontal extent of these measurements (Bergen et al., 2009; Bradbury et al., 2005). Furthermore, field measurements are not always standardised, are lacking for many remote areas that are difficult to access, and are inefficient in capturing change (Bergen et al., 2009).

Remote Sensing can be used as an alternative to such field based methods. Passive multispectral optical sensors such as Landsat and MODerate-resolution Imaging Spectroradiometer (MODIS) are

useful for classifying vegetation type and horizontal forest structure at low resolutions for larger landscape scales (Bergen et al., 2009) and stereo-photogrammetry can also provide vegetation height information (Bradbury et al., 2005). Active sensors such as SAR (Synthetic Aperture Radar) and InSAR (Interferometric SAR) can also provide observations related to forest aboveground biomass and vegetation structure (Waring et al., 1995; Saatchi et al., 2007). For valuable biodiversity assessment, SAR, InSAR and airborne Light Detection And Ranging (LiDAR) hold an advantage; forest canopies present a surface porous to the emitted energy, allowing information to be collected from the top of the canopy and lower canopy layers (Chasmer et al., 2006; Lefsky et al., 2002). This allows the height and sometimes density of vegetation elements or layers to be calculated in relation to the ground (Lindberg et al., 2012). Like other remote sensing techniques LiDAR provides a means of data collection in areas of restricted or limited access and can generate high density sampling data rapidly and more efficiently than field methods. This is particularly evident at landscape levels (Lefsky et al., 2002; Bradbury et al., 2005).

This research had the opportunity to utilise two airborne LiDAR datasets collected over Chopwell Woodland Park in the North-East of England under leaf-on and leaf-off conditions to investigate the relationship between LiDAR derived and field measured forest structure diversity under different seasonal capture conditions. Chopwell Woodland Park is comprised of stands ranging in biodiversity, maturity and level of management and also encompasses areas of ancient woodland (woodland that has been continually present since 1600, a category only 16% of UK woodland can claim to be a part of).

The following sections within Chapter 2 aim to contextualise this study within the literature through the analysis of key studies and outlining of important concepts. This review was critical in the formulation of the aims and objectives which are stated in Chapter 3 after a full appraisal of the literature enabled a detailed premise to be set.

2. LITERATURE REVIEW

2.1 The LiDAR System

An airborne LiDAR system is mounted upon an aircraft equipped with a Global Positioning System (GPS) and Inertial Measuring Unit (IMU) which allow calculation of precise location in easting (x) northing (y) and height (z) and angular orientation (the pitch, roll and heading) of the sensor with respect to the ground (Wehr and Lohr, 1999). The laser scanning system itself is comprised of the laser source, the laser detector, the scanning mechanism, the timing mechanism and the computing power to process and record vast amounts of data in real-time to extract the geo-referenced points (Thiel and Wehr, 2004). Aside from this, as with any GPS activity, airborne LiDAR capture requires a surveyed ground base location to be established in or near to the project area (Lillesand et al., 2014). LiDAR systems emit repetitive laser pulses towards the earth's surface and measure the time taken for them to return. Scanning takes place as the aircraft motion displaces the laser beam. The laser is also deflected across the flight path by a device such as an oscillating mirror to create a swathe of pulses following the aircraft's line of flight (Wagner et al., 2004). Different systems perform different swath patterns (z pattern, parallel pattern, sinusoidal pattern) which are generally acquired in many overlapping parallel strips to enable dense point clouds and adequate data coverage (Mallet and Bretar, 2009). The travelling time taken by the emitted pulse to reach the earth's surface and return to the system directly relates to the distance from the sensor to the ground or whatever may be above the ground (Wagner et al., 2004) using the formula:

$$\boldsymbol{R} = \boldsymbol{c}\frac{\boldsymbol{t}}{\boldsymbol{2}}$$

R = range (distance between sensor and target)

c = speed of light or 0.3m/nanosecond

t = time interval between pulse emission and detection

(Baltsavias, 1999)

Such distances are then mapped into 3D point clouds representative of the surface beneath the scanner, typically accurate to 100-150mm in plan and height (Mallet and Bretar, 2009). The received signal intensity of backscattered pulses is additionally measured providing radiometric information about the surveyed data that can later be utilised during classficiation or edge detection (Höfle and Pfeifer, 2007; Jutzi and Stilla, 2006). As these are active systems (they provide their own energy source and do not rely on light energy from the sun) the data do not suffer from illumination shadows that may be present in photogrammetrically derived data, however object occlusion is still present.

Light from LiDAR scanner laser sources is highly collimated (strong and tightly focused) and monochromatic with a very narrow spectral width typically within the near infrared region of the electromagnetic spectrum (Wagner et al., 2004). The laser diverges from the source into a diffraction cone making the footprint approximately circular but varying with scan angle and topography (Baltsavias, 1999). Typically, laser footprints are classed as large or small. Large footprint systems such as NASA's Land Vegetation and Ice Scanner (LVIS) and the Scanning LiDAR Imager of Canopies by Echo Recovery (SLICER) have a wide divergence angle for the laser beam so that it illuminates a large (10 – 30 metre) footprint (Chasmer et al., 2006). Often few footprints are recorded for each scan line but the entire return pattern of energy versus time (height) is recorded in great detail. Most large footprint systems are confined to use in research and are less available for commercial use (Mallet and Bretar, 2009). Small footprint systems use a narrow divergence angle resulting in footprints typically 10cm-1m and operate at a much higher frequency and can also distinguish multiple returns from each fired pulse.

2.2 Airborne LiDAR and Forestry

As highlighted in Chapter 1, LiDAR data are incredibly valuable for monitoring forestry characteristics and parameters. Each laser pulse fired can provide returns from differing layers of the canopy. Returns that arrive back first may come from the very top of the canopy and subsequent returns may represent lower layers or even the ground. The application of airborne LiDAR in forestry can offer a wealth of forest characterisation and measurement data which can be of critical importance in forest growth models, biodiversity assessment and in the derivation of estimates of carbon sequestration, standing timber volume, and biomass (Lim et al., 2003).

2.2.1 Study Scale

LiDAR forestry studies are undertaken at scales varying from individual tree level to country-wide or international investigations. Stand level LiDAR data are considered to produce information on the physical dimensions of timber volume, or large structural characteristics and features typically derived are height percentiles and densities calculated from the height distributions. This ignores any spatial x/y distributions over the plot extent (Næsset, 2002). Conversely an individual tree approach can be advantageous when classifying individual species or delineating individual trees as structural features, which can be separated from the point cloud using assumptions based on the physiology of different types and species of tree.

Li et al. (2013) undertook tree species identification by analysing tree crown structural features to capture detailed foliage and branching patterns that differ systematically among species. Results were compared to trees in the field and analysis of the clustering of returns in 3D space showed they were related to the biomass distribution within different species crowns. This study demonstrated the incredible amount of detail that can be captured for each individual tree but

raises questions surrounding how such detail can be utilised at larger scales without incurring significant time and processing power. Morsdorf et al. (2004) suggest that single tree metrics can be aggregated to cover larger scales. This is akin to how field measurements of individual trees are often aggregated to larger scales and again introduces the trade-off between amount of detail in metrics calculated from individual trees and the horizontal extent of these metrics can be extrapolated to.

It is, however, important to note that this level of detail would likely be superfluous in larger scale studies. For example, Zimble et al. (2003) investigated the separation of structure classes at the stand and landscape level. Simply undertaking statistical analysis of LiDAR data over a given area produced valid and valuable conclusions without having to undertake a computationally expensive methodology. Ideally there needs to be a compromise between the quantity and duration of analysis techniques and the real level of detail required for any research project. Much management in the UK is undertaken at the stand level and it may be argued that remote sensing measurements for biodiversity assessment would ideally be related to this scale. If no further spatial detail is necessary, less time and effort in data analysis is spent whilst information relevant to the management of a stand can still be obtained (Townsend Peterson and Kluza, 2003).

2.2.2 Full Waveform and Discrete Return LiDAR Systems

LiDAR systems themselves can be grouped into two main categories: full waveform or discrete return. Some systems have both full waveform and discrete return capabilities. Both of these systems continuously emit light and measure the phase difference between the transmitted and received signal to determine distance of occlusive objects from the system (Mallet and Bretar, 2009). The difference between the two system types comes in the way the returning signal is recorded. Full waveform systems digitise the continuous returning signal, recording the entire

shape of the returning wave. Discrete return systems record discrete echoes where the return signal has exceeded a set threshold (Jutzi and Stilla, 2006).

Each have their advantages and disadvantages when used in forestry analysis. By recording the power of the entire return signal, full waveform systems are often able to obtain height information beneath the tallest canopy. For discrete return systems, the return signal diminishes in power as it intercepts canopy surfaces making returns from the ground sometimes more difficult. However with larger footprint systems a signal is still recorded from the ground in nearly all footprints, providing estimates of total canopy height (Lefsky et al., 1999a). Lefsky et al. (1999a) used full-waveform LiDAR data to ascertain the age of forest stands using the vertical distribution of the canopy produced within a waveform. Older stands (characterized by canopy gaps and trees of multiple ages and sizes) exhibited a more even vertical distribution of canopy components compared to younger, even-aged stands which had a majority of their canopy materials in the top portion of the canopy.

Discrete return systems are more commonly small in footprint and can provide exact locations and detailed information on scales as small as a singular tree crown (Lefsky et al., 2002). However due to their spatially focused nature these systems can encounter problems such as missing the very tops of trees and, in forests with much understory vegetation, never reaching the ground (Lim et al., 2003). Lindberg et al. (2012) used discrete return and the full-waveform digitisation LiDAR data to estimate vegetation volume profiles. Both systems showed good agreement with ground data however it was shown that waveform data provided the best results by compensating for the shielding effects of higher vegetation layers that discrete return data suffered from.

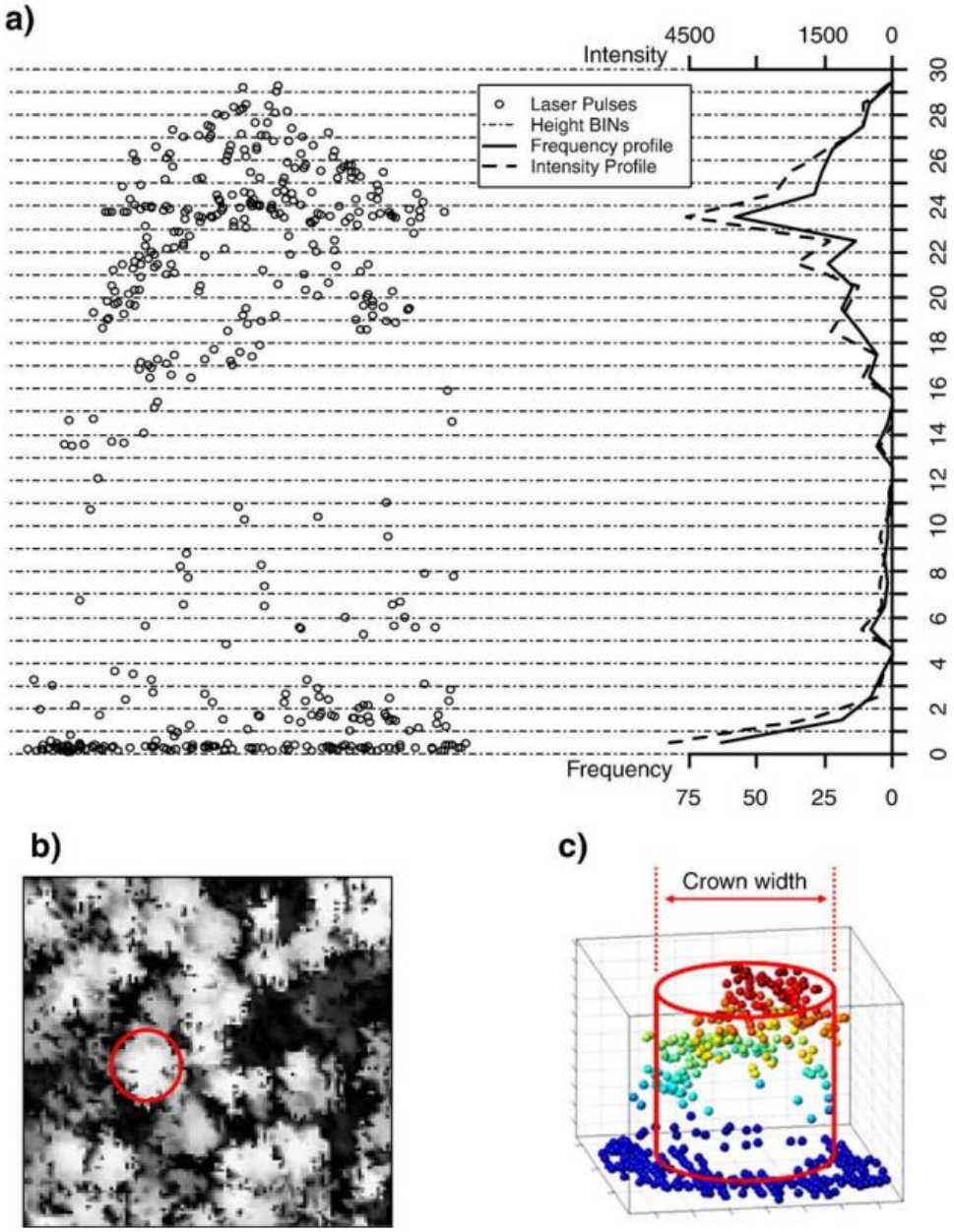

Figure 1. a) Laser hits within a tree crown footprint, with frequency and intensity vertical profiles; b) A model of the canopy height with the highlighted location of the tree crown shown in "a"; c) The tree crown footprint shown in 3D (Popescu and Zhao, 2008)

Issues such as occlusion when using discrete return systems can often be ameliorated by increasing the point density. There are studies which have taken discrete return LiDAR data integrated over a test site at an individual tree scale (Popescu and Zhao, 2008) or stand scale (Chasmer et al., 2006), and then plotted these returns as frequency by height (see Figure 1). This technique provides a

distribution similar to intensity waveforms acquired from full waveform LiDAR systems and can provide general summaries of the vertical forest structure and canopy layers at stand scales.

2.2.2 Utilising the Point Cloud vs. Point Cloud Products

LiDAR studies of forest structure often attempt to derive metrics such as tree height and crown dimensions and then utilise allometric relationships or statistical analysis to derive other valuable characteristics such as biomass, volume, crown bulk density, and canopy fuel parameters. For example, tree or vegetation height is a function of species composition, climate and site quality and can also be used to model stand biomass and volume (Lim et al. 2003). Lefsky et al. (1999b) calculated stem diameter of trees from LiDAR data which could then be used as an input for many traditional predictive models of biomass and volume. These characteristics can be calculated from either the LiDAR point cloud or by constructing surfaces or grid based metrics. Choosing to work with the LiDAR point cloud itself involves pre-processing the data to ensure questionable returns caused by errors in time registration, or from atmospheric effects, are removed. These errors are easily identified as exaggerated depressions or spikes with improbable ranges in the three-dimensional point cloud (Axelsson, 2000).

A high proportion of studies involving utilisation of LiDAR datasets to estimate forest structure metrics at a stand scale do so by constructing models of the relationship between the response variable of interest and LiDAR derived auxiliary variables from the point cloud. Hall et al. (2005) used the LiDAR point cloud to estimate variables including stand height, total aboveground biomass, foliage biomass, basal area, tree density, canopy base height and canopy bulk density. Metrics developed from the LiDAR point cloud were used in regression models, which were fit to field estimates of the stand structural variables. A regression model for mean stand height explained slightly under 60% of the variability of the 41 sites, based on the mean height of the upper 50% of first returns and the standard deviation of all first returns greater than 3 metres.

Amable et al. (2004) integrated small footprint discrete pulse LiDAR data over forest stands within the UK into histograms of return heights and plots of laser height against easting per stand. Plots of height against easting enabled distinct boundary layers between differing canopy components to be identified (see Figure 2). In addition to characterising vertical structure, the cumulative height distributions from the histograms also provided very clear discrimination between the vegetation classes involved. The techniques used in this study can provide sound qualitative information about vegetation structure and layering in forest stands. Comparison to more detailed ground data would have added an additional element of great interest to this research.

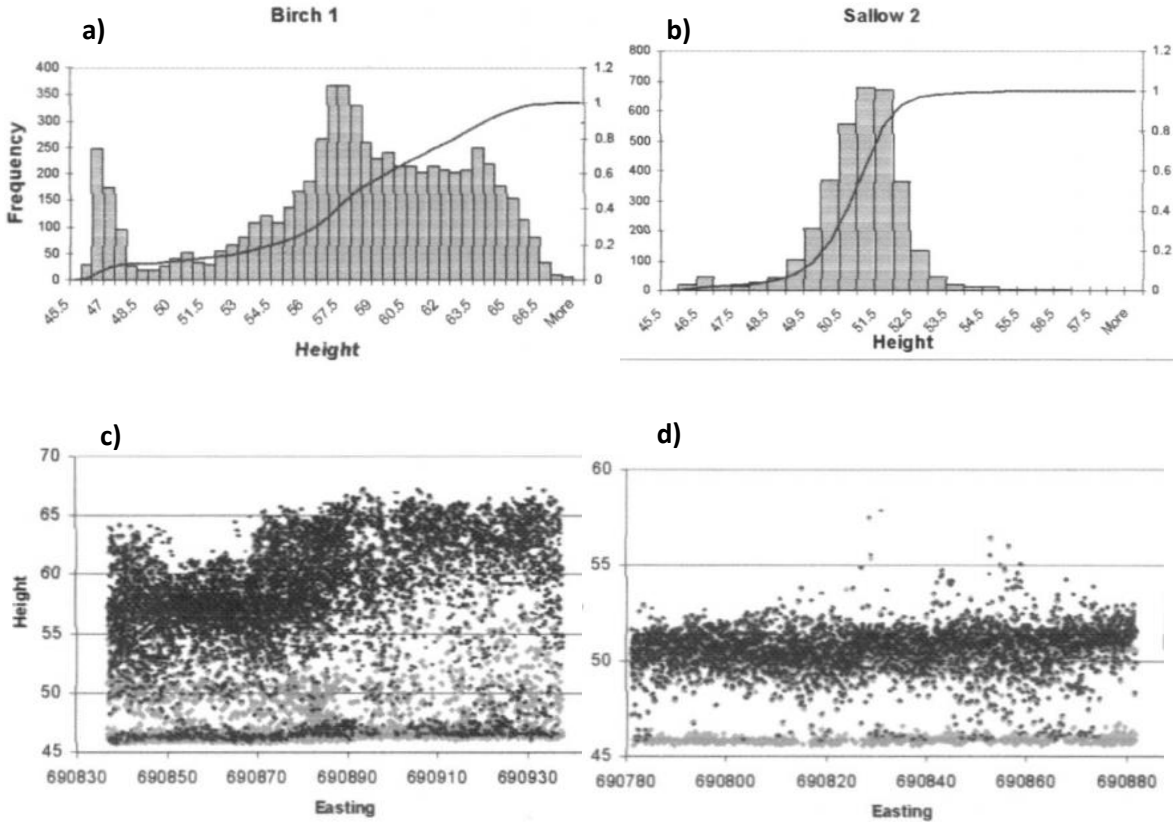

Figure 2. a) and b): Histograms displaying LiDAR return heights from two structurally different woodland environments. c) and d): Corresponding plots of LiDAR return height by Easting. First returns are the darker markings, last returns are the lighter markings. Distinct canopy boundary layers can be identified in both plots (Amable et al., 2004).

Instead of working with the LiDAR points themselves one may choose to further visualise data by creating 2D or 3D gridded datasets. Much focus has rested on the ability of LiDAR data to be used to calculate canopy tree height and models of canopy height (CHMs) can be constructed from the point clouds. This is after interpolation of ground and none ground returns into separate surfaces to create a Digital Terrain Model (DTM) and Canopy Surface Model (CSM) respectively, which can be differenced to create a CHM. CHMs can be used in conjunction with algorithm controlled segmentation which aims to isolate individual trees or tree groups and analyse their structural metrics (Solberg et al., 2006). Popescu and Zhao (2008) delineated individual tree locations from CHMs which they then combined with vertical segmentations of the point cloud at each location. The frequency points within each vertical segment was plotted (see Figure 1 page 9), with the vertical components of the individual tree clearly described. Coops et al. (2007) used a "canopy volume" modelling approach involving the assessment of the absence or presence of LiDAR returns (taken to represent returns from foliage) and their relative occlusiveness within volumetric pixels (voxels) which test sites were divided into.

Care must always be taken when solely working with models and gridded datasets as information from the original 3D point cloud can be lost when data are interpolated or generalised. The loss of information can be significant, especially in the case of forested areas where multiple echoes are registered. Points at different elevations but with similar x, y coordinates are difficult to represent in such a form (Axelsson, 2000). On the other hand as discussed earlier in this section, using point data alone can involve long processing times. Morsdorf et al. (2004) utilised both surface models and the point cloud itself to limit information loss and speed up processing. Iterative cluster analysis to delineate tree crowns (a process usually run on the CSM or CHM) was undertaken on the point cloud itself to divide the feature spaces into areas containing values similar to each other. They did however utilise local maxima derived from the CSM as seed points from which to run the cluster analysis; a process faster than determination of the seed points from the raw data itself. Geometric

properties were then derived from the individual tree clusters. Using the data in this way integrates the best of using both surfaces and the point cloud.

Utilisation of 3D and 2D grids and surfaces can simplify complex forested environments in a way that makes them easy to conceptualise but this inevitably leads to the loss of data precision. The scale of such loss may be acceptable considering how much information is needed to achieve a study's aims and objectives and at what scale a study is operating at. Often integration of some form of 3D grid, especially DTMs, during LiDAR analysis can be a useful 'tool'.

2.3 Airborne LiDAR for Biodiversity Studies

As described in Clawges et al. (2008) applications of LiDAR data in biodiversity research are focused on three main areas:

1) Correlating LiDAR-derived data with potential species occurrence
2) Utilizing LiDAR-derived estimates to examine aspects of habitat quality
3) Establishing correlations between LiDAR-derived and field-based estimates of vegetation structure

These areas provide the structure for this section.

2.3.1 Correlating LiDAR-Derived Metrics with Species Presence

Swatantran et al. (2008) provides a good example of a study that utilises LiDAR to calculate forest structure attributes and then uses these to delineate potential habitat areas. They processed LVIS data to produce maps of forest structure and later combined these with stressed and dead

vegetation maps from Airborne Visible Infrared Imaging Spectrometer (AVIRIS) data. This in turn was used to pin point habitat 'hotspots' based on historical records of habitat preferences of the Ivory Billed Woodpecker (*Campephilus principalis*).

Nelson et al. (2005) provide a further example of LiDAR in this application as they used airborne LiDAR to measure canopy height and canopy closure to create habitat suitability maps. These delineated potential habitat areas for the Delmarva fox squirrel (*Sciurus niger cinereus*), usually prevalent in tall dense forests with an open understory. LiDAR data often must be integrated with other datasets to pinpoint actual habitat, but workflows such as this are a practical tool to identify potential habitats.

2.3.2 Utilising LiDAR-Derived Estimates to Examine Aspects of Habitat Quality

Studies also endeavour to link LiDAR derived forest metrics with habitat quality assessment (usually for a specific species) so areas associated with high habitat quality might be linked to the possibility of species prevalence. Hinsley et al. (2002) examined the relationship between LiDAR derived mean vegetation height around Great tit (*Parus major)* and Blue tit (*Cyanistes caeruleus*) nest boxes to mean chick mass (used as a surrogate for breeding success and, therefore indirectly, habitat quality). These researchers found that for Great Tits mean chick mass decreased with mean vegetation height and for Blue Tits mean chick mass increased with mean vegetation height. Hill et al. (2004) then produced a predictive map of reproductive performance in Great Tits based on a LiDAR-derived woodland canopy height model and the statistical relation between mean canopy height and mean nestling body mass.

Broughton et al. (2006) evaluated detailed territory maps of Marsh Tits *(Poecile palustris)* using airborne LiDAR data and found substantial differences between the vegetation structure within

Marsh tit territories and that of adjacent locations not occupied by the bird. In particular, Marsh Tits were found to occupy sites comprised of mature trees with a sub-canopy shrub layer and to avoid sites containing many small, young trees

Goetz et al. (2007) derived canopy structure metrics including canopy height and the vertical distribution of canopy elements from LVIS data taken over temperate Maryland, USA, forests. They then assessed the suitability of using said metrics as predictors for bird species presence with reference to bird survey data collected at referenced grid locations. The vertical canopy distribution information was consistently found to be the strongest predictor of species richness.

2.3.3 Establishing Correlations between LiDAR-Derived and Field-Based Estimates of Vegetation Structure

Research in this field also concentrates on analysis between LiDAR-derived and field-based estimates of vegetation structure important to various species. Clawges et al. (2008) examined the relationship between vegetation structure indices calculated from LiDAR-derived vegetation heights and corresponding field-based measurements to establish the utility of LiDAR data in representing vegetation structure in a Pine (*Pinus*)/Aspen (*Populus*) forest in South Dakota, USA. In this study, an index of tree vegetation density estimated from LiDAR data was significantly correlated with two field-based indices. The tree vegetation density index had a higher correlation than a tree stem density index, perhaps because the former came closer to representing the vegetation volume associated with trees, which may correspond better to the number of LiDAR returns from all parts of the tree (not just the trunk).

Hyde et al. (2005) and Hyde et al. (2006) also found a significant correlation between measures of vegetation structure derived from LiDAR, such as canopy height, canopy cover and biomass, and

on-the-ground field observations. These were then used in the creation of habitat maps to guide management of common forest species. This indicated that LiDAR-derived data could be used to replace field-derived vegetation data traditionally used to characterize avian habitat.

Structural diversity is the most straightforward measurement that indicates the potential biodiversity and habitat suitability of a forest stand. Ozdemir and Donoghue (2013) assessed the relationship between tree height, DBH, crown length and crown width diversity measured in the field and LiDAR derived variables and texture measures generated from the point cloud and CHMs. Models constructed accounted for up to 85% of the variance of tree height diversity, 68% of the variance of DBH diversity and around half of the variance for crown shape diversity measures. Measurement of forest vertical structure and structural diversity is vital in many forest biodiversity studies and LiDAR datasets can be invaluable tools with which this can be measured.

2.4 LiDAR Datasets Collected during Leaf-on and Leaf-off Conditions

Sections 2.2 and 2.3 demonstrate the abundance of studies utilising LiDAR datasets to explore forest structure. Most studies tend to use leaf-on LiDAR datasets to assess forest biophysical parameters as during leaf-on canopy conditions one may expect a greater chance of the laser pulse being returned from the highest parts of the canopy due to the presence of occlusive leaves (Hill and Broughton, 2009). However, some studies have also identified advantages that leaf-off LiDAR datasets could provide in forested environments. The differences between variables derived from seasonally different LiDAR datasets will be explored in this section.

The intensity data derived from LiDAR data are directly related to the spectral reflectance of the target material (Ahokas et al., 2006). Because deciduous species lose leaves during winter this directly affects their reflectance and can provide a more obvious distinction between coniferous

and deciduous species during winter months. Reitberger et al. (2008) found that when utilising the intensity and pulse width of full waveform LiDAR datasets to classify trees to deciduous or coniferous groups the best case classification accuracy for the leaf-on dataset was 85% but a 96% accuracy level was achieved using the leaf-off dataset. Kim et al. (2009) also found better species separation in the intensity data from a leaf-off LiDAR dataset as opposed to a leaf-on dataset.

In deciduous woodland it is expected that laser pulse penetration will differ greatly between leaf-on and –off canopy conditions with the possibility of increased penetration to lower canopy layers and the ground likely during leaf-off periods (Hill and Broughton, 2009). Hill and Broughton (2009) demonstrated that the integration of a leaf-off LiDAR dataset with a leaf-on made it possible to map the understorey layer in broad-leaf deciduous woodland to a high level of accuracy. It has also been suggested that despite the increased penetration in leaf-off conditions a significant portion of returns may still be reflected from the upper canopy layers of deciduous stands. Brandtberg et al. (2003) found no significant underestimation of the true deciduous tree heights by the maximum laser-derived heights when utilising a leaf-off LiDAR dataset. This could be because leaf-off LiDAR datasets with increased numbers of ground returns are likely to produce more accurate DTMs and in turn could produce more accurate tree height estimations (Ørka et al., 2010). In coniferous stands, where the leaves are not lost from the trees in winter, penetration of the laser pulse through the upper canopy layers may not change but penetration through a decreased understorey to the ground is likely (Hill and Broughton, 2009).

2.4.1 Investigating LiDAR Derived Forest Metrics from Leaf-on and Leaf-off LiDAR Datasets

A selection of studies directly compare the ability of leaf-on and leaf-off LiDAR datasets to assess forest biophysical parameters. In the coastal Pacific Northwest Gatziolis et al. (2010) evaluated the

accuracy and precision of LiDAR derived estimates of tree height under both leaf-on and –off canopy conditions. With a study area comprised of both coniferous and deciduous species under varying degrees of management and spread over complex terrain and steep slopes, the LiDAR associated error in tree height estimation from both the leaf-on and leaf-off datasets were larger than that seen in most studies. The authors did note that the LiDAR error accounted for less of the total tree height whilst utilising the leaf-off dataset (LiDAR error exceeded 10% of tree height for 55% of the trees the authors had precise measurements for and 38% of the plots distributed across the study area) as opposed to the leaf-on (LiDAR error exceeded 10% of tree height for 60% of the trees and 43% of the plots).

In the North-eastern USA Wasser et al. (2013) compared leaf-on and leaf-off LiDAR estimates of canopy height and fractional canopy cover with plot measurements collected within riparian buffer zones with a diverse range of trees and vegetation. Mean height, coefficient of variation (CV) of LiDAR points and decile and quartile percentile height values were calculated from each dataset. Histograms illustrating the frequency distribution of laser pulse returns throughout the canopy were also constructed. CV describes the overall spread of returns throughout the canopy (a larger dispersion generating a larger CV) while percentile height values often show strong relationships to tree height. Canopy height, canopy base height, diameter at breast height (DBH), fractional canopy cover and species were collected from the eighty test plots in the field. The overall dispersion of laser pulses throughout the canopy (CV) under leaf-off conditions was 6.9% greater than that found in the leaf-on canopies but varied depending on tree type. Observed differences between leaf-on and leaf-off CV values in conifer plots were small (difference of 1.1%) whereas largest differences between leaf-off and leaf-on CV values were observed in deciduous plots with a more open canopy (difference of 11.4%).

When comparing the LiDAR derived metrics and field measurements it was found that the LiDAR percentile values estimated field measurements well in both leaf-off and leaf-on conditions but

again varied with vegetation type. Differences between leaf-on and -off were largest again in the open deciduous canopies where returns were triggered lower down in the canopy during leaf-off conditions. Despite the differences in the pulse distribution throughout the canopy there were large similarities in LiDAR top of the canopy percentile estimates under both canopy conditions within deciduous plots, in agreement with Brandtberg et al. (2003). This demonstrates the potential ability of LiDAR datasets to still produce returns from the very top of the canopy even under leaf-off conditions.

A small collection of studies have touched on this subject in Europe. Whilst investigating the capability of small footprint airborne LiDAR to map canopy heights over complex topography Hollaus et al. (2006) also compared the products derived from a leaf-on and -off LiDAR dataset collected over their field sites in Vorarlberg, Austria. The study had two test areas covered by both flight campaigns, the first containing many deciduous trees and some coniferous. In this location there were considerably fewer ground hits under forest canopy in summer resulting in too few points with which to interpolate a DTM. The authors suggest that this is a result of the large numbers of deciduous trees in the study area. Additionally, it is mentioned that coniferous tree crowns are more transparent for infrared laser pulses in winter than in summer. When comparing the CSMs constructed for both LiDAR datasets the summer CSM was found to be consistently higher or roughly of same height as the winter CSM. A second test site was dominated by coniferous trees and allowed the study of the penetration of the laser beam depending on seasonal conditions through a canopy that does not greatly differ between seasons. The penetration capability (described in this instance as the percentage of total LiDAR returns with height differences to the terrain surface less than 0.5m) for the winter first pulse data is 17% and those of the summer data 13%. The authors summarise that for dense coniferous forests the penetration rate is very low and is 4% higher for winter than for summer conditions.

Working in broad-leaved, mixed wood and needle leaved forests in Europe Duong et al. (2008) compared and combined multiple tracks of large footprint full-waveform LiDAR data collected by the Geoscience Laser Altimeter System (GLAS) on the Ice, Cloud and land Elevation Satellite (ICESat) during two different epochs (February 2003 (leaf-off), September 2003 (leaf-on)). This was with the aim of determining the change in forest structure by seasonal influences. As the two datasets were obtained from repeated tracks many footprints from both datasets overlapped entirely or had some common topographic overlap. By comparing the shape of the returned waveform integrated across the test sites per dataset differences were observed in the height of median energy (a height measure of the median of the intensity in the returned waveform) over broad-leaved areas between the two epochs (a 148% change), much smaller than coniferous areas (36% change winter to summer). Ratios of ground return energy to canopy return energy also changed noticeably over time: 67% in broad-leaved, 62% in mixed-wood, and 47% in conifers. This study highlights the clear differences in LiDAR-derived structural metrics that can be obtained from LiDAR datasets collected during different seasons.

A large proportion of studies considering the difference between leaf-on and –off LiDAR datasets have taken place in Scandinavian Forests. One of the most prominent is that of Næsset (2005) which analysed how canopy conditions from a leaf-on and leaf-off LiDAR dataset affected various laser derived canopy metrics and biophysical properties of forest stands within a forest inventory in Norway. In this study first and last returns were considered separately with percentiles of the canopy returns, maximum return height, mean return height and CV of return height created for each return type and each LiDAR dataset. These LiDAR derived metrics were used as independent variables in multiple regression where relationships were created between these and tree mensuration data collected in the field. These estimated regression models were then used to predict biophysical tree properties of interest in a further set of field plots not included in the training data so they could be independently validated.

The Næsset (2005) study found that in mixed forest the last return datasets were generally influenced more by the canopy conditions that the first return data and that canopy height measurements of the lower and intermediate parts of the canopy are more affected by canopy conditions than the maximum canopy heights. Additionally in agreement with Wasser et al. (2013) it seemed the CV of return height was significantly higher under leaf-off conditions, and the accuracy of estimated biophysical properties in mixed forest was the same or slightly improved under leaf-off conditions.

These findings are echoed in Ørka et al. (2010), a similar study assessing the relative abilities of a leaf-on and –off datasets to assess biophysical parameters of a single tree in a forest reserve in south-eastern Norway. The authors found that the largest discrepancies in LiDAR return height between the two LiDAR datasets occurred in deciduous plots where, under leaf-off conditions, a larger proportion of last and single returns were reflected from the ground. The first returns seemed unaffected by the loss of leaves in deciduous plots as these were still being reflected from the same depth in both datasets. Furthermore, significantly more accurate tree species discrimination was obtained during the leaf-off conditions. The classification accuracies were in the order of 10 percentage points higher in overall accuracy.

In Finnish managed boreal forests, Villikka et al. (2012) tested a leaf-on and –off LiDAR dataset in a forest inventory in which deciduous and coniferous trees needed to be separated. They also investigated the appropriateness of mixing leaf-off and leaf-on data for the estimation of plot volumes of deciduous and coniferous trees. Using a similar workflow to both Næsset (2005) and Ørka et al. (2010) separate height distributions were calculated for the first and last pulse data for each plot with various height based LiDAR metrics calculated. Assessing the linear regressions that the authors created to estimate plot volume it was found that the leaf-off estimates were always more accurate than leaf-on estimates in coniferous-dominated and deciduous-dominated sample plots. The authors conclude that the leaf-off regression models applied to leaf-on data caused

systematic overestimation and, correspondingly, the leaf-on models applied to leaf-off data caused underestimation. When analysing leaf-on and –off affinity for classifying a plot as coniferous or deciduous the leaf-off dataset generally provided considerably more accurate estimates than leaf-on data. This was still the case even after the leaf-on LiDAR dataset had been combined with features from aerial imagery. Especially at lower heights, the distributions between coniferous and deciduous plots differ considerably in leaf-off data. This tendency cannot be seen in the case of leaf-on data. It can also be seen that the distributions of pine and spruce follow each other quite closely and do not differ between leaf-on and leaf-off data

There is a wealth of evidence to suggest that LiDAR datasets penetrate through the canopy differently under leaf-on and –off canopy conditions. The difference is greater in deciduous and mixed stands (Næsset, 2005; Ørka et al., 2010; Villikka et al., 2012; Wasser et al., 2013) but differences in penetration have also been witnessed in some coniferous stands (Hollaus et al., 2006; Duong et al., 2008). Last and single echoes seem more affected by canopy conditions than first echoes suggesting that canopy conditions have a lesser influence on maximum height obtained than on the distribution of pulses through the canopy. Increased penetration to the ground in winter conditions has been shown to create more accurate DTM models (Hollaus et al., 2006) and studies indicated that data acquisition in leaf-off conditions can be a means to improve the accuracy of biophysical properties estimated and predicted in a mixed or deciduous forest (Ørka et al., 2010; Næsset, 2005; Wasser et al., 2013; Gatziolis et al., 2010). Datasets taken under different canopy conditions appear to be so different in cases that their combination could introduce bias and lower the accuracy of species estimations (Villikka et al., 2012). Considering the large differences in biophysical parameters generated from seasonally different LiDAR datasets it would be of interest to assess the effect specifically on tree size diversity estimations of forest stands. Additionally, a large proportion of these studies have taken place in more managed Scandinavian forests with lower levels of species diversity or forested areas markedly different to those found in the UK; It

would be advantageous to see if significant differences between leaf-on and –off datasets would still be present in UK forests.

It is important to note that though the studies in this section largely come to similar conclusions after comparing and combining multi-temporal LiDAR datasets the very nature of doing so can overlook undesired effects which can confound the assessment of canopy condition on LiDAR estimation. Tree growth, systems configurations and positional error between surveys should all be assessed in detail when combination or comparison of LiDAR datasets is taking place. These issues are covered in detail in the next section.

2.4.2 Difficulties of Comparing and Combining LiDAR Datasets

Differences in LiDAR return distributions obtained using different airborne LiDAR sensors are well documented in the literature (Hopkinson, 2007; Næsset, 2005; Næsset et al., 2006; Chasmer et al., 2006). In addition, differences in flight altitude and speed during survey can result in varying point density and canopy penetration between surveys and can confound the analysis of the effects of changing canopy conditions alone.

Wasser et al. (2013) utilised two different LiDAR datasets collected with separate scanning configurations. To account for the different point densities between the leaf-on and –off LiDAR datasets due to the different pulse repetition frequencies, flying height and number of returns collected per pulse the leaf-on point cloud was thinned to be comparable to the lower resolution, leaf-off LiDAR dataset. This reduced the effect of the varying point densities between the two surveys had on LiDAR estimated biophysical parameters. To account for the remaining influence of differing LiDAR flight parameterization between datasets, Wasser et al. (2013) compared leaf-off and leaf-on LiDAR derived metrics generated from conifer dominated plots where year-round

needle retention somewhat negated the influence of changing canopy condition. Differences attributed to LiDAR flight configuration detected within these plots were assumed to propagate to all other forest plots. In this instance the authors found that sensor and flight altitude effects accounted for small differences (less than 0.5 m) in top of the canopy penetration. It is likely the effects were more pronounced within and towards the bottom of the canopy. By understanding the influence of sensor and flight altitude effects the authors could then better assess to what extent variability in LiDAR biophysical parameter estimations between datasets were due to changing canopy conditions.

Though Næsset (2005) utilised the same instrument in both leaf-on and –off LiDAR surveys, between these surveys the scanner underwent an upgrade affecting the pulse energy and peak power. Components associated with signal reception were also replaced or adjusted and altitudes between the two survey flights were also very slightly different. The effects of the increased flying height when capturing the leaf-on dataset was corrected based on findings from Næsset (2004) and used a linear relationship between change in flight altitude and the effects on the laser metrics. It is accepted by the authors that this assumption had not been confirmed with further study so there lies the potential for inaccuracies with this method. When again comparing datasets within the coniferous forest plots, the first return measurements of canopy height tended to be unaffected or shifted somewhat upwards by system upgrade and ground penetration was reduced, whereas the last return data indicated unaffected or downwards shifted canopy heights and increased penetration. Though systematic shifts in canopy heights and canopy penetration were revealed these accounted for less than 20–30% of the observed differences between the two acquisitions for most of the variables. Overall the effects of canopy conditions on the laser-derived height and canopy metrics seem to be of a magnitude on an order of 10–50 times the effects of flying altitude.

In research by Ørka et al. (2010), which utilised leaf-on and leaf-off data acquired using the same sensor and identical parameters, and an additional leaf-on dataset acquired using a different

sensor, the authors found that estimations of individual tree properties were fairly accurate in all acquisitions with RMSE ranging from 0.76 to 0.84 m for tree height and from 3.10 to 3.17 cm for stem diameter. This was only after all datasets had been co-registered so that the distributions matched spatially.

Co-registration of multi-temporal LiDAR datasets is incredibly important in comparative studies. Shifts in x, y and z can be due to LiDAR system errors (originating in the laser instrument, IMU or GOS), survey characteristics (point density, flight altitude, scan angle) and interpolation errors. Generally little information is included in the studies covered in this section as to how each dataset was co-registered if at all. There are a few exceptions, for example Næsset (2005) co-registered all returns from each dataset utilised in the study over a public road where systematic shifts by datasets away from a DTM created from the leaf-on data were clearly identified on the flat surface and corrected.

Authors often utilise a DTM created from one survey to normalise the heights of other surveys. Villikka et al. (2012) utilised the DTM created from leaf-on LiDAR data to calculate 'height above ground' for both the leaf-on and -off datasets so that returns from both datasets were registered to the same DTM. Wasser et al. (2013) utilised only the leaf-off ground returns to create a DTM that was used to create the CHM for both leaf-on and -off datasets. This method somewhat ignores any differences in x, y and z that may have been present between subsequent surveys due to systematic shifts.

Hill and Broughton (2009) were also faced with difficulties of co-registration of the leaf-on and –off LiDAR datasets used in their study as their point distributions did not match spatially. To overcome this both datasets were interpolated into Digital Surface Models (DSMs). A DTM was created from the leaf-off last returns and the subtraction per grid cell of the DTM from each of the DSMs created normalised DSMs where height was expressed in metres above ground level. The accuracy of the

DTM was assessed using terrain measurements recorded throughout the study site with an electronic total station. Again, though the authors assess the accuracy of the DTM there is no correction of any potential spatial differences between the two datasets. Any spatial differences between the datasets will have propagated through to the CHM, DSMs or height normalised LiDAR generated using the DTM from a different survey. This could introduce underestimates or overestimates of LiDAR point height above ground and therefore effect estimates or pulse penetration or canopy height estimation.

A further complication that could influence LiDAR derived heights between surveys is the growth or disturbance of the trees and vegetation. To account for this factor field sites could be visited to ensure no managed felling or natural tree fall had taken place between data collection and survey flights (Næsset, 2005). Additionally, some authors have applied corrections derived from tree growth models to the LiDAR data from subsequent surveys to ensure that datasets are comparable through time (Wasser et al., 2013; Næsset, 2005). Næsset (2005) applied different corrections to the first and last returns in subsequent LiDAR surveys according to the effects of growth on the laser-derived metrics observed by Næsset and Gobakken (2005) using the same sensor (ALTM 1210).

2.5 Literature Review Conclusions and Research Premise

There is a body of evidence linking biodiversity to selected forest structure metrics. It is clear that stand variation in tree height, diameter, distribution of biomass, crown characteristics and canopy cover are all important considerations in biodiversity conservation in forested landscapes (Hall et al., 2011) and can be used as an indicator of overall species diversity (Kimmins, 1997).

As an alternative to costly field collection of such variables airborne LiDAR survey holds an advantage. Vegetation canopies present a surface to the laser which is porous to energy allowing realisation of the vertical canopy structure (Lefsky et al., 2002; Chasmer et al., 2006). Like other remote sensing techniques LiDAR provides a means of data collection in areas of restricted or limited access and can generate high density sampling data rapidly and more efficiently than field methods, particularly at landscape levels (Lefsky et al., 2002; Bradbury et al., 2005). The three dimensional representations of vegetation structure provided by LiDAR can play an important role in ascertaining microclimate conditions, availability of niche space and habitat quality (Brokaw and Lent, 1999) and can therefore be a critical component of effective forest ecosystem management (Lefsky et al., 2002; Proulx and Parrott, 2009).

There have been many studies investigating the relationships between LiDAR derived structure metrics and those collected in the field though fewer studies are concerned with assessing tree size diversity metrics. There has been very little focused research into the effect of the time of LiDAR data collection, be it during the summer leaf-on period or winter leaf-off period, specifically on LiDAR derived forest structure diversity metrics. The studies covered in section 2.4 demonstrate that LiDAR datasets collected under differing canopy conditions can have a significant effect on the derived forest biophysical parameters. The general consensus is that LiDAR datasets collected during leaf-off canopy conditions are shown to have the same and higher levels of accuracy when estimating forest structure metrics compared to leaf-on LiDAR datasets. However the most focused studies investigating this topic are based in managed Scandinavian forests with relatively low levels of species diversity. Many of the remaining studies investigating leaf-on and -off LiDAR datasets are involved with sites with vegetation conditions that are very different to those found in the UK: Though Hill and Broughton (2009) utilised LiDAR datasets collected under different canopy conditions to map understorey, no studies directly comparing LiDAR derived tree size diversity metrics under leaf-on and off conditions have taken place in forests in the UK. It is uncertain whether these observations would hold in the UK forest environment.

Undertaking analysis of the structural diversity of a range forest stands applicable to UK species composition and management techniques would be advantageous to UK forestry management in terms of biodiversity assessment. Additionally, working at the stand level is at a scale which forest management bodies like the Forestry Commission make conservation priority decisions and so is ideal to provide meaningful analysis that can be practicable in management processes (Townsend Peterson and Kluza, 2003). It may also be of use to other airborne LiDAR system users to assess the relative accuracy of LiDAR derived tree size diversity metrics obtained during any season and combined between seasons. Additionally a robust method of co-registration and standardisation between multi-temporal datasets will allow conclusions to be drawn with increased confidence.

3. RESEARCH AIM AND OBJECTIVES

The aim of this research is to assess and compare the accuracy of forest structural diversity metrics calculated from a purposely wide range of forest stands and LiDAR surveys collected under leaf-on and leaf-off conditions.

Key research questions:

1. How does the seasonal time of capture impact upon the LiDAR point distributions and structural diversity metrics generated from the LiDAR point cloud?
2. What is the relative accuracy of models describing tree size diversity metrics generated from leaf-on LiDAR derived diversity metrics, leaf-off LiDAR derived diversity metrics and models generated from a mix of the two?
3. Can this tell us anything about when is best to undertake airborne LiDAR survey when modelling forest structure diversity and assessing biodiversity?

In answering these questions this project will attempt to:

1. Co-register the leaf-on and leaf-off LiDAR datasets sufficiently to remove any systematic bias between surveys;
2. Qualitatively and quantitatively compare forest structure and structural diversity metrics calculated from leaf-off and –on LiDAR datasets to one another to better understand the potential influence of growth and differing survey characteristics between epochs and better isolate the influence of seasonal capture conditions;
3. Assess the relative capability of leaf-on and -off LiDAR derived structural diversity metrics to describe true structural diversity through assessment against field data;
4. Assess what the outcomes mean for LiDAR survey planning for forest biodiversity investigations in the UK.

4 MATERIALS AND METHODS

4.1 Data Collection in the Field

4.1.1 Field Site

The field site was chosen in this study aims to cover as full a range of structural variability as possible. This is so that the results obtained and techniques used can be applied beyond to a wide range of forest types and landscapes throughout the UK. Chopwell Woodland Park, in the North East of England, is one such forest which fits this requirement. It is mixed coniferous and deciduous woodland of 360 hectares (3.4 km^2) located on the northern slopes of the Derwent Valley, 10 miles southwest of Gateshead in the North East of England (see Figure 3).

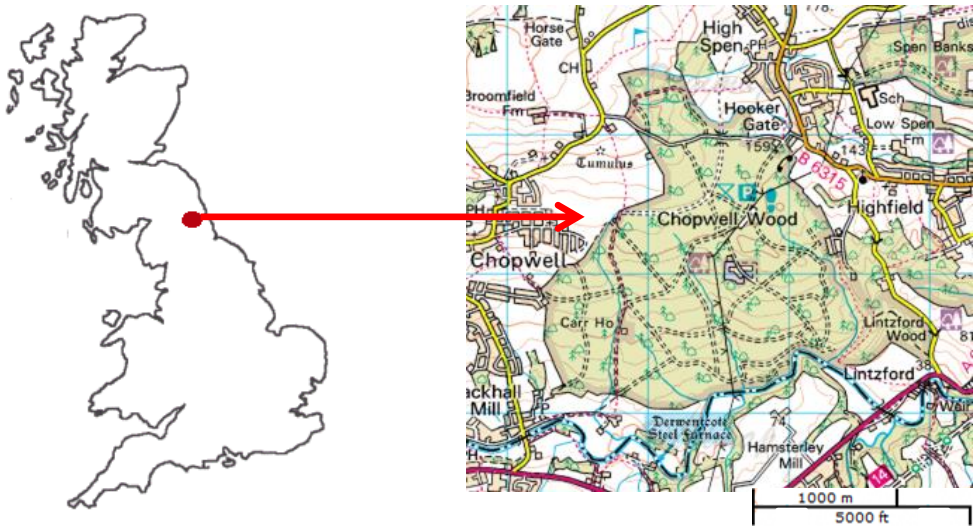

Figure 3. Study site location (EDINA, 2013) at latitude -54.916193° longitude -1.791604°

The terrain in Chopwell Woodland Park has minor undulations and an elevation range between 44 to 222m above sea level, most of which is associated with an escarpment leading to the river Derwent. It is classified as an Ancient Woodland site by the UK Forestry Commission (2009), a

designation reserved for only 2% of the country's forested area and one of the rarest habitats in the UK.

Initially consisting of a mix of deciduous trees, mainly Oak (*Quercus*) and Hazel (*Corylus*), the wood has undergone many changes since its original 'Wildwood' state. After timber from the wood was felled during the 16th and 17th centuries for shipbuilding and bridge repairs it was replanted with Larch (*Larix*), Oak and Elm (*Ulmus*) and large areas of Scots Pine *(Pinus sylvestris*). When the Forestry Commission took over management of the wood in 1923 further replanting of Pine, Fir (*Abies*), Spruce (*Picea*) and Larch took place. In 2005 the wood was designated under the Plantation on Ancient Woodland Site (PAWS) scheme which prevents further planting of any trees not native to the area. Therefore, despite its varied planting history, the current forest design plan for Chopwell Wood is based on natural regeneration of species or planting of native species (Searle, 2000). As a result, the Forestry Commission are currently removing areas of conifer to help the forest return to its original cover of native trees, whilst thinning forest crops (removing, for example, one in every five trees) and occasionally harvesting full areas. Because of this the range of tree species, plantation years and silvicultural practices there is a wide variety of structural characteristics and stand types (pure conifer, mixed conifer, pure deciduous, mixed deciduous, mixed deciduous and conifer, all of varying age class and levels of spacing (Forestry-Commission, 2009)). This variation within the site provides an excellent environment to assess the ability of multi-epoch LiDAR datasets to calculate variables surrounding forest structural diversity.

Aside from the structural suitability of Chopwell Woodland Park to this study, the forest is also of interest to National Grid UK, an electricity transmission network operator and the system operator for England and Wales, as its extent encompasses the locations of two electricity transmission line corridors. Aerial LiDAR surveys are particularly suited to visualisation of the transmission line towers and cables rarely detected using other remote sensing methods. It is for this reason that Chopwell Woodland Park has two airborne LiDAR surveys flown over it, the original aim of which was to cover

the transmission lines running through the forest. The requirements for both surveys ensure that shared coverage of at least parts of the forest that could be used to assess structural characteristics is provided.

4.1.1.1 *Existing Sample Plots*

In this study measurements collected in the field provide a dataset that can be used to assess the accuracy of LiDAR derived forest structure metrics. These metrics were to be calculated from a leaf-on and leaf-off aerial LiDAR dataset and so coverage of both of these would need to extend over all of the sample plots used. Measurements were collected from 30 individual sample plots throughout the forest. Nineteen of these were provided by previous research carried out by Ozdemir and Donoghue (2013) who utilised them to investigate the relationships between the plot-level tree size diversity and diversity variables derived from airborne LiDAR. Though the 2013 study provides measurements from 27 sample plots within Chopwell Woodland Park, only nineteen of these were fully covered by both the leaf-on and the leaf-off LiDAR datasets analysed in this research (see Figure 4 page 33).

Ozdemir and Donoghue (2013) undertook a purposive sampling strategy when selecting sample plots based on the criteria of age, percentage canopy cover, tree species and species diversity. As the number of sample plots available from the 2013 study was limited, and amounted to only a subset of a former full dataset, there were concerns that the structural diversity within the dataset was insufficient to provide a comprehensive assessment of the research aim. To investigate this a simple assessment of species composition, number of tree stems per square metre and tree height statistics was undertaken (see Table 1 page 34). Metrics related to tree height were chosen as representations of structure within each plot as tree height is easy to conceptualise and in itself is a function of other measured variables such as DBH (Lim et al., 2003). The Coefficient of L Variation

(L-CV) of tree height was chosen as a representation of structural heterogeneity. Coefficient of Variation (CV), analogous to the L-CV has been shown to be a good indicator of structural complexity (Bolton et al., 2013). L-CV, identical to the Gini Coefficient utilised in many studies to convey forest structure diversity (Peck et al., 2014; Lei et al., 2009) is more robust to outliers and reasonably unbiased in small samples . This is important as the diversity of species, age and management level of the field sites in Chopwell Woodland Park mean that Tree Height outliers, and smaller sample sizes are present which would adversely affect many other descriptive statistics. In this instance an L-CV value of 1 would indicate the highest heterogeneity and 0 would indicate complete homogeneity.

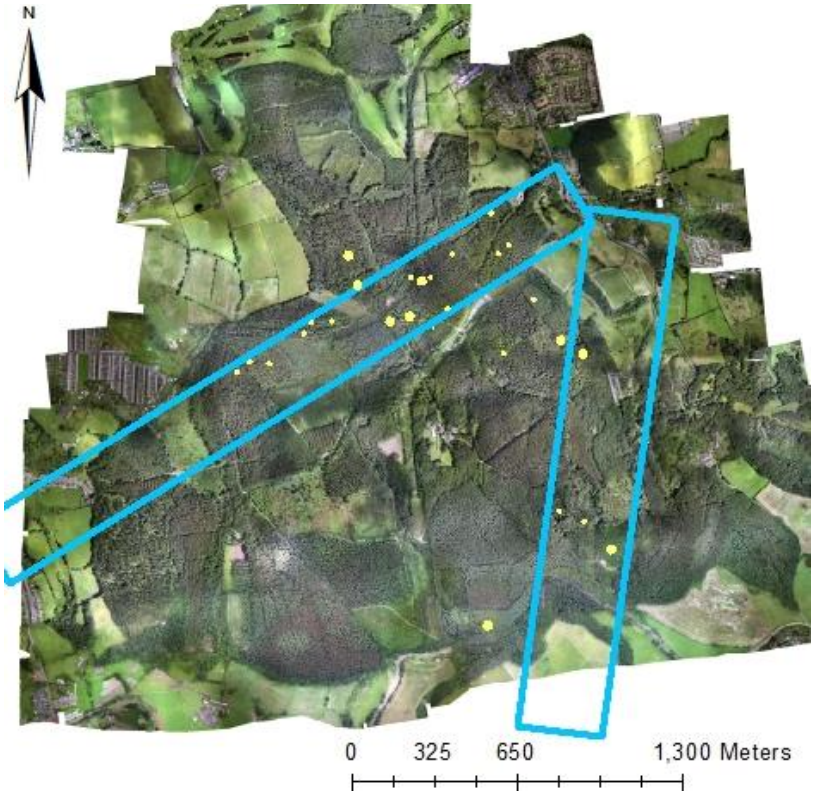

Figure 4. Orthomosaic captured July 2009 during the first LiDAR acquisition. LiDAR data from the 2011 survey is only available within the blue boundaries whereas LiDAR data from the 2009 survey is available across the entire forest. Yellow circles represent all Chopwell Woodland field data sample plots available from the Ozdemir and Donoghue (2013) study.

					Tree Height		
Plot	Plantation Year	Deciduous	Evergreen	Trees Per Hectare	Mean	Range	L-CV
1	1908	75	25	525	19.84	34.4	0.276
2	1963	69	31	438	17.2	25.5	0.201
3	1985	100	0	1275	17.38	20.6	0.126
4	1980	46	54	1400	14.61	22	0.175
5	1954	100	0	275	22.88	7.2	0.048
6	1949	95	5	525	19.12	22.8	0.155
7	1944	100	0	567	19.85	12.2	0.088
8	1924	100	0	1000	21.8	11.8	0.079
9	1943	100	0	375	24.83	4.3	0.022
10	1943	96	4	525	18.47	18.6	0.192
11	1920	3	97	750	19.24	11.9	0.061
12	1984	0	100	2917	18.53	19	0.112
13	1908	67	33	875	13.48	18.8	0.215
14	1923	100	0	900	16.66	17.1	0.196
15	1969	23	77	475	20.26	13	0.076
16	1954	100	0	325	22.29	14.6	0.103
17	1947	88	12	650	17.21	18.5	0.168
18	1963	6	94	550	19.36	15.7	0.083
19	1943	100	0	725	14.8	15.3	0.172

Table 1. Information surrounding each of the 19 plots available from *Ozdemir and Donoghue (2013)*. Plantation year was provided by the Forestry Commission sub-compartment database *(Forestry-Commission, 2013)*. Green boxes represent a dominance of either evergreen or deciduous (an assemblage above 90%) and yellow boxes demonstrate a mix.

Table 1 shows that there are at least three examples of evergreen coniferous dominated plots, deciduous dominated plots and plots with an even mix of the two within the pre-existing field data. Each of these assemblages are useful in different ways: Field data collected from purely evergreen coniferous stands can be used in conjunction with LiDAR derived metrics from multiple datasets to identify differences due to possible changing understorey conditions, survey characteristics or growth as one would expect the foliage mass between surveys to be similar. Analysis of deciduous dominated plots could highlight the differences in LiDAR derived metrics between datasets that are

likely attributed to both changing understorey and overstorey seasonal conditions. Plots which are a mixture of the two may be useful as an intermediate comparison.

Figure 5 highlights that the range of tree height diversity (THdiv) in the existing sample plots is relatively small (0.022-0.276) with only a small number of plots at the higher, or more diverse, end. Therefore, when choosing additional field sample plots to improve the current selection an aim to increase this range would increase the structural diversity available to study. As finding incredibly low diversity of tree height in complex natural systems is rare, even when they are highly managed, additional sample plots were chosen to increase the L-CV of tree height in order to enhance the structural heterogeneity of the field dataset.

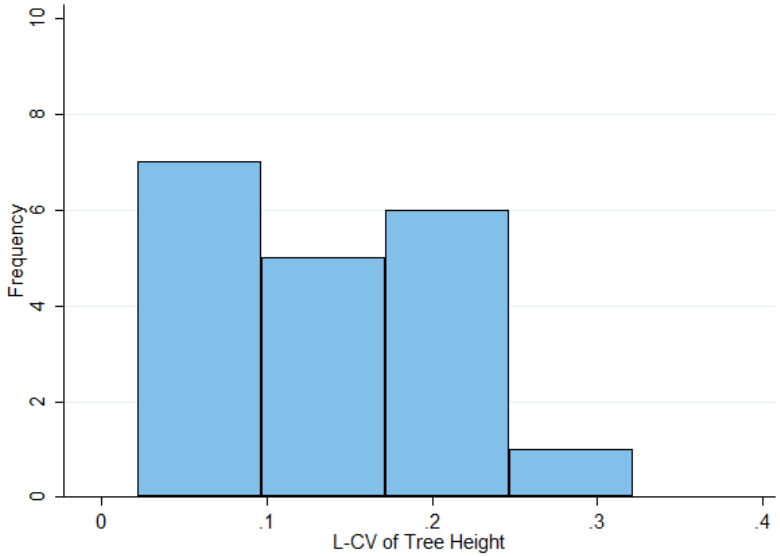

Figure 5. Histogram showing L-CV of Tree Height measurements from the 19 Chopwell Woodland plots available from previous research *(Ozdemir and Donoghue, 2013)*

To identify ways this range could be increased regression analysis was undertaken using potential independent variables available from the field data or the Forestry Commissions GIS sub-compartment dataset (Forestry-Commission, 2013) (which provides density of tree stems, total number of discrete species per plot, plantation year and percentage of deciduous trees among coupe characteristics) against L-CV as the dependant variable. The only independent variable which

significantly (95% significance) described around 30% of the tree height variation was the total number of discrete tree species in each plot. Other potential predictor variables showed some relationships to L-CV but they were weak and below any confidence levels.

4.1.1.2 Delineating Additional Sample Sites

Through the statistical analyses undertaken in section 4.1.1.1 it was endeavoured that additional plots should display high species diversity in order to achieve higher L-CV of tree height and therefore structural diversity. In addition, currently underrepresented species in the field sites, such as Oak and Birch, widely present in woodland throughout the UK, should be sought to ensure a dataset as representative of UK woodland as possible. As the majority of existing plots were dominated by deciduous species it was endeavoured that as many evergreen species dominated sites as possible would also be sought.

Potential new plots were isolated with the aforementioned characteristics in mind using the Forestry Commission GIS sub-compartment dataset (Forestry-Commission, 2013) providing information on plantation year, primary secondary and tertiary species present, habitat and their relative abundance within each coupe. Reconnaissance visits to the forest before additional data collection took place enabled any incongruities between the forest itself and the Forestry Commission database to be spotted. Chopwell Woodland Park is a working forest with various stands thinned each year. These initial visits were also used to identify these areas of recent thinning. It is important to note at this point that the potential of thinning at the pre-existing field sites between the field data collection and the two LiDAR survey dates was ruled out through correspondence with the Forestry Commission. Thinning after LiDAR data collection would cause significant forest structure change preventing the use of said areas as ground control plots. Out of an initial nineteen candidate areas that were covered by both LiDAR datasets and displayed

favourable characteristics, eleven sites were deemed viable after many sites displayed evidence for recent thinning. The careful consideration and addition of these eleven sample sites did indeed increase the range of L-CV and therefore the range of THdiv from 0.254 to 0.367 (see Figure 6).

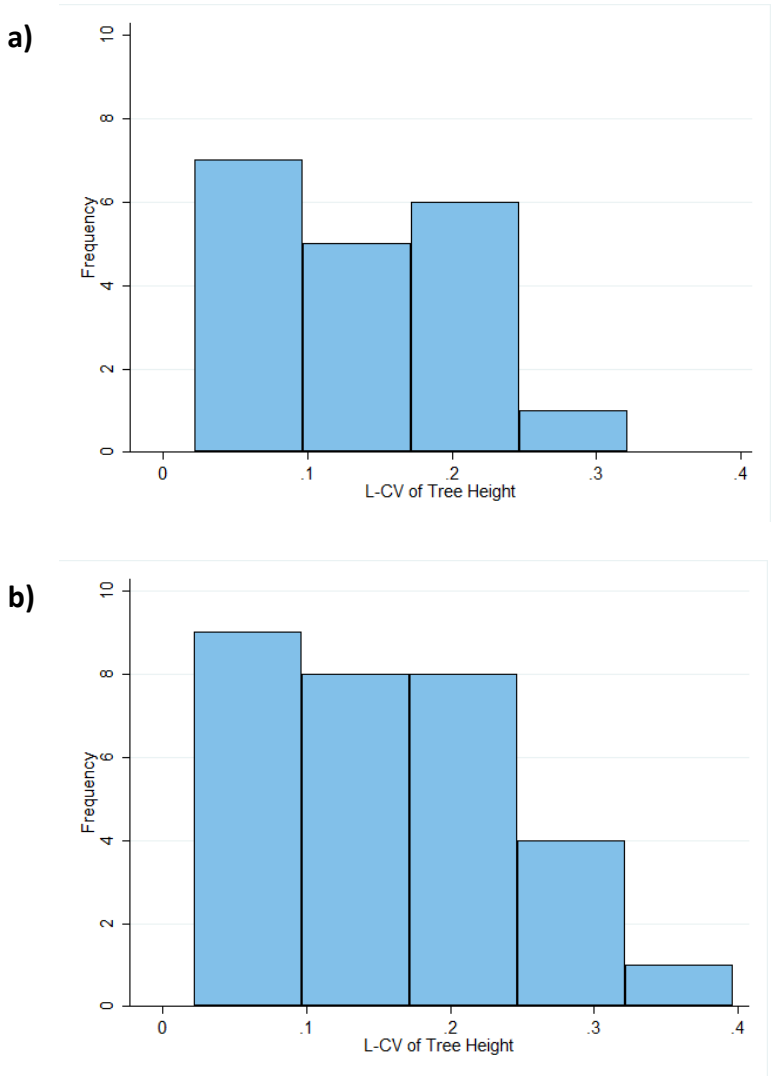

Figure 6. L-CV of tree height before (a) after (b) addition of new sample sites.

4.1.2 Field Data Collection

Data collected for sites 1-19 took place during May, June and July 2011 and more recent data collection for sites 20-30 took place during February and March 2013. Sample plots were of a circular shape, the centre of which was referenced using a hand-held GPS (the accuracy of which is

addressed later in this chapter). As the plots delineate hypothetical boundaries it is likely that trees from outside of the perimeter may overhang the boundary or tree stems within the plot may have portions of their crowns outside (Frazer et al., 2011). To compensate for this effect, and any error associated with the handheld GPS, approximately 5m of forest exhibiting a similar species composition and structural characteristics surrounded every plot to act as a buffer.

Typically Forest management bodies such as the Forestry Commission use plot sizes of 0.01 to 0.05 hectares (100 to 500 square metres) as a representative sample of trees within a stand depending on tree spacing (Mackie and Matthews, 2008). In this study three different plot sizes (100, 400 and 1256m^2) were adopted, some larger than sizes used by the Forestry Commission to ensure a very detailed description of each stand. The choice of plot size was, like methods adopted by the Forestry Commission, based on the tree spacing and homogeneity of species and age. Particularly densely planted homogenous age and species stands were surveyed using the smallest plot size as this was time efficient and would still provide an adequate representation of the structure and species in the stand. Gobakken and Næsset (2009) found that structural metrics calculated from airborne LiDAR data are less sensitive to variations in plot size and GPS error in dense homogenous stands than complex and heterogeneous stands. The largest plot size was used when surveying stands with particularly large tree spacing which were generally more species and structurally diverse. In these instances using the conventional smaller plot sizes resulted in small tree counts with a species mix not completely representative of the larger stand so an increased plot size was chosen. Larger plot sizes have been found to exhibit greater spatial overlap between ground-reference and LiDAR datasets for any given GPS error. Additionally Hinsley et al. (2009) report that the standard deviation (SD) of differences between metrics calculated using incorrect plot positions and ground-truth positions were smaller for larger field plots.

The field data collection process follows that used by Ozdemir and Donoghue (2013) to ensure conformity with existing data and occurred as follows: At each site four biophysical tree

characteristics were obtained for each tree (DBH $\geqslant 8$): DBH, Tree Height, Crown Length, and Crown Width. The DBH of each tree was measured using a diameter tape at 1.3m above the ground surface. When the tree resided on a slope DBH was measured from the uphill side looking downhill to ensure conformity throughout the data, though slopes were uncommon and usually very gentle.

The height of each tree was ascertained through the use of a Vertex-III ultrasonic hypsometer, widely used for forest mensuration applications. The handheld device works using ultrasonic communication with an associated T3 transponder unit. The transponder unit was placed at a height 1.3m on the trunk of a tree and then the vertex was used to ascertain tree height. Whilst standing in a position where both the transponder and the very top of the tree are visible, the Vertex can be used to measure the distance and angles of inclination between the user and the transponder and treetop using ultrasound and an embedded digital inclinometer. The system can correct the measured height to include the 1.3m the transponder has been placed at. This process calculates the height of any tree to the nearest 10cm (Božić et al., 2005). The Vertex was also used to collect crown length and crown width. Crown length describes the height from the top of the tree to the lowest live branch forming part of the canopy and crown. The crown width was calculated by measuring the length of two orthogonal axes of the tree crown (the diameter of the maximum axis and the axis at 90°) and taking an average.

Before any use of the Vertex, and intermittently throughout use, the instrument was calibrated as changes in humidity, air pressure, and temperature have a distorting effect of the range and extension of the ultrasound waves (around 2cm per 1°C). As these atmospheric conditions change regularly, regular calibration minimises the detrimental effect (Božić et al., 2005).

4.1.3 Resultant Field Metrics

From each of the allometric measurements collected in the field (tree height, DBH, crown length and crown width) the L-CV was calculated as a representation of diversity. The variables shown in Table 2 were also calculated.

Trees Per Hectare	The number of trees per hectare in each plot –from the field data.
Tree Species Number	The discrete number of species -from the field data.
Percentage of Deciduous Trees	The relative percentage of deciduous trees per plot - calculated from the field data.
Plot Age	An indicator of the average age of trees in each plot - inferred using the Forestry Commissions sub-compartmental database (Forestry Commission, 2009) which, though generalised over large areas, gives an indication of the planting year in each stand.

Table 2. Summaries of secondary field variables

These secondary variables were obtained so that, alongside the primary field diversity metrics, their relative influence on the LiDAR derived structure diversity metrics could be assessed. Table 3 shows correlations between all field variables and as expected variables such as DBH diversity (DBHdiv), Tree Height diversity (THdiv), Crown Length diversity (CLdiv) and Crown Width diversity (CWdiv) are highly correlated. On the other hand, the secondary variables are generally less correlated with one another.

		n	***nsp***	***%D***	***age***	***THdiv***	***DBHdiv***	***CLdiv***
Trees per Hectare	***n***	1						
Tree Species Number	***nsp***	-0.29	1					
% Deciduous	***%D***	-0.27	0.15	1				
Plot Age	***age***	-0.36*	0.03	0.03	1			
Tree Height Diversity	***THdiv***	-0.13	0.39*	0.23	0.28	1		
DBH Diversity	***DBHdiv***	-0.02	0.35	0.11	0.33	0.92**	1	
Crown Length Diversity	***CLdiv***	0.18	0.05	0.02	0.30	0.75**	0.80**	1
Crown Width Diversity	***CWdiv***	0.06	0.07	0.08	0.32	0.60**	0.72**	0.74**

Table 3. The Pearson's correlation of all field variables**.** *=statistically significant at the 95% CI **=statistically significant at the 99% CI.

4.2 LiDAR data

4.2.1. LiDAR Data Acquisition

As shown in Table 4 the 2009 dataset was collected by Network Mapping Ltd during the summer leaf-on period for deciduous trees. Trees would have been under full leaf at the time with understorey vegetation close to its maximum growth. The 2011 dataset was collected by the National Environmental Research Council (NERC) Airborne Research Facility (ARSF) with a sensor mounted upon Dornier 228-101 NERC research aircraft in conditions where the understorey was advanced but leaves had not begun bud burst.

	Leaf-on LiDAR Survey	**Leaf-off LiDAR Survey**
Acquisition date	18th-19th July 2009	23rd March 2011
System	Optech ALTM 3100EA	Leica ALS50-II
Platform	Helicopter	Fixed wing Plane
Laser Type	Discrete Pulse	Discrete Pulse
Beam Deflection	Oscillating Mirror	Oscillating Mirror
Wavelength	1064	1064
Flying Height	300m a.g.l.	800m a.g.l.
Pulse Rate (kHz)	100	87
Point Density	~25ppm²	~60ppm²
Returns	up to four	first and last
Survey Characteristics	wide area	two multiple pass corridors
Pulse discrimination distance	2.14m	2.8m
Pulse discrimination method	Constant fraction discriminator	Constant fraction discriminator

Table 4. A summary of the two LiDAR surveys analysed in this research. A.g.l. stands for above ground level and ppm² stands for points per square metre.

4.2.2 Pre-Processing of the LiDAR Datasets

The 2009 airborne LiDAR data were pre-processed by Network Mapping Ltd. GPS and IMU data were processed through Applanix POSPac 5.0 under the loosely coupled GNSS mode using

information from two ground-based stations. Optech's Dashmap software was used to process the trajectory and range information into a georeferenced point cloud in ODN (Ordnance Datum Newlyn) and the British National Grid projection. As shown in Table 4 (page 41) this was a wide area survey and coverage of the whole of Chopwell Woodland Park and past its boundaries was obtained.

The 2011 airborne LiDAR data were delivered as ASCII files containing the x, y, z coordinates of all first and last returns in the Universal Transverse Mercator (UTM) zone 36-North projection and WGS84 datum. These were transformed to British National Grid projection and Ordnance Datum Newlyn to match the 2009 survey. As shown in Table 4 page 41, in contrast to the 2009 survey, this flight consisted of multiple passes over transmission line corridors. This provided two survey corridors around 300m in width centred along the power lines but capturing the surrounding forest, resulting in over 60ppm².

It is important to note that though the NERC ARSF provided some initial quality control observations with regards to the 2011 leaf-off LiDAR survey (discussed in section 4.3.2) this dataset was not corrected for any geometric distortions. On the other hand, Network Mapping Ltd assessed the absolute accuracy of the 2009 dataset using 85 ground truth points and removed a 6cm systematic bias from the point cloud.

4.2.3 Initial Assessment of the LiDAR Datasets

There are some notable differences between the two datasets (see Table 4 page 41) such as the height of the surveys, the point density achieved, the pulse discrimination distance and the return numbers per pulse. As multiple returns were collected during the 2009 survey, only first and last returns were used during analysis in this research for the same reason as vertical forest structure

could be realised in more detail with multiple LiDAR returns making the derived metrics less directly comparable.

The use of only the first and last returns from each survey will also have reduced the effect of the different pulse discrimination distances between the two LiDAR sensors. This discrimination distance refers to the resolution within which the sensor can identify individual returns from the received waveform. The presence of this in each sensor means if there are targets distributed at distances less than the range with which the sensors in this study can discriminate returns in the LiDAR's 'line of sight', then these targets can be missed (Ussyshkin and Theriault, 2011). Situations such as this will most likely be present in the complex vertical distributions of branches and foliage natural forest systems are comprised of. The difference of around 65cm could have resulted in differing levels of vertical detail between surveys, but as mentioned it is thought the effect is reduced by only using the first and last returns. This might be seen as an unnecessary loss of potential vertical detail from the study, however in the authors' opinion the ability to more directly compare the two LiDAR datasets is important, and the very high point densities of the surveys potentially negates any detail lost. Within Chopwell Woodland Park the stands with the highest tree densities are coniferous (Forestry-Commission, 2013), which, due to the nature of their foliage and thin conical shape, are expected to still provide enough penetration of the laser at high point densities so that first returns are collected from the lower canopy layers. Deciduous stands with more occlusive leaves tend to be widely spaced within the wood, providing a similar expectation of returns from the lower layers.

There is also a large discrepancy between survey point densities due to the nature of each survey, one being a wide area and one confined to two corridors flown multiple times. This resulted in the 2009 leaf-on wide area dataset having only 50% overlap between neighbouring flight lines but the 2011 leaf-off dataset having almost 100% overlap of four flight lines in both of the captured

corridors. This issue is analysed in more detail and rectified during section 4.3 LiDAR Post-Processing.

The differences in flying height between surveys will affect the of the laser footprint on the ground. Differences in footprint size between datasets can manifest in differing success of laser pulses to hit the apices of trees or achieve a high penetration rate through the forest canopy (Wulder and Franklin, 2003). Despite this, studies have not found significant differences in canopy structure metrics between flying heights (and resultant footprint sizes) where flying heights differ at the scale seen in this study (Yu et al., 2004a; Persson et al., 2002; Takahashi et al., 2010). Studies where data is compared at higher altitudes are more variable but are usually also under the influence of differing point densities (Yu et al., 2004a; Persson et al., 2002), a characteristic which is made comparable in this study and documented in section 4.3 LiDAR Post-Processing.

Another main difference is the time between LiDAR surveys likely resulting in vegetation growth. If we take for example the species Sitka Spruce (*Picea sitchensis*), grown commercially for timber due to its' high yield volumes in a comparatively short time, it often has a yield class of 14 (producing 14 cubic metres per hectare per year (Forestry-Commission, 2015)). Based on Forestry Commission growth models of Sitka Spruce between the ages of 20-45 it is possible that this species alone could have increased in height by 0.54-1.08m in the time between the two LiDAR surveys (approximately one and a half years) (Jenkins, 2009). These growth rates are heavily dependent on management practises and tree age, neither of which can be specified to an acceptable level in this research to retrieve an accurate prediction. In terms of tree growth across all sites between LiDAR surveys the growth of coniferous species such as Douglas Fir (*Pseudotsuga menziesii*) and Corsican Pine (*Pinus nigra*) will likely be in this region, however the majority of plots within this study are comprised of deciduous trees like Beech (*Fagus*) and Oak, the latter sometimes having a yield class of only 4 suggesting significantly less growth volumes (Wasser et al., 2013).

A further influence on derived height metrics from the LiDAR datasets is tree removal or damage (which there was evidence for in some sites though it was difficult to estimate when this had occurred), and the different understorey conditions between surveys. The changes in understorey mass between surveys can affect the penetrability of the laser to the ground. Differences in ground penetration between surveys could contribute to tree height underestimation in one and not the other. Tree removal or damage between surveys could lead to inconsistencies between the direct field measurements (tree height, crown length and width and DBH) and the equivalent LiDAR metrics between survey dates. Diversity metrics are not expected to be largely effected during the time period however to assess any differences LiDAR derived diversity metrics will be compared in purely coniferous plots, to assess the effects of growth, tree removal or damage and changing survey characteristics in this research.

4.3 LiDAR Post-Processing

For each survey dataset, all points were loaded into the LiDAR processing package TerraScan (Soininen, 2015). The process functions embedded within TerraScan are automated but customisable and macros can be quickly written and used to batch process large point clouds. The software also allows for multiple flights to be loaded and processed simultaneously but separately. This provided an ideal environment for the management and comparison of the two surveys analysed in this research.

4.3.1 Initial Filtering of the LiDAR Datasets and Assessment of Relative Accuracy

This research draws comparisons between diversity metrics calculated from two separate LiDAR surveys, but it is impractical to expect any two surveys to capture an entire area homogenously,

especially when different scanning systems are used as with this study. There may be differences in track spacing and overlap along flight strips dependant on how the survey was flown which can prevent regular coverage (Baltsavias, 1999; Mallet and Bretar, 2009). The latter was particularly apparent in this research, the multiple pass style of survey the 2011 leaf-off dataset meant it exhibited, on average, twice the point density of the 2009 leaf-on survey. This was still true when the intermediate returns from the 2009 survey were excluded from analysis. There has been much research surrounding the effects of point density on the assessment of LiDAR metrics such as tree height (Treitz et al., 2012; He and Li, 2012; Lovell et al., 2005; Gobakken and Næsset, 2008). As a very general rule, accuracy of calculated structural metrics decreases and RMSE increases as pulse density decreases (He and Li, 2012; Lovell et al., 2005; Jakubowski et al., 2013). However, the accuracy of these LiDAR derived structure metrics remains relatively high until very small point densities, typically less than 1ppm^{2,} above which little difference is seen (Goodwin et al., 2006; Tesfamichael et al., 2010; Takahashi et al., 2010; Jakubowski et al., 2013). The datasets in this research demonstrate significantly higher point densities (approximately 25ppm² and 60ppm² respectively) and so are not expected to demonstrate any great differences in accuracy of structural diversity metrics that could be attributed to the differences in point density. However, as the pulse density of the 2011 dataset was twice as numerous as the 2009 and the procedure to reduce it to a relative level was moderately simple this process was undertaken regardless. This would eliminate even the smallest advantage the larger point density would offer and make structural diversity metrics from the two datasets more directly comparable. By removing four of the total eight flight strips from the two multiple pass corridors the 2011 survey was comprised of, the average point density over the whole 2011 dataset was reduced to approximately 23ppm² from over 60. Figure 7 (page 47) shows the different proportions of returns from the two datasets at the plot level and averaged between all plots. There are plots where there are comparatively greater proportions of returns for either the leaf-on and –off datasets. Datasets where a low proportional point density does not reflect low frequency (as the lowest point density is around 20ppm²) but should highlight

where datasets have a high frequency of returns – the benefits of which are unlikely to be of significance (Treitz et al., 2012). On average the datasets have comparable return frequencies.

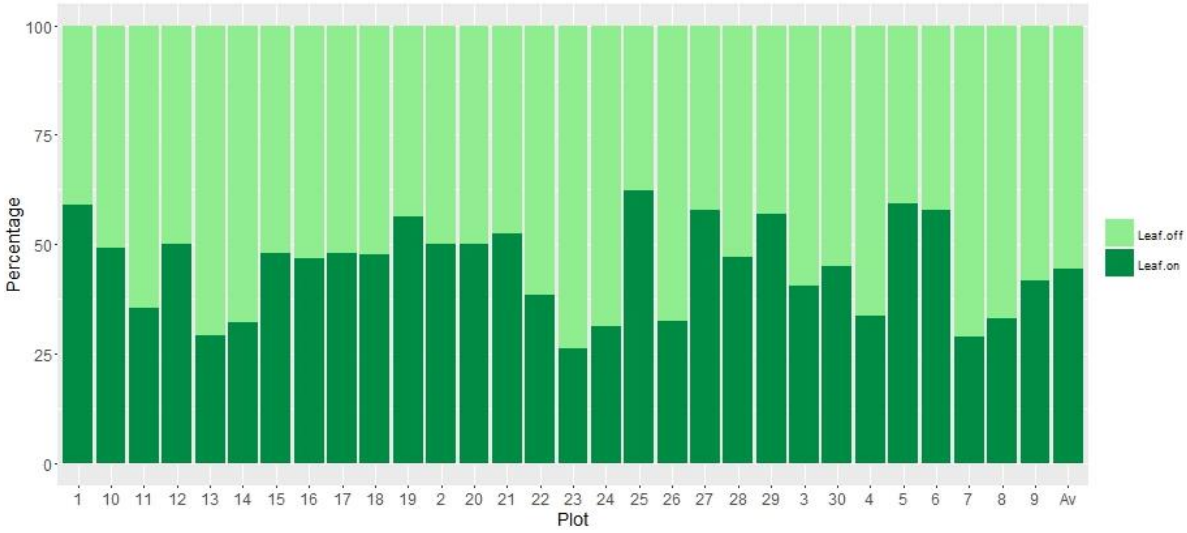

Figure 7. Relative proportions of return numbers from each dataset, separated by plot number. The last bar relates to the average across all plots.

Before any further processing could take place a preliminary filtering of outliers and classification of the ground was undertaken. LiDAR outlier points were identified as points below the true ground surface and significantly above the vegetation canopy. These errors may be caused by recording inaccuracies in the IMU or due to some laser pulses being reflected between a number of surfaces before returning to the sensor. This causes a time delay, which then means an inaccurate range distance is calculated (Watt, 2005). If these points remained the LiDAR returns from each survey would have a wide vertical range containing false features significantly affecting the performance of ground classification algorithms.

A multi-step macro was written in TerraScan to undertake this initial filtering of outlier points and classification of a ground surface (see Table 5 page 48). This macro was run initially on a flight line by flight line basis for each dataset. This is so relative alignment between flight lines could be

assessed through spatial analysis of the flight strip ground models per survey and corrected where necessary. It was then run over each dataset as a whole to create a seamless ground model.

Step	Overview
1. Classify returns to a default point class	Point classifications held in LiDAR returns are removed as classification varies between providers.
2. Classify low and isolated returns to an outliers point class	Enables erroneous points lower than the true ground to be removed from further analyses or ground classification. In order to avoid misclassifying acceptable LiDAR returns the procedure requires user inputted thresholds pertaining to distance and radius surrounding each point.
3. Classify ground returns	Described in detail in this section.
4. Classify outliers by distance from ground surface	Returns 5.5 standard deviations below the ground and returns above 50m were assigned to the outlier point class. Maximum tree height recorded in field was 45.5m so this eliminates high altitude outliers caused by weather influences or birds.
5. Assign remaining default points to vegetation point class	All returns remaining in the default class (those neither assigned to ground or outlier point classes) were classified as vegetation.

Table 5. A summary of the LIDAR filtering and classification macro.

Arguably the most important stage of the classification and filtering stages is the accurate classification of the ground. The ground model is a key element used when calculating tree height from the LiDAR data. TerraScan employs the progressive densification method (Axelsson, 2000; Axelsson, 1999) to classify a ground surface. The powerful algorithm is especially suited to the filtering of vegetation. It works by iteratively building a Triangulated Irregular Network surface model (TIN) based around determining a neighbourhood minima within a moving window of specified size. It is important that the area of the window will enclose at least one confident ground hit from a LiDAR return and therefore should be the maximum possible distance between LiDAR ground returns (which could be related to the maximum size of an above ground object within the dataset for example). The routine then builds up iteratively from the selected low points, adding new laser points, and is controlled by specified iteration parameters. These parameters describe

the iteration angle (the largest acceptable angle between points and the current TIN surface) and the iteration distance (the smallest allowable distance to each triangle node) (see Figure 8). When no further points remain within the iteration parameters the iterative process finishes and selected points are classified as ground.

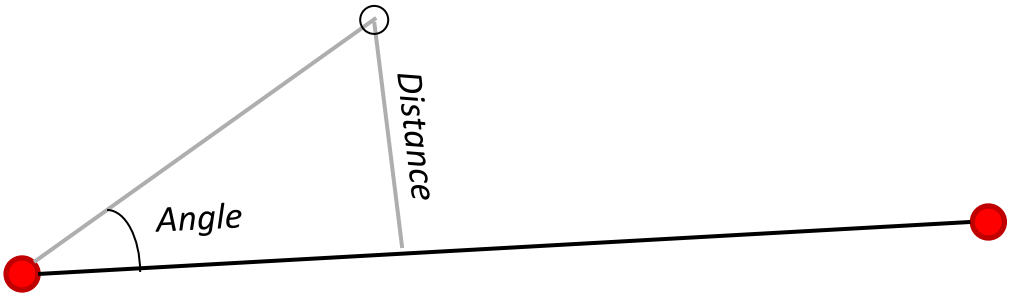

Figure 8. Iteration distance and iteration angle between candidate points (Soininen, 2016).

During ground classification the smaller the iteration parameters the less eager the routine is to iterate upwards through the point cloud which could be undesirable in hilly or mountainous terrain with steep terrain angles. As a result, the values describing the iteration parameters need to be considered in the context of the actual terrain and probable density of ground hits. As objects such as buildings will most likely be the largest obstacle to LiDAR ground hits, the maximum length and width of buildings in the survey area were considered as the input for the window size (15m). The decision to increase this a further 2m to 17m was taken so the chance of obtaining a true ground hit was increased, particularly in large areas of dense canopy. If the window size is too small points which actually fall on low vegetation or lower canopy layers risk being classified as 'ground' and can lead to an overestimation of the terrain surface (Kraus and Pfeifer, 1998; Zakšek et al., 2006; Hyyppä et al., 2005; Hollaus et al., 2006). This value was not increased any further amid concerns that it would compromise the quality of an interpolated DTM. To further control the iteration process and prevent artificial terrain gradient the routine offers an input for terrain angle which was taken as 50°. This was based on previous terrain measurements collected in the field (Landy, 2011). The

iteration distance was set as 1.4m and angle set as 6°, parameters suitable for the sloping but not hilly terrain of Chopwell Woodland Park.

Once a ground classification had been obtained for each flight strip it allowed for further filtering routines which rely on filtering by distance from ground surface. Often during this initial filtering and classification some erroneous returns remain classified as ground. These can be easily identified after the macro has completed by visual assessment of the TIN (see Figure 9). Additionally, some high outlier points are often misclassified as vegetation (see Figure 9). To fix these issues and improve the quality of the classification both datasets were manually checked throughout and any misclassified LiDAR reclassified.

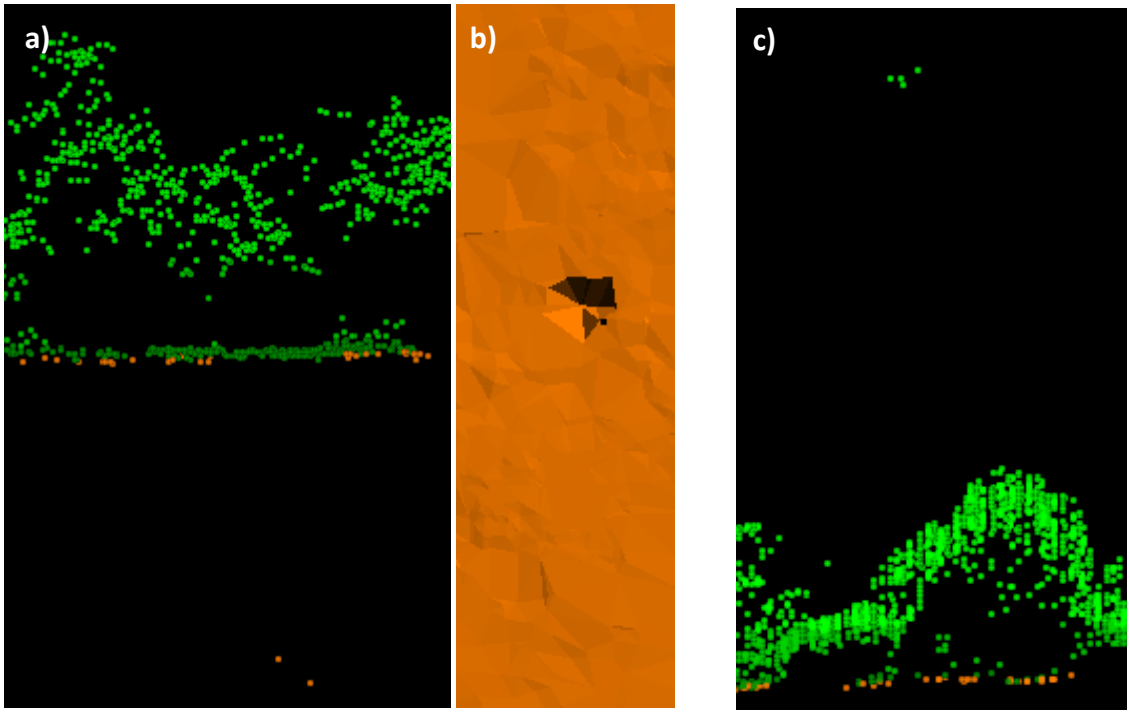

Figure 9. a) Spurious low LiDAR returns incorrectly classified as ground (brown points). b) Incorrectly classified ground points easily identified by spiked depressions in the ground model. c) A return from a bird incorrectly classified as vegetation (green).

After achieving a preliminary ground surface for each flight strip an assessment of the relative and absolute alignment of the LiDAR flight strips and datasets was possible. Due to the strip-wise

acquisition of LiDAR surveys, any systematic errors can affect the coordinate offsets for each strip separately. Existence of systematic errors in airborne LiDAR data has been acknowledged by both users and data providers. These errors can be attributed to the individual components of the data acquisition system (GPS, INS, and rangefinder systems) as well as to their integration. With two surveys and multiple flight strips it was important at the beginning to identify and solve any relative alignment issues between flight strips caused by systematic errors in the LiDAR system. If left in the dataset these systematic errors can degrade the accuracy of the laser footprint and create offsets between overlapping strips of data (Ma et al., 2014). Initial quality control comments provided by the NERC ARSF identified some misalignment between flight strips in the 2011 leaf-off survey potentially up to 7cm. Visual analysis of the 2009 leaf-on LiDAR data (see Figure 10) also identified flight strips misalignment in this survey.

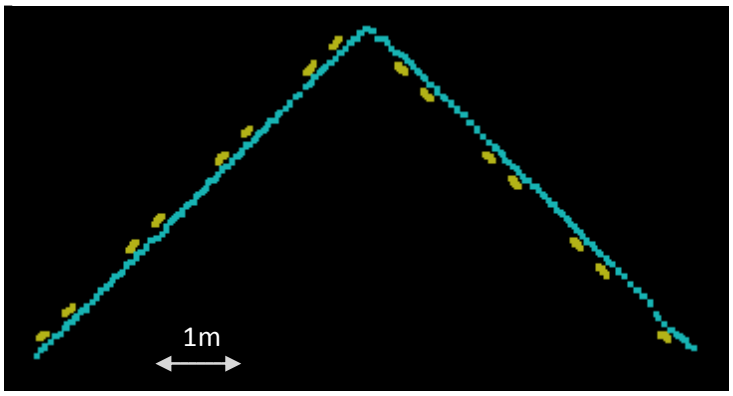

Figure 10. Misaligned LiDAR flight strips (each flight strip coloured differently) from the 2009 LiDAR dataset. This cross section is through a pitched roof.

TerraSolid's TerraMatch software was chosen to automate the assessment and solving of misalignment in height between flight strips for each survey individually. The 'find match' command utilises a triangulated model from the classified ground returns per flight strip and compares any overlapping ground surfaces. Any observed differences in gradient are translated into a constant elevation correction value for each flight strip which TerraMatch can also apply. Though further matching algorithms exist, the TerraMatch software was freely available to the author and has been

utilised and recommended by studies as being suitable for the removal of discrepancies between LiDAR flight strips (Shi and Shi, 2011).

After this initial classification and flight strip alignment the filtering and classification macro was run once more. There were a few modifications: all but points in the outlier class were classed to default to begin the macro and the macro was run over the whole dataset so that the ground classification would not be not limited to each flight strip but seamless between the flight strips of a survey. Omitting outliers ensured they were not misclassified as ground or vegetation. Additionally, they were not able to have an adverse effect on the ground classification routine.

4.3.2 Correction of Absolute Accuracy

Taking steps to correct the misalignment between LiDAR flight strips solves any relative accuracy discrepancies. To correct the absolute accuracy, or the accuracy of each survey's point cloud with reference to its' true location, comparison to ground truth data is necessary. At this point during processing only the 2009 survey data had been checked for absolute accuracy by the provider. The data were assessed in x, y and z against 89 ground control points and vectors manually drawn from these points describing road markings identifiable in the LiDAR intensity data. Though the 2009 survey had been analysed against Ordnance Survey vectors before delivery, no correction to the absolute accuracy was applied. The notation provided by the NERC ARSF found no misalignment in easting or nothing but identified that a correction to height may need to be undertaken. To facilitate the standardisation of the two surveys to one another, they were overlaid for visual analysis (see Figure 11 page 53). Through taking cross sections over rigid structures such as roads and buildings and viewing the intensity data it became clear that the surveys aligned in easting and northings but were consistently misaligned in height. As steps had been taken to ensure the 2009 survey was correct for absolute accuracy the entire 2011 survey underwent a transformation which 'shifted'

the data +14cm in height to align with the former. Omitting any discrepancies in x, y and z between the two surveys lessens the possibility that differences identified in metrics derived from each LiDAR dataset are due to absolute accuracy error (Vepakomma et al., 2008).

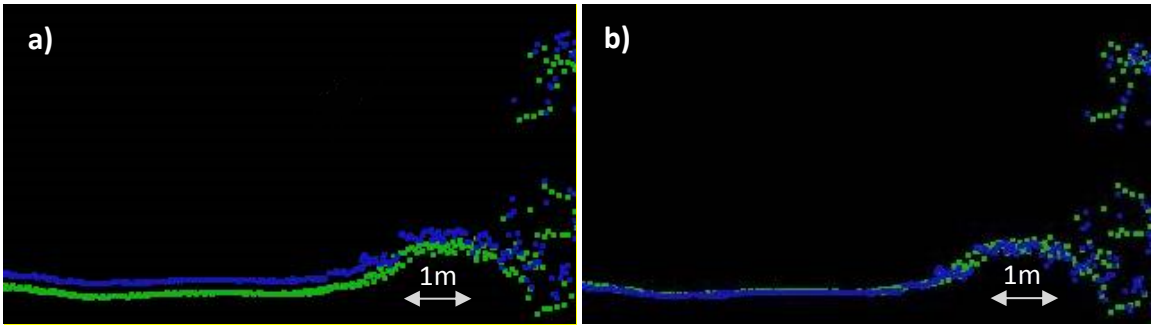

Figure 11. Cross section through the LiDAR data over a road and soft verge. a) Vertical misalignment present between the two LiDAR surveys (green is the 2011 leaf-off survey, blue is the 2009 leaf-on survey). b) after correction.

4.3.3 LiDAR Data Management

4.3.3.1 Clipped Las Files

Due to the way the LiDAR data had been processed in TerraScan the data from each survey was in a tiled format. Though any LiDAR data collected from forest surrounding the sample plots was vital during the triangulation of the ground classification algorithm at this stage it was deemed superfluous. For ease of management each survey point cloud was clipped to the 30 circular sample plots via shapefiles delineating their boundaries. This resulted in 60 LAS files, two for each sample plot. Each circular las file held an elevation with reference to the OSGB36 Newlyn datum. This reference elevation is useful for comparison of the interpolated ground models created from each dataset, as elevation differences between these would highlight changes in the penetrability of the canopy and understorey vegetation.

4.3.3.2 Normalising Canopy Height

In order to compare the structural diversity metrics between datasets collected at different dates, the standardisation of point heights is obligatory (Vepakomma et al., 2008). This standardisation was undertaken by creating normalised canopy heights from the original sample plots from each survey. This requires negating the height above Newlyn Datum provided by each plot's classified ground model to the las files for each associated plot. This resulted in each point holding an elevation above ground level instead of above the local datum with classified ground points holding a height of 0m.

4.3.4 LiDAR Derived Metrics

To assess and describe the empiracle diversity realtionships the LiDAR display with the field data, a large variety of variables were calculated from the LiDAR returns within each plot. These variables could be directly compared between surveys and plots due to the standardisation of each dataset.

The mean and percentile metrics described in Table 6 (page 55) were chosen to provide insightful summaries of the datasets which could be compared between leaf-on and –off datasets and within plot types to better understand the pulse penetration between datasets. The diversity metrics described in Table 6 page 55 (indicated with a *) were specifically chosen as metrics well suited to model tree size diversity in the field plots based on existing studies discussed in section 2.4.1. SD, skewness, kurtosis and CV of the height distribution of returns in each plot provide a summary of canopy structure based on the shape and dispersion of the distribution (Donoghue et al., 2007). Additionally, L-CV of canopy return heights was chosen to provide a diversity statistic less sensitive to skewness and small sample sizes. Laser-based height percentile ratios, utilised by Ozdemir and

Donoghue (2013), provide information about the diversity of vertical canopy layers and was shown to be a good estimator of stand based tree size diversity.

LiDAR return height derived metrics per plot	Reference
Mean	*mean*
25th percentile	*P25*
50th percentile	*P50*
75th percentile	*P75*
90th percentile	*P90*
99th percentile	*P99*
Coefficient of Variation	*CV**
Skewness	*skew**
Kurtosis	*kurt**
Standard Deviation	*SD**
Variance	*var**
The Coefficient of L Variation	*L-CV**
Ratio means of 99th and 25th percentiles	*P99/25**
Ratio means of 99th and 50th percentiles	*P99/50**
Ratio means of 99th and 75th percentiles	*P99/75**
Ratio means of 99th and 90th percentiles	*P99/90**

Table 6. LiDAR derived metrics calculated from each plot with the corresponding reference. * specifically indicates diversity metrics.

Metrics were derived from the clipped las files which had been normalised to height above ground rather than the local datum. Variables were calculated from returns which fell between 2m and 45m above the ground surface. Those hits with a height of less than 2m above the ground were excluded to eliminate the effects of understorey and terrain. This is a commonly used approach, utilised to help improve the quality of canopy height metric estimations (Næsset, 2002; Næsset and Bjerknes, 2001; Yu et al., 2004b; Hudak et al., 2008). Heights above 45m were excluded as these were unlikely to be hits from vegetation, being significantly higher than the tallest trees recorded in the field data.

4.4 Further Analysis

In order to assess the relationships between field and LiDAR derived diversity Ordinary Least Squares regression analysis was undertaken using field derived diversity variables as dependant variables and LiDAR derived diversity metrics as independent variables.

4.4.1 Testing Regression Assumptions

In total ten models were constructed using independent variables from one LiDAR dataset at a time and a combination of the two where appropriate. Most statistical tests rely upon certain assumptions about the both the dependant and independent variables used that need to be fulfilled. When these assumptions are not met this may lead to less trustworthy conclusions through over- or under-estimation of statistical significance (Weisberg, 2005).

In order to assure the validity of each model the following assumptions should were endeavoured to be adhered to:

1. **Independent and dependant variables should be normally distributed**.
2. If one expects a valid t-test and F-test result (which in this study we require to directly compare models between surveys) then **the residuals from the regression models need to be normally distributed.**
3. **The residuals should display homogeneity of variance** as if the model is well fitted there should be no pattern to the residuals plotted against the fitted values.
4. **The independent variables should not show strong linear relationships to one another.** If there is a perfect linear relationship between two (collinearity) or more (multicollinearity) independent variables the estimates for a regression model cannot be uniquely computed.

5. **The independent variables should show a strong linear relationship with the dependant variable**. If this assumption is violated, the linear regression will try to fit a straight line to data that does not follow a straight line
6. **The regression model should be correctly specified and not omit important relevant variables** that could better describe the variance in the dependant variable. Additionally, if irrelevant variables are included in the model the common variance they share with included variables may be wrongly attributed to them directly affecting estimation of regression coefficients.

Each assumption will be tested statistically and graphically. Though avoided wherever possible, selected models violated one or more of these assumptions. These regressions were undertaken using the Robust Standard Errors method rather than the Ordinary Least Squares method, a regression method designed to not be overly affected by violations of the aforementioned assumptions. The following subsections will summarise the statistical and graphical tests undertaken and provide example test results and graphics from these, the full set can be found in the Appendices.

4.4.1.1 Assessing variables for normality

During regression model construction it became clear that some predictor variables exhibited evidence for non-normality and curvilinearity. Variables with a non-normal distribution can distort relationships and significance tests so those showing evidence for non-normality were transformed to correct this (see Table 7 page 58). Normality was assessed visually against a reference 'normal' distribution and by statistically testing the skewness and kurtosis for normality. For example, kurtosis from the leaf-on dataset displayed a divergence from a normal distribution through visual analysis (see Figure 12 page 58). When analysing the relationship between leaf-on kurtosis and

other diversity variables (see Figure 13 page 59) leaf-on kurtosis displayed a curvilinear correlation with many other variables.

Leaf-on/-off Variable	Transformation
Kurtosis	Log
P99/25	Inverse
P99/50	1/square
P99/75	1/cubic

Table 7. Summary of each transformed variable

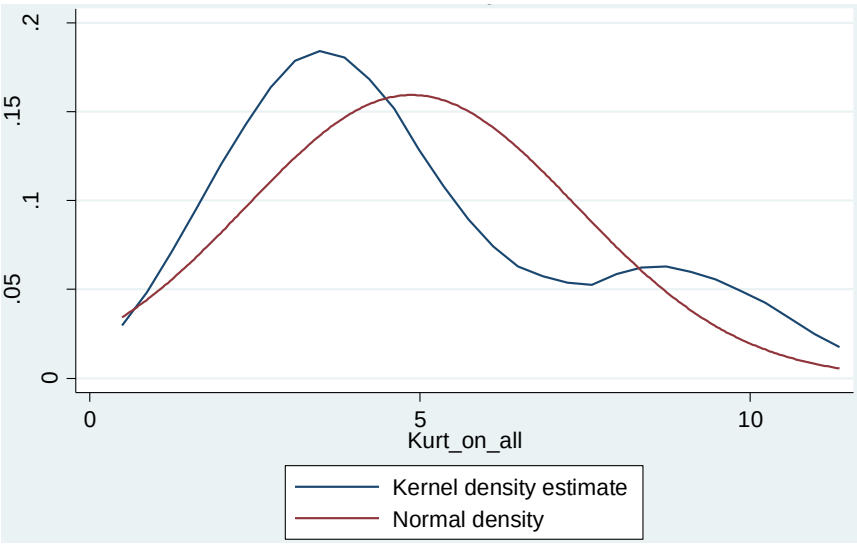

Figure 12. The density distribution of leaf-on kurtosis (blue) plotted against a "normal" distribution (red).

After a log transformation of leaf-on kurtosis the distribution greatly improved and no longer significantly diverged from a normal distribution (see Figure 14 page 60). Not all variables required a transformation and for those that did the simplest and easiest to conceptualise transformation was chosen. Table 7 summarises the variables that were transformed and Appendix 1 gives further detail. The same variables from each survey often shared similar distributions and so to maintain continuity the same transformation was applied. Most of the variables that required transformation were transformed using as low a complexity transformation function as practical however P99/50

and P99/75 underwent a slightly more complex transformation in order to meet normality requirements.

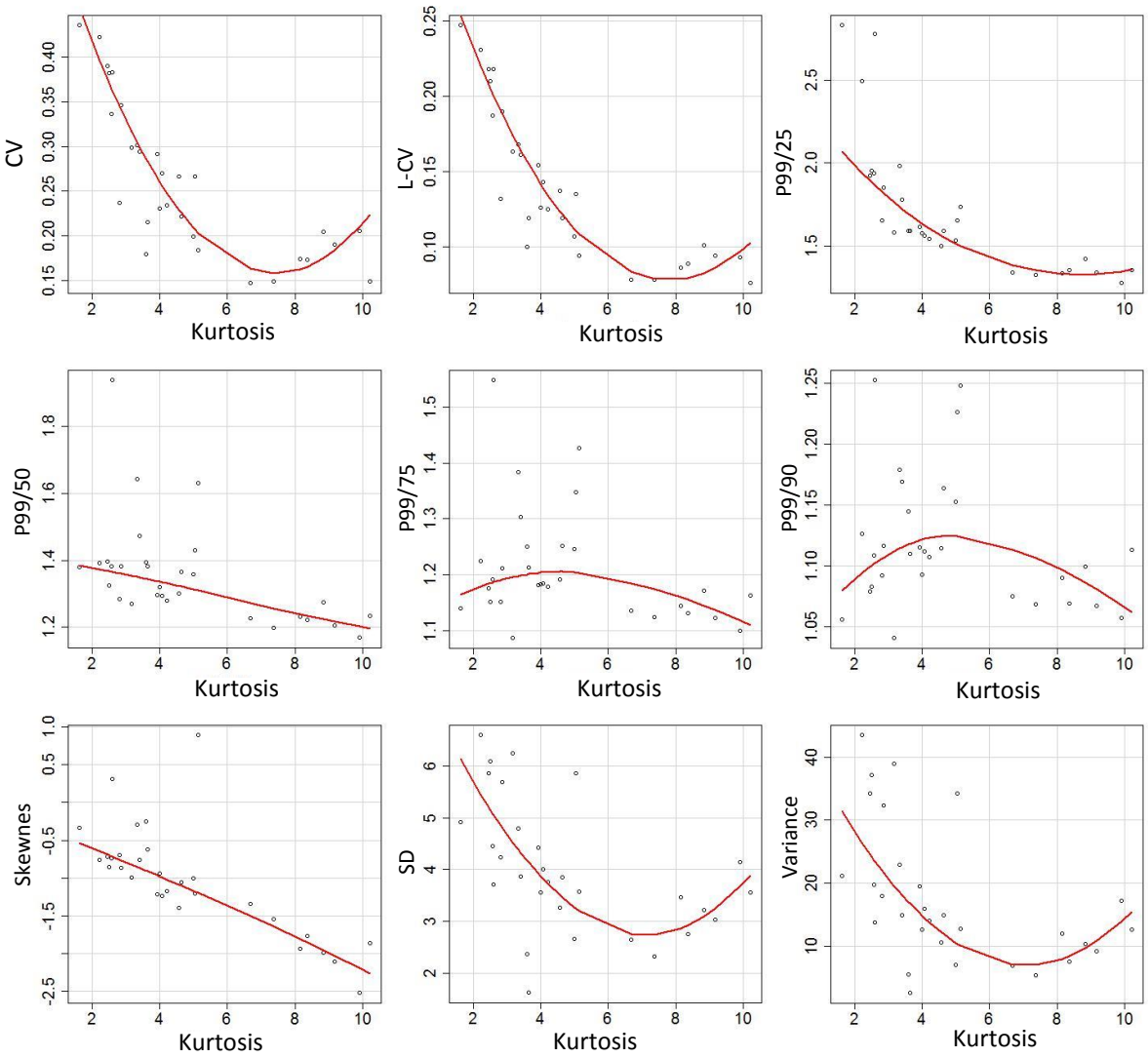

Figure 13. Correlations between leaf-on kurtosis and other leaf-on variables with a smoothed line.

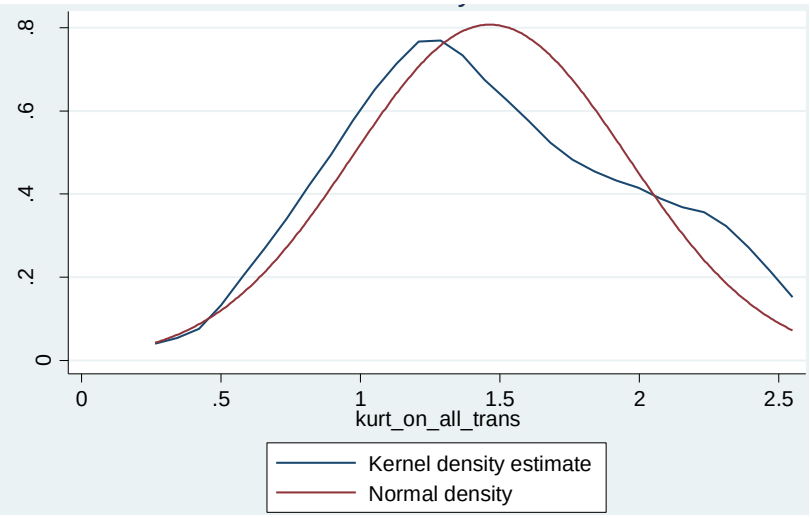

Figure 14. The density distribution of log transformed leaf-on kurtosis (blue) plotted against a normal distribution (red).

4.4.1.2 Assessing residuals for normality

To test the normality of the distributed residuals from each constructed model the density distributions were plotted for comparison against a reference normal distribution. In addition, a quantile plot (a plot of the ordered values of one or more variables against the quantiles of a uniform distribution for the same number of values) was created for each model. Confidence bounds have been added at the 95% interval so the reader can interpret the plot with greater ease (examples for Models 1 and 2 are shown in Figure 15 page 61).

The statistical test for normality based on skewness and kurtosis was also undertaken on each models' residuals where a significant result (< 0.05) rejects the null hypothesis that this variable is normally distributed (see Table 8 page 61). The skewness and kurtosis normality results were assessed alongside the graphical representations to judge normal or none normal distributions.

The distributions of residuals for most models created (including Model 2 shown as an example in Figure 15 page 61 and Figure 16 page 62) show little or no statistically significant evidence for non-

normality. Model 1 displays evidence for non-normality in kurtosis of the density distribution and the statistical analysis of the kurtosis (value of 0.03<0.05). The quantile plot shows residuals for Model 1 fall outside of the confidence bounds so this model was constructed using Robust Standard Errors.

Model 1 $THdiv = 0.233905 - 0.090259\log(Kurt_{lon}) + 0.003075Var_{lon}$

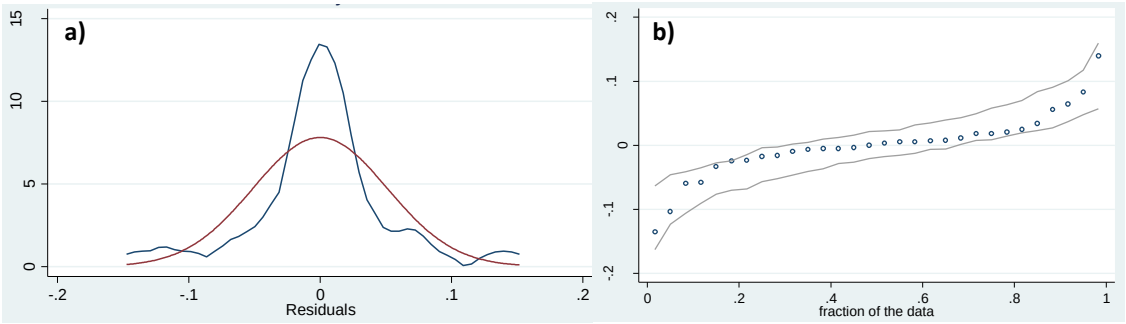

Model 2 $THdiv = 0.233218 - 0.091749\log(Kurt_{loff}) + 0.003367Var_{loff}$

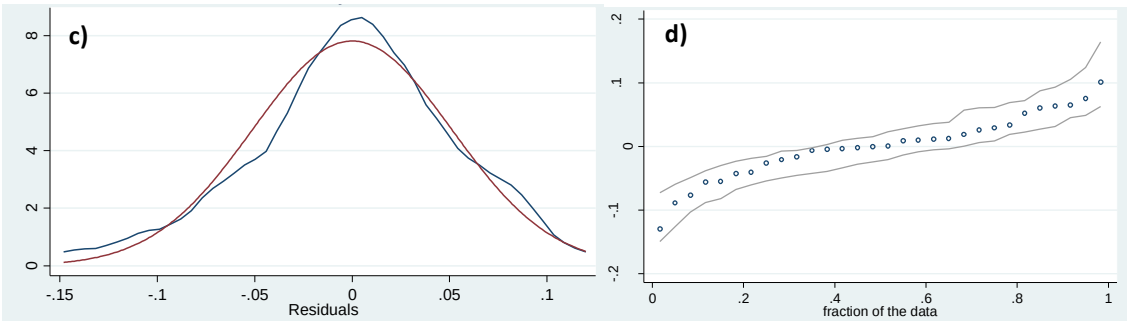

Figure 15. Example density plots and quantile plots from two models. The density plots (a and c) show the residual density distribution (blue) alongside a normal distribution (red). The quantile plots (b and d) show residuals (circles) within normality confidence bounds (lines).

	Skewness test result and indication of normality	Kurtosis test result and indication of normality
Model 1	Result: 0.87 Indicates normal skewness	0.03 Indicates none normal kurtosis
Model 2	0.35 Indicates normal skewness	0.49 Indicates normal kurtosis

Table 8. Results of the skewness and kurtosis normality tests. A value < 0.05 indicates none normality.

4.4.1.3 Testing Homogeneity of Residuals

To assess homogeneity of residuals the residuals from each model were plotted against the fitted values from the same model. Points on this plot are expected to be randomly distributed around the reference line (y=0). Any noticeable pattern in the data such as a narrowing to either side, towards the centre or a curvilinearity would indicate heteroscedasticity of residuals (see an example in Figure 16). There are also inferences from the Breusch and Pagan (1979) test and the Cameron and Trivedi (1990) White's test – where in both a p value <=0.05 indicates a rejection of the null hypothesis that the variance of the residuals is homogenous and accepting the alternative hypothesis that the variance is not homogenous (see Table 9).

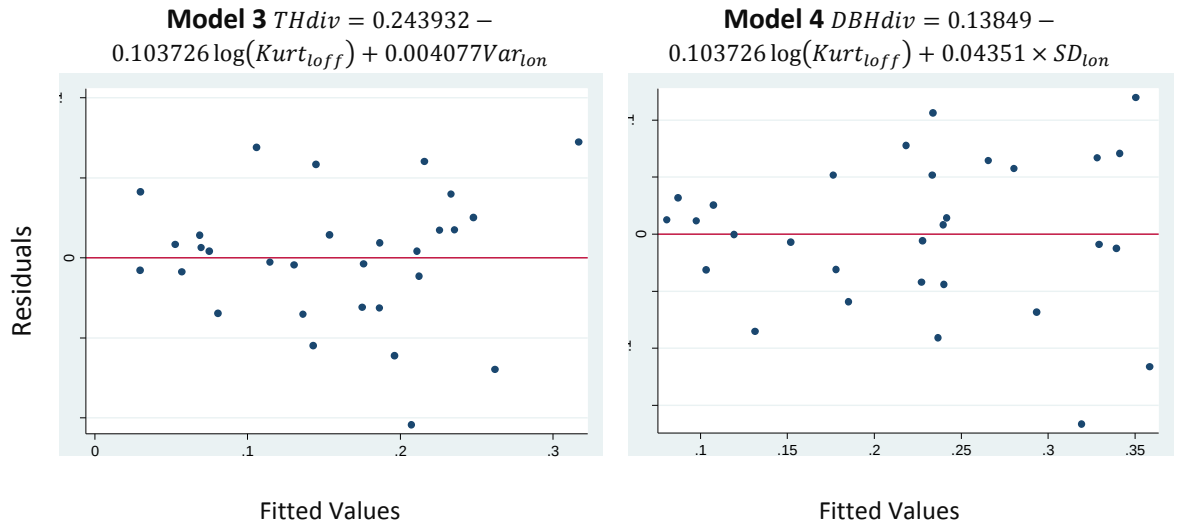

Figure 16. Plot of residuals against fitted values for models 3 and 4

	Model 3	*Model 4*
Breush-Pagan test	*p*=0.05	*p*=0.01
White's test	*p=0.09*	*P=0.38*

Table 9. The resultant *p*-values of the Breusch-Pagan and White's tests for models 3 and 4

Model 3 (see Figure 16 and Table 9) is an example of a model showing slight statistical evidence of heteroscedasticity but little graphically significant evidence with a relatively random point

distribution and *p*-values only just over 0.05. Conversely model 4 shows some graphical evidence for non-homogeneity with a widening of the point distribution from y=0 as fitted values increase and statistically significant evidence of heteroscedasticity through acceptance of the Breush-Pagan test's alternative hypothesis.

4.4.1.4 Avoidance of Collinearity and Multicollinearity and Correct Specification of Models

	Model	VIF	Link test *p*-value	RESET *p*-value
1	$THdiv = 0.234 - 0.090\log(Kurt_{lon}) + 0.003Var_{lon}$	1.43	0.21	0.22
2	$THdiv = 0.233 - 0.092\log(Kurt_{loff}) + 0.003Var_{loff}$	1.34	0.43	0.38
3	$THdiv = 0.245 - 0.104\log(Kurt_{loff}) + 0.004 \times Var_{lon}$	1.08	1.68	0.30
4	$DBHdiv = 0.139 + 0.087Skew_{lon} + 0.044SD_{lon}$	1.43	0.42	0.78
5	$DBHdiv = 0.791 + 0.103Skew_{loff} + 0.048SD_{loff} - 0.576P99/90_{loff}$	1.58	0.88	0.71
6	$DBHdiv = 0.115 + 0.004Var_{loff} + 0.064Skew_{loff} + 0.433CV_{lon}$	1.25	0.36	0.60
7	$CLdiv = 0.285 + 0.065Skew_{lon}$	N/A	0.63	0.97
8	$CLdiv = 0.35 + 0.568\frac{1}{P99/75_{loff}{}^3} - 0.892\frac{1}{P99/50_{loff}{}^2} + 0.002Var_{loff}$	6.60	0.89	0.67
9	$CWdiv = 0.267 - 0.051\log(Kurt_{lon})$	N/A	0.72	0.60
10	$CWdiv = 0.286 - 0.061\log(Kurt_{loff})$	N/A	0.70	0.84

Table 10. Equations for constructed models (values all to 3 decimal places) and outputs of tests for model specification: inflation factor, RESET and Link Test p-values

The Variance Inflation Factor (VIF) was calculated for independent variables from each model. This assesses whether the variance of the coefficient estimate is being inflated by multicollinearity (O'brien, 2007). The values shown in Table 10 are well below the level acceptable for multiple regression (which should be approximately 10 at the most (StataCorp., 2013)). As some models only contain one independent variable this test is not applicable in these cases. The Link Test (Pregibon, 1979) tests model specification and assesses the hypothesis that no further independent variables could have a significant influence within the model except by chance. An insignificant *p*-value greater than 0.05 would indicate the test has failed to reject the assumption that the model is

specified correctly. The RESET, or Ramsey (1969) regression specification-error test for omitted variables is similar to the Link Test and an insignificant *p*-value greater than 0.05 would indicate the test has failed to reject the assumption that the model has no omitted variables. Table 10 (page 63) demonstrates that all statistics from these tests indicate no statistical probability of problems of multicollinearity, collinearity and misspecification (omitted key variables) in any of the models.

4.4.1.5 Assessing the Linearity of Relationship between Independent and Dependant Variables

To assess the linearity of the relationship between the independent and dependant variables, augmented component-plus-residual plots (also known as an augmented partial residual plots) as described by Mallows (1986) were constructed (see Figure 17 as an example of these from model 8). The plots for each independent variable against the model's dependant variable also include a line of best fit and locally weighted smoothing to aid in the reader's interpretation. If the smoothed line differs substantially from the line of best fit it indicates a non-linearity between a dependant and independent variable. None of the relationships between dependant and independent variables in any of the models showed concerning non-linearity.

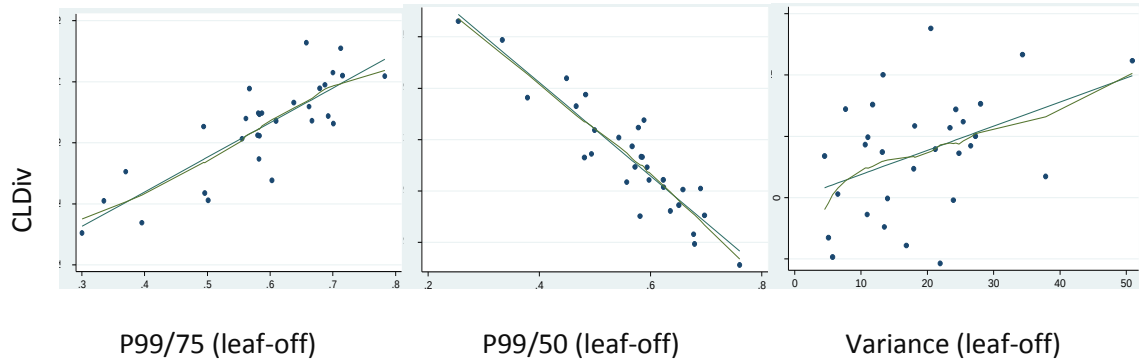

Figure 17. Augmented component-plus-residual plots for all independent variables in Model 8 describing CLdiv

5. RESULTS AND ANALYSIS

5.1 Field Data

Field data collected in 2013 were combined with field data collected from Ozdemir and Donoghue (2013) to provide a comprehensive dataset describing the tree assemblages in each plot. Table 12 page 66 demonstrates that 16 of 30 field plots are deciduous dominated (where deciduous tree species accounted for ≥90% of total species type), four plots are evergreen dominated (where evergreen coniferous tree species accounted for ≥90% of total species type) and the remainder are mixed. Stem density per hectare ranges from 151 to 2917 and there are 11 discreet dominant tree species.

Table 11 shows the ranges between minimum and maximum values for all diversity metrics are large with THdiv having a particularly large range. CWdiv does not seem very varied despite the mix of evergreen and deciduous tree types in the study.

	Minimum	**Maximim**	**Mean**	**σ**
THdiv	0.022	0.389	0.156	0.086
DBHdiv	0.046	0.470	0.224	0.109
CLdiv	0.094	0.408	0.218	0.072
CWdiv	0.103	0.375	0.192	0.057

Table 11. Summary statistics of tree size diversity indices for the 33 survey plots.

Plot	No. of Trees	Trees per Hectare	Planting Year	Primary Species	Assemblage	Min. TH	Max. TH	Mean TH	THdiv	DBHdiv	CLdiv	CWdiv
1	21	525	1908	Sycamore	**Mixed**	4.6	39	19.84	0.276	0.33	0.277	0.177
2	55	438	1963	Birch	**Mixed**	5	30.5	17.2	0.201	0.338	0.235	0.227
3	51	1275	1985	Japanese Larch	**Deciduous**	5	25.6	17.38	0.126	0.147	0.207	0.195
4	56	1400	1980	Corsican Pine	**Mixed**	2.6	24.6	14.61	0.175	0.228	0.213	0.207
5	11	275	1954	Japanese Larch	**Deciduous**	18	25.2	22.88	0.048	0.046	0.172	0.103
6	21	525	1949	Oak	**Deciduous**	4.4	27.2	19.12	0.155	0.196	0.185	0.157
7	34	567	1944	Beech	**Deciduous**	12.2	24.4	19.85	0.088	0.146	0.16	0.127
8	60	1000	1924	Beech	**Deciduous**	14.9	26.7	21.8	0.079	0.145	0.148	0.193
9	15	375	1943	Japanese Larch	**Deciduous**	23.7	28	24.83	0.022	0.072	0.116	0.143
10	21	525	1943	Japanese Larch	**Deciduous**	8.2	26.8	18.47	0.192	0.242	0.212	0.182
11	30	750	1920	Scots Pine	**Evergreen**	10.1	22	19.24	0.061	0.119	0.107	0.132
12	175	2917	1984	Douglas Fir	**Evergreen**	8.3	27.3	18.53	0.112	0.248	0.276	0.189
13	35	875	1908	Acer/Birch/Douglas Fir	**Mixed**	4.6	23.4	13.48	0.215	0.34	0.318	0.236
14	54	900	1923	Beech	**Deciduous**	9.7	26.8	16.66	0.196	0.32	0.337	0.375
15	19	475	1969	Scots Pine	**Mixed**	12.5	25.5	20.26	0.076	0.119	0.149	0.18
16	13	325	1954	Japanese Larch	**Deciduous**	12.2	26.8	22.29	0.103	0.153	0.121	0.112
17	26	650	1947	Oak/Japanese Larch	**Mixed**	4.8	23.3	17.21	0.168	0.222	0.218	0.16
18	22	550	1963	Scots Pine	**Evergreen**	7.8	23.5	19.36	0.083	0.093	0.094	0.122
19	29	725	1943	Birch/Acer/Oak	**Deciduous**	6.6	21.9	14.8	0.172	0.256	0.167	0.21
20	14	350	1925	Ash	**Deciduous**	15.6	33.6	25.49	0.135	0.185	0.209	0.152
21	19	151	1942	Oak	**Deciduous**	2.8	27.4	18.18	0.243	0.225	0.26	0.197
22	23	575	1907	Holly	**Mixed**	1.9	37	15.32	0.389	0.47	0.408	0.3
23	11	275	1910	Beech	**Mixed**	29.7	39.1	34.05	0.046	0.133	0.191	0.252
24	12	796	1908	Douglas Fir	**Mixed**	3.2	36.2	22.19	0.231	0.296	0.32	0.218
25	11	275	1934	Japanese Larch	**Deciduous**	5.5	31.9	20.82	0.273	0.327	0.233	0.208
26	11	275	1988	Beech	**Deciduous**	7.9	31.9	18.81	0.203	0.285	0.257	0.217
27	14	350	1942	Ash	**Deciduous**	4.5	25.6	14.53	0.273	0.412	0.263	0.262
28	22	1947	1980	Birch	**Deciduous**	7.2	15.4	12.02	0.101	0.126	0.23	0.161
29	24	600	1947	Beech	**Mixed**	6.8	31.6	15.58	0.253	0.395	0.247	0.23
30	15	375	1969	Corsican Pine	**Evergreen**	18.3	24.8	22.47	0.071	0.109	0.212	0.149

Table 12. A summary of the ground truth measurements collected in the field and the resultant diversity metrics (L-CV). Also shown are the inferred plantation dates from the Forestry Commission Compartmental Database (Forestry-Commission, 2013). The planting years included in this table are generalised and mostly do not take into account any restocking practises which have occurred. Regardless they are included as additional information to provide the initial plantation year of each stand.

Table 13 shows that evergreen coniferous plots are the least represented (only 4 plots), most densely planted (average of 1148 trees per hectare) and have the lowest tree size diversity metrics (0.082 to 0.148) and lowest species diversity (on average 2 species per plot). Deciduous plots on the other hand are most prevalent (16 plots) and are the least densely planted plots (an average of 615 trees per hectare). Mixed plots have higher average diversity metrics than deciduous or evergreen plot types (0.194 to 0.287).

	Deciduous	Mixed	Evergreen
No. of Plots	16	10	4
Average Thdiv	0.151	0.194	0.082
Average DBHdiv	0.205	0.287	0.142
Average CLdiv	0.205	0.258	0.087
Average CWdiv	0.187	0.219	0.148
Average Tree Species per Plot	3	4	2
Average Trees per Hectare	615	661	1148

Table 13. A summary of the average diversity, tree species per plot and tree density variables by dominant tree type. The highest values are highlighted in red and the lowest in blue.

Figure 18 and Table 14 page 68 demonstrates there is a strong positive correlation (r = 0.90 significant at the 99% confidence interval (CI)) between the average tree height and DBH in this dataset. This differs between deciduous, mixed and coniferous plots (r values of 0.84, 0.99 and 0.91 respectively) but only deciduous and mixed plots show significant relationship. Plots 28 and 23 have the smallest and largest tree sizes respectively. Plot 28 was in a relatively new stand of Birch trees and 23 in a well established mixed plot of Beech, Corsican Pine and Sitka Spruce with all of the trees measuing taller than 29 metres. There is lateral spread of the plot positions away from the x y resulting in a loose distibution.

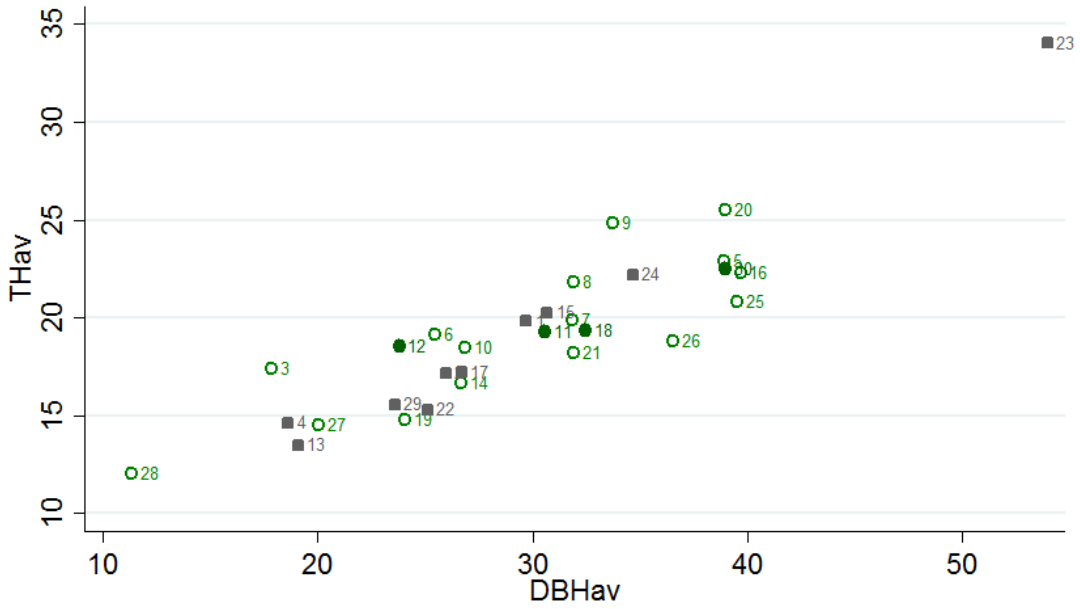

Figure 18. Scatter graph to show the relationship between the average DBH and Tree Height measured for each plot. Open circles represent deciduous plots, filled circles evergeen plots and squares mixed plots.

	TH Diversity	DBH Diversity	CL Diversity	CW Diversity
TH Diversity	1.00			
DBH Diversity	0.92	1.00		
CL Diversity	0.75	0.80	1.00	
CW Diversity	0.60	0.72	0.74	1.00

Table 14. Pearson's product-moment correlation (r) matrix of tree size diversity variables (all significant $p<0.01$)

Table 14 and Figure 19 page 69 demonstrate that a significant (99% CI) positive relationship (r=0.92) is shown between THdiv and DBHdiv in the dataset indicating increased diversity in tree height per plot is highly correlated to an increase in the DBH diversity. Evergreen plots display lower DBHdiv and THdiv than most of the mixed and deciduous plots and show no statistically significant relationship between THdiv and DBHdiv alone. The mixed and deciduous plots display greater relationships (r=0.92 and 0.93 respectively at the 99% CI) with deciduous plots 5 and 9 (both comprised of only Japanese Larch) displaying the lowest THdiv and DBHdiv and mixed plot 22 (located in ancient woodland) the highest.

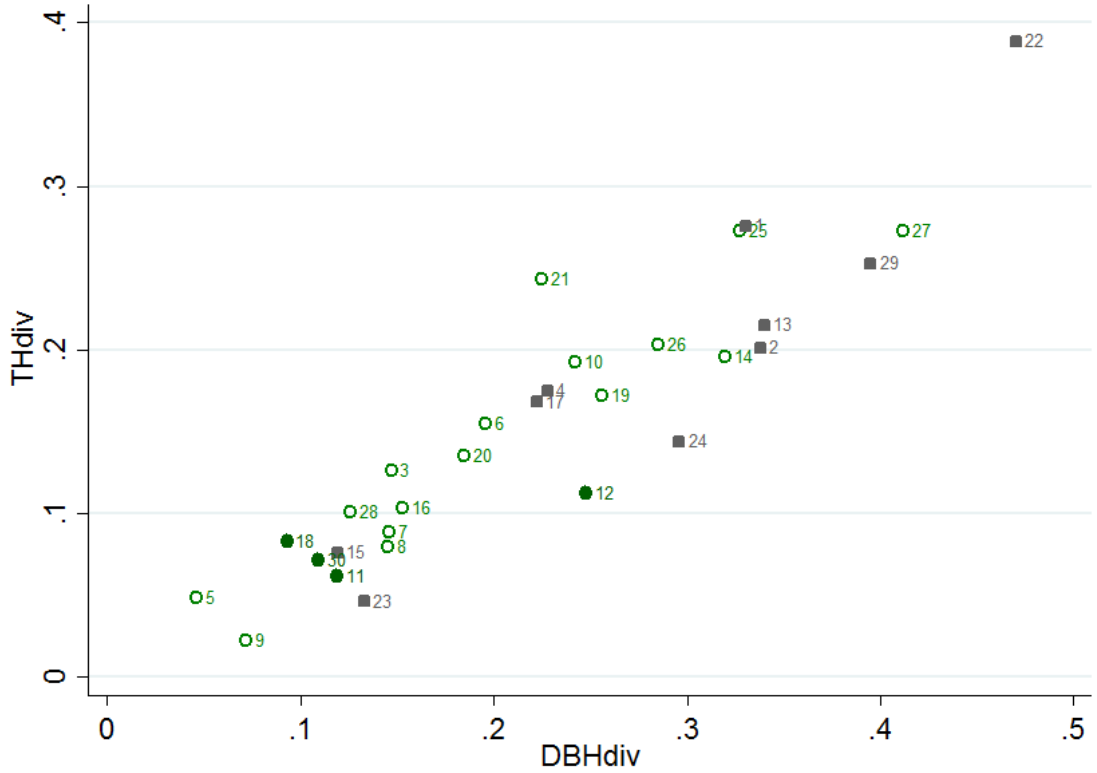

Figure 19. Scatter graph to show relationship between THdiv and DBHdiv. Open circles represent deciduous plots, filled circles evergeen plots and squares mixed plots.

The relationship between CLdiv and CWdiv shown in Figure 20 page 70 and Table 14 page 68 in evergreen plots is the strongest positive relationship with an *r* of 0.96 at the 99% CI. This is much stronger than the relationship across all plot types between these variables (*r* = 0.74 99% CI). Mixed plots show no statistically significant correlation between CLdiv and CWdiv. The correlation in deciduous plots has an *r* of around 0.81 at the 95% CI. Plots 22 and 14, mixed and deciduous plots display the highest CLdiv and CWdiv respectively.

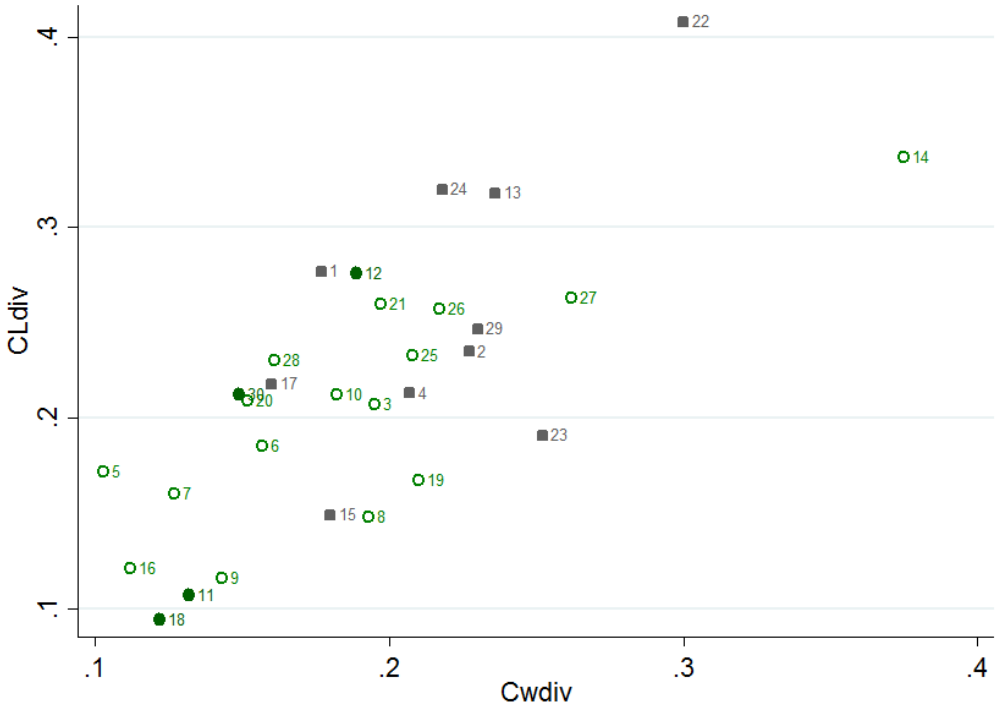

Figure 20. Scatter graph to show relationship between CLdiv and CWdiv. Open circles represent deciduous plots, filled circles evergeen plots and squares mixed plots.

When assessing which stand types would increase the structural diversity of the dataset in section 4.1.1.1 species diversity appeared to be a strong contributory factor (describing around 30% of the tree height variation at the 95% CI). Figure 21 page 71 shows that a small (r=0.39) but significant (90% confidence) correlation is still present with the additional plots added. However, when considering each plot type alone no statistically significant correlation is seen.

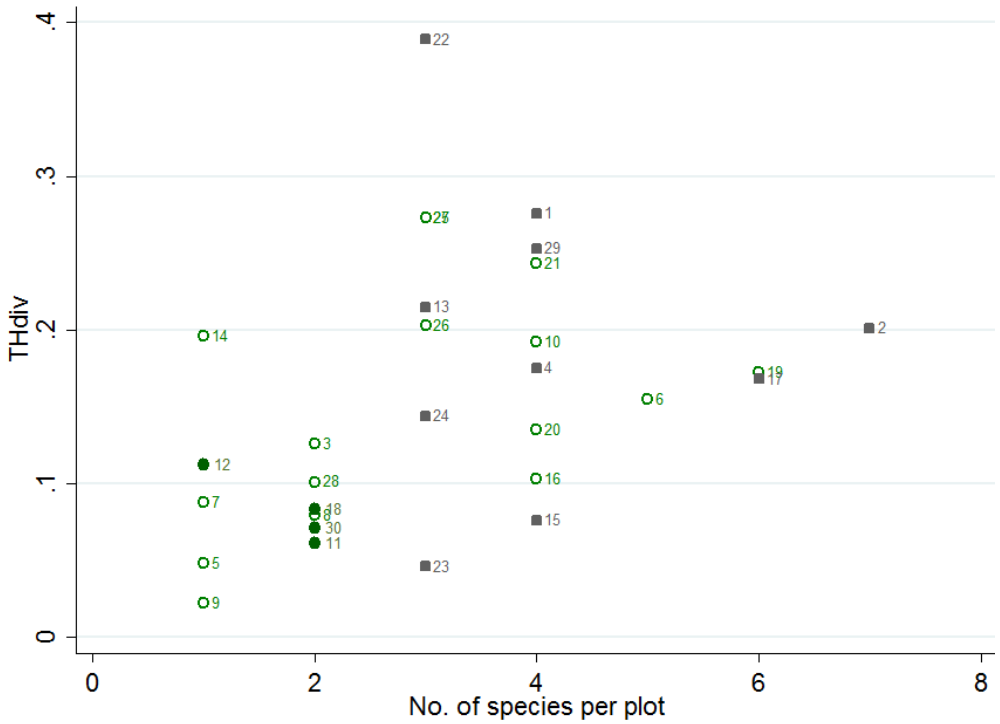

Figure 21. Scatter plot to show the relationship between species diversity and THdiv in each of the sample plots.

5.2 LiDAR Data

5.2.1 Initial LiDAR Dataset Observations

Clipped las files (see section 4.3.3.1 Clipped Las Files) were assessed first allowing the direct comparison of the distribution of returns throughout both datasets without any ground correction to the elevation. As described in section 4.2.3 Initial Assessment of the LiDAR Datasets ground returns may be overestimated depending on understorey conditions and so assessing the LiDAR before ground elevation correction eliminates this influence on the data.

Figure 22 (page 73) shows that though minimum and maximum return heights from the two surveys are similar in each plot, the leaf-off LiDAR dataset displays consistently lower minimum and higher maximum return height values than the leaf-on LiDAR dataset. The difference between the

maximum returns from leaf-on to leaf-off LiDAR datasets was 0.56-1.07 metres. The distribution of LiDAR returns in the leaf-off datasets are more skewed towards the ground, most obvious in the deciduous plots and less apparent in the evergreen plots with the exception of plot 12. Table 15 shows that upper return height percentiles (P75 and greater) are statistically significantly different between surveys for evergreen plots. The difference in height percentiles between leaf-on and –off LiDAR metrics in evergreen plots is likely a product of survey system configuration changes or capture differences rather than seasonal foliage changes. Therefore, applying a correction of the difference in metrics between leaf-on and leaf-off LiDAR datasets over evergreen plots to LiDAR metrics in deciduous and mixed plots may negate the influence of changing survey characteristics and growth. Corrected values show that in the mixed and deciduous plot percentiles (aside from P25 for deciduous plots and P90 for mixed plots) and the mean of return heights were lower under leaf-off conditions.

	Deciduous				**Evergreen**			**Mixed**			
	D		σ	Dcorr	D		σ	D		σ	Dcorr
P25	-0.86	A	2.241	-0.30	-0.56	B	0.52	0.22	A	2.15	0.78
P50	-0.35	A	0.782	0.20	-0.55	B	0.31	-0.10	A	1.44	0.45
P75	-0.25	A	0.526	0.45	-0.70	*A	0.25	-0.40	A	1.00	0.30
P90	-0.25	*B	0.462	0.46	-0.71	*A	0.28	-0.83	*A	0.94	-0.13
P99	-0.20	**B**	0.420	0.64	-0.84	**A	0.26	-0.66	*A	0.69	0.18
mean	-0.36	A	1.159	0.25	-0.61	B	0.41	-0.10	A	1.53	0.51

Table 15. A summary of the differences 'D' between percentiles and the mean calculated from the leaf-on and –off LiDAR datasets. A positive 'D' indicates that leaf-on metrics were that amount of metres higher than leaf-off metrics. A negative 'D' indicates that leaf-on metrics were that amount of metres lower than leaf-off metrics. 'A' indicates normally distributed variables that underwent a paired t-test. 'B' indicates non-normally distributed variables underwent the sign rank test. *=statistically significantly different at the 95% CI **=statistically significantly different at the 99% CI. Dcorr corresponds to the difference values corrected for the difference between surveys in evergreen coniferous plots. σ represents the standard deviation.

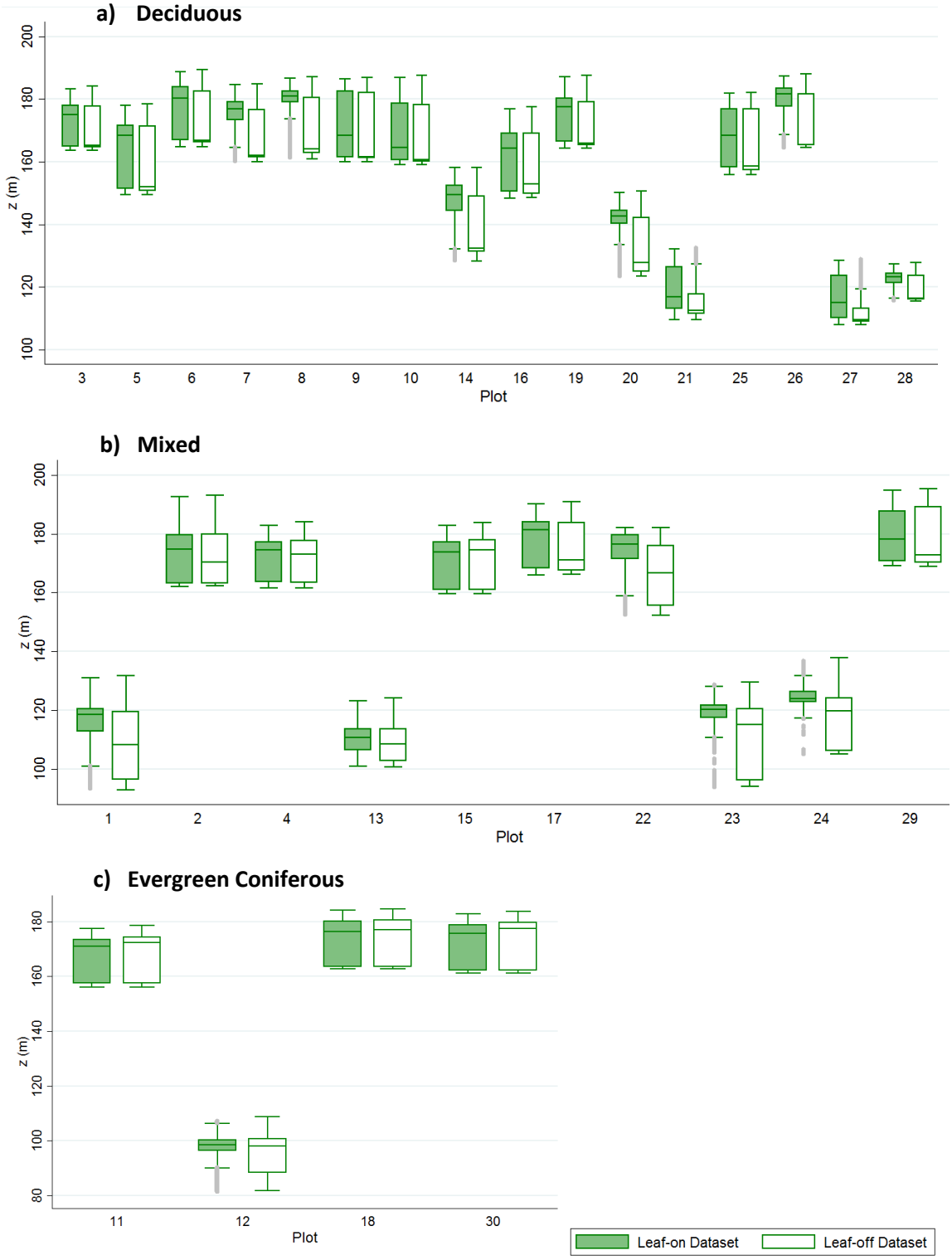

Figure 22. Box plots of LiDAR return heights. The whiskers of the box plot represent the range of values within 1.5 x the interquartile range and grey markings on each graph represent returns outside of these boundaries. a: Deciduous plots. b:Mixed plots. c: Evergreen plots.

5.2.2 Ground Classification

With tree growth, leaf loss, understorey growth and potential tree fall all occurring between surveys a feature that we can be sure will have stayed more constant is the topography beneath the vegetation. As mentioned in section 2.4 overestimation of the ground surface can be a problem through dense canopies. Table 16 page 75 presents an assessment of the significance of difference between the distribution of ground classified return elevation for each survey. The table shows the average of the ground classified heights is statistically significantly different between the two surveys. Leaf-on ground classified points in most (22) plots have a greater mean elevation than the leaf-off survey plots. This is not the case over all plots. Some plots (e.g. plot 24) have a statistically insignificant difference between average ground classification elevation and some plots display a negative difference between average ground classification elevation from leaf-off to -on indicating that the average leaf-off LiDAR ground classification elevation was lower than the leaf-on average ground classification elevation.

		Mean z (m nearest cm)		
	Plot	leaf-on	leaf-off	Leaf-on-Leaf-off
Deciduous	3	164.64	164.54	0.1**
	5	150.86	150.75	0.11*
	6	165.93	166.07	-0.14**
	7	161.49	161.34	0.15**
	8	163.07	162.86	0.21**
	9	161.26	161.14	0.12**
	10	160.13	160.01	0.12**
	14	130.65	130.84	-0.19**
	16	149.72	149.63	0.09**
	19	165.41	165.29	0.12**
	20	124.54	124.59	-0.05
	21	112.12	111.68	0.34**
	25	157.59	157.4	0.19**
	26	165.18	165.14	0.04**
	27	109.37	109.21	0.16**
	28	116.04	116.03	0.01
	Average	**147.36**	**147.28**	**0.08**
Mixed	1	96.03	96.01	0.02
	2	162.98	162.97	0.01
	4	163.03	162.94	0.09**
	13	102.16	101.97	0.19**
	15	160.57	160.55	0.02
	17	167.32	167.11	0.22**
	22	153.77	154.28	-0.51**
	23	95.59	95.75	-0.16*
	24	105.92	105.84	0.08
	29	170.24	169.93	0.31**
	Average	**137.76**	**137.74**	**0.03**
Evergreen	11	157.11	157.08	0.03
	12	N/A	N/A	N/A
	18	163.43	163.32	0.11**
	30	161.99	161.88	0.11**
	Average	**160.84**	**160.76**	**0.08**

Table 16. A summary of the mean height of the classified ground points in each sample plot. A t-test was undertaken to assess whether there was any bias in the ground height classifications between surveys. * indicates <0.05 p value. ** indicates <0.001 p value. No * indicates the difference between height distributions was not statistically significant.

When further assessing the distribution of ground returns in plot 22 (see Figure 23 page 76), with an average elevation of 153.8m for leaf-on compared to 154.3m from the leaf-off survey, a large difference between the density and the elevation range of ground returns between surveys is

apparent. This is also common to plots 23 and 14, which also display a significant negative ground difference. Conversely plot 6, again with a negative average ground elevation from leaf-on to -off, had a much more comparable ground point density (see Figure 23) and though statistically significantly different there is little visually detectable bias between ground classification elevation distributions.

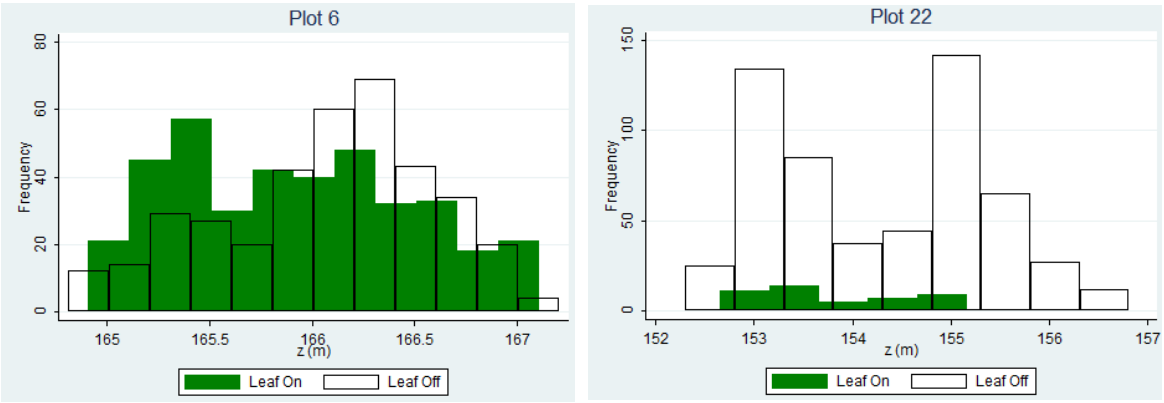

Figure 23. Histogram showing the height distribution of ground returns from both leaf-on and off datasets at plot 22 (left) and plot 6 (right).

Evergreen plots 18 and 30 (see Figure 24) displayed a significant positive difference between the ground classification elevations from the leaf-on to –off conditions.

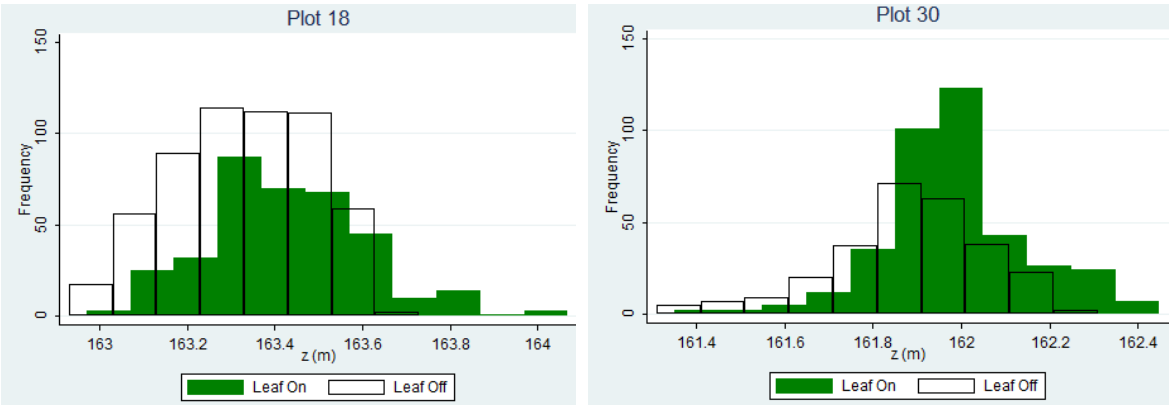

Figure 24. Histogram showing the height distribution of ground returns from both leaf-on and off datasets at plot 30 (left) and plot 18 (right).

5.2.3 First and Last Returns

Sections 5.2.1 and 5.2.2 describe initial observations gathered from each LiDAR dataset as a whole and the direct comparison between the two. This section looks in more detail at the differences between the first and last pulse penetration through the canopy. This is after normalisation to height above ground which makes the data easier to visualise and compare but will be influenced by the accuracy of the ground classification.

With reference to Table 16 page 75, the mean elevation of the first and single returns seem higher in the leaf-off than leaf-on dataset, hence the negative values displayed here, this is most apparent in the deciduous plots. When looking at the corrected maximum return heights (as corrected mean return heights stay constant) Table 16 shows that the largest differences in both return types is seen in deciduous plots (0.42m difference first and single returns, 0.91m difference last returns).

The mixed and evergreen plots show no statistically significant difference in the ability of the first/single and last pulses to penetrate through a leaf-on and –off canopy. This is in agreement with Figure 22 (page 74) where little difference is seen in the penetrability of LiDAR pulses in muti-temporal evergreen plots (aside from plot 12). However, the variable differences between pulse distributions in leaf-on –off in mixed plots shown in Figure 22 is not echoed in Table 16 page 75 by the grouped LiDAR returns.

To further explore the differences in more detail, visual analysis of a selection of plots was undertaken. The leaf-off first returns in plot 7 (see Figure 25 page 79), a deciduous plot primarily composed of Beech, intermittently hit the very lowest of the canopy layers, understorey and ground whereas a larger proportion of the leaf-on last returns reflect from within the canopy. A higher

proportion of first returns have penetrated lower through the canopy and some returns can be seen from understorey and ground, more so than the leaf-on first returns.

First and Single Returns – difference leaf-on - leaf-off								
	hmean	σ		hmax	σ		hmean-corr	hmax-corr
Deciduous plots	-0.45	0.78	*	-0.22	0.27	*	-0.45	0.42
Mixed plots	-0.65	0.39	NS	-0.65	0.39	***	-0.65	-0.01
Evergreen plots	0.00	0.38	NS	-0.64	0.36	NS	0.00	0.00

Last Returns - difference leaf-on - leaf-off								
	hmean	σ		hmax	σ		hmean-corr	hmax-corr
Deciduous plots	7.41	4.91	**	0.94	1.05	**	7.71	0.91
Mixed plots	4.27	6.51	NS	-0.21	0.64	NS	4.57	-0.19
Evergreen plots	-0.30	3.72	NS	0.03	0.81	NS	0.00	0.00

Table 17. Summary of the differences in height metrics for first (and single) and last returns between leaf-on and –off datasets. hmean = difference in average mean return height across plot type, hmax = difference in average maximum return height across plot type. A positive Hmean or Hmax indicates leaf-on metrics > leaf-off metrics. A negative Hmean or Hmax indicates that leaf-on metrics < leaf-off metrics. σ = standard deviation of the differences. It also describes whether the leaf-on and leaf-off hmean and hmax are significantly different. NS=Not significant *=significant 0.05 **=significant 0.01 ***=significant 0.001. hmean-corrected and hmax-corrected correspond to values for hmean corr and hmax corr for the differences in evergreen coniferous plots.

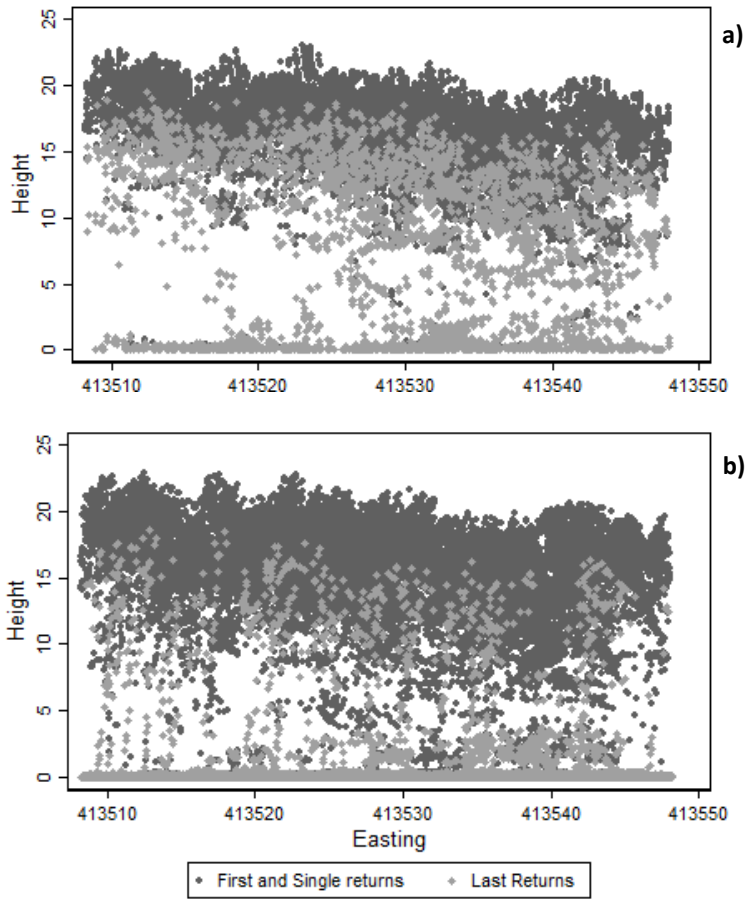

a) Plot 7 Leaf-on

b) Plot 7 Leaf-off

Figure 25. A plot of return height by easting from each survey over plot 7. a) Under leaf-on conditions. b) Under leaf-off conditions.

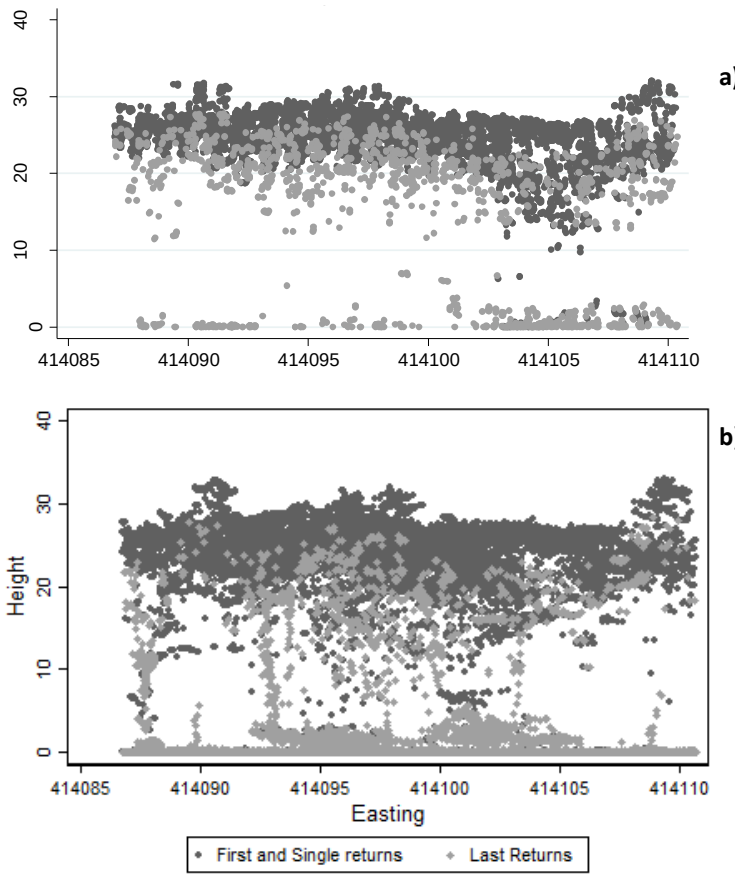

a) Plot 23 Leaf-on

b) Plot 23 Leaf-off

Figure 26. A plot of return height by easting from each survey over plot 23. a) Under leaf-on conditions. b) Under leaf-off conditions.

The representations of plot 23 (see Figure 26 page 79) demonstrate how a mix of deciduous and evergreen species that, though present in a relatively even mix and have differing rates of growth, result in a low THdiv (see Table 12 page 66). In both survey datasets a clear continuous height canopy can be seen from first/single returns with only a few coniferous trees extending above this layer. Again the realisation of the lower canopy is much improved in the leaf-off survey without compromise of the upper canopy realisation. Penetration to the ground in the leaf-on LiDAR dataset is severely limited and the leaf-off maximum return height is noticeably higher (around 33m as opposed to around 31m for the leaf-on survey).

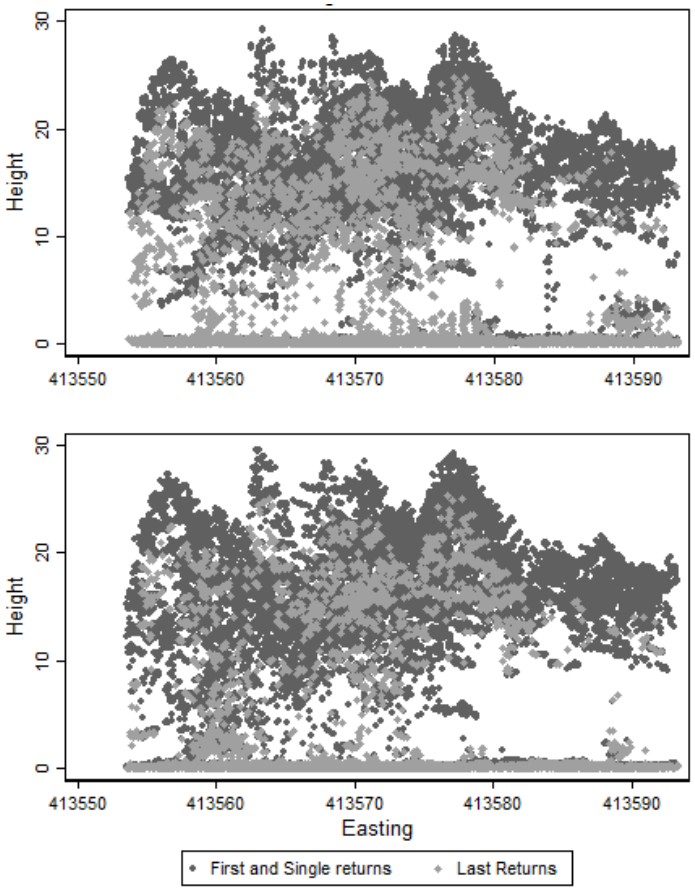

a) Plot 2 Leaf-on

b) Plot 2 Leaf-off

Figure 27. A plot of return height by easting from each survey over plot 2. a) Under leaf-on conditions. b) Under leaf-off conditions.

The tree species diversity in plot 2 is the highest of the surveyed plots (with 7 different tree species surveyed) but it has a low THdiv (see Table 12 page 66). Both coniferous and deciduous tree shapes

can be seen clearly in the graphics from both surveys (see Figure 27 page 80) but the leaf-on dataset seems to have far more last returns reflecting from the canopy. There does not seem to be a large difference in the penetration of first and last returns to the classified ground and both seem to have returns from some form of understorey and the lower branches.

Plot 22, shown in Table 12 page 66 to have the highest THdiv and DBHdiv, has a unique structure (see Figure 28). Though the point density for the leaf-on dataset in this plot is slightly lower than the leaf-off (approximately 21ppm² and 25ppm² respectively) there are large visual differences. There is a distinct difference between first and last point distributions between survey conditions. The penetration of the first returns through the leaf-on canopy is restricted with few first returns reaching the ground. Visibility of the understorey can be found in the leaf-off dataset with smaller Holly trees and bushes towards the lower right.

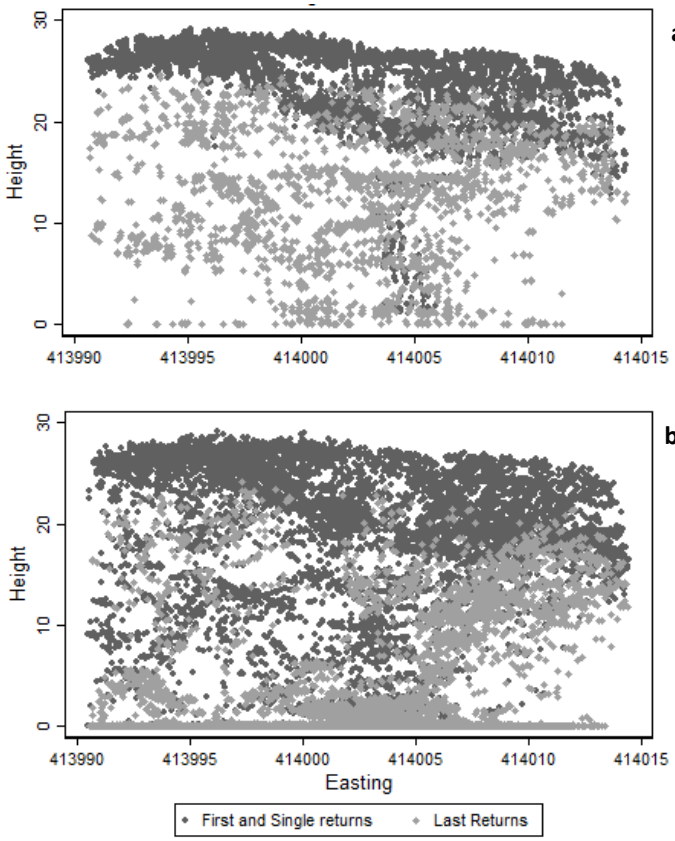

a) Plot 22 Leaf-on

b) Plot 22 Leaf-off

Figure 28. A plot of return height by easting from each survey over plot 22. a) Under leaf-on conditions. b) Under leaf-off conditions.

Plot 11 (see Figure 29) is a good example of evergreen plot pulse distribution under leaf-on and -off conditions. The only substantial difference that can be spotted between plots is the thickness of the low level understorey between surveys. Aside from this the point distributions between datasets seem very similar. Plot 12 (see Figure 22 page 73) was identified as having unusual changes in pulse penetration from an evergreen plot between seasons, Figure 30 (page 83) displays the difference in pulse penetration in more detail. It is clear that the pulse penetration of the first/single returns is much higher under leaf-off conditions in contrast to the other evergreen plots. When analysing this plot in more detail utilising the maximum heights in a 1x1m gridded format to create a rasterised CHM it is clear that multiple lines of thinning from a northwest to southeast direction had taken place leading to this openness of canopy (see Figure 31 page 83). Because of this plot 12 had to be removed from further inclusion in the study. After similar analysis of the remaining plots in this way, plot 12 was the only one to display this thinning. This reduced the number of evergreen coniferous dominated plots to three.

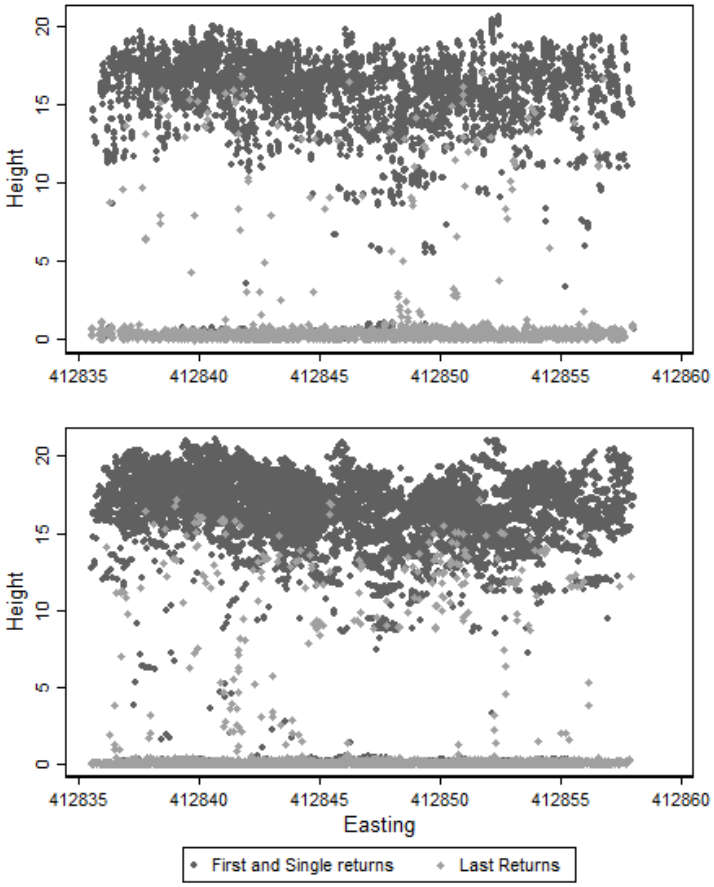

a) Plot 11 Leaf-on

b) Plot 11 Leaf-off

Figure 29. A plot of return height by easting from each survey over plot 11. a) Under leaf-on conditions. b) Under leaf-off conditions.

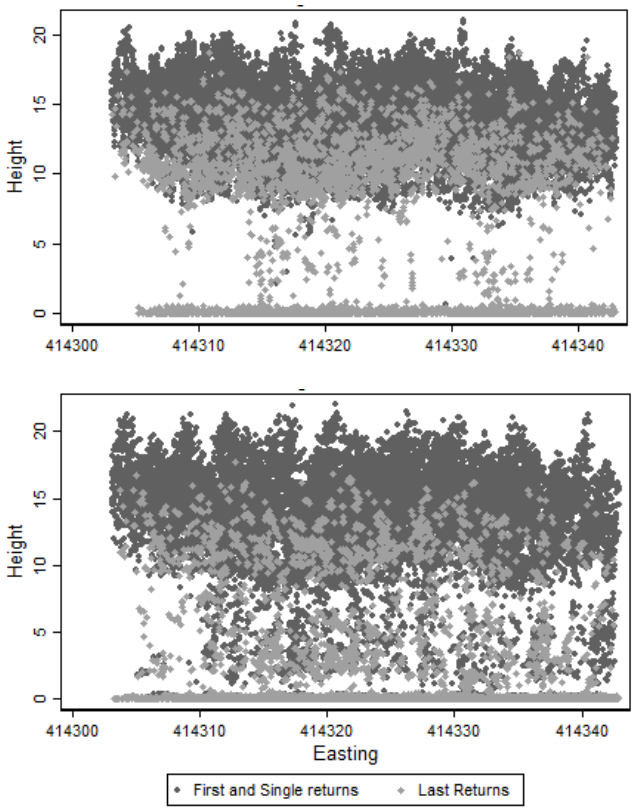

a) Plot 12 Leaf-on

b) Plot 12 Leaf-off

Figure 30. A plot of return height by easting from each survey over plot 12. a) Under leaf-on conditions. b) under leaf-off conditions.

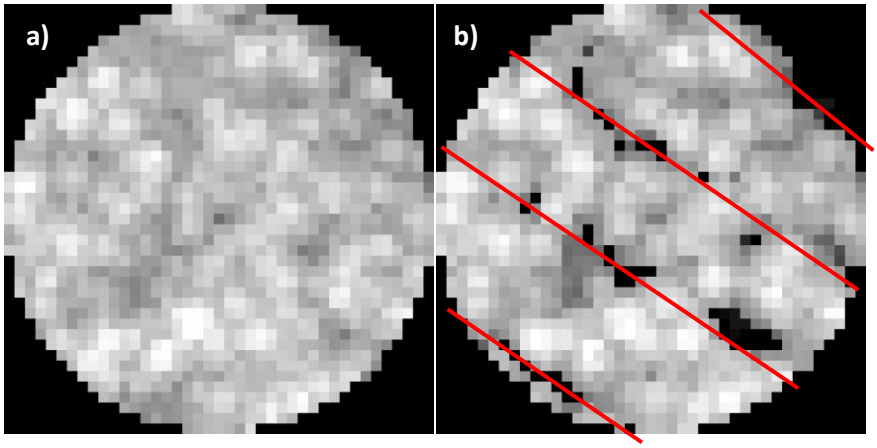

Figure 31. 1x1m gridded maximum canopy heights for plot 12. The scale is from dark to light: low to high. a) Leaf-on. b) Leaf-off with corridors of removed trees indicated.

This section has demonstrates the differences between the pulse distributions of the leaf-on and –off datasets. The leaf-off returns over deciduous and some mixed plots seem to be much more skewed towards the lower elevations than the leaf-on returns but the point distributions within evergreen plots (aside from plot 12 which has been removed from analysis) do not seem to differ

substantially between seasons. The leaf-off point distributions show a larger height range than the leaf-on.

5.2.4 Forest Diversity Metrics

This section focuses on the tree size diversity metrics calculated from the terrain normalised point clouds (see section 4.3.3.2) using LiDAR >2m from the ground surface. The differences between mobilisations has shown to affect all LiDAR point distributions (see sections 5.2.1 to 5.2.3 First and Last Returns). Differences in calculated diversity metrics between surveys can be seen in Table 18. Table 19 (page 85) explores whether the differences in the diversity metrics averaged over each plot group are statistically significantly different between surveys.

Variable	**Mean**	**SD**	**Min**	**Max**		**Mean**	**SD**	**Min**	**Max**
Leaf-off					**Leaf-on**				
CV	0.265	0.076	0.137	0.407	CV	0.285	0.160	0.145	0.999
skew	-1.199	0.687	-3.240	0.200	skew	-1.047	1.325	-6.120	2.520
kurt	5.266	2.937	2.210	15.530	kurt	4.873	2.503	1.630	10.210
SD	4.200	1.201	2.120	7.130	SD	4.458	2.500	1.630	15.920
var	19.008	10.513	4.490	50.900	var	17.454	10.922	3.640	43.440
P99/25	1.655	0.330	1.240	2.776	P99/25	1.702	0.396	1.278	2.829
P99/50	1.358	0.173	1.147	1.984	P99/50	1.334	0.213	0.557	1.939
P99/75	1.208	0.098	1.085	1.493	P99/75	1.211	0.102	1.087	1.548
P99/90	1.111	0.046	1.050	1.234	P99/90	1.091	0.167	0.255	1.252
L-CV	0.141	0.046	0.073	0.233	L-CV	0.139	0.05	0.076	0.247

Table 18. Descriptive statistics surrounding the LiDAR derived diversity metrics

In Table 19 (page 85) the only statistically significant difference in calculated diversity between the two surveys (within each group) can be seen in skewness and kurtosis in the deciduous plots and the ratio of the 99th and 25th percentile in the mixed plots. Variance and kurtosis have large differences within the evergreen plots (-0.558 and -0.520 respectively) (though the difference is not significant) but other diversity variables show smaller differences between surveys.

	Deciduous			Evergreen			Mixed		
	D		σ	D		σ	D		σ
SD	-0.048	A	0.856	-0.085	A	0.705	-0.433	A	0.849
var	0.002	A	8.787	-0.558	A	4.023	-4.028	A	7.853
skew	0.248	**B	0.274	0.083	A	0.596	0.072	A	0.406
kurt	-0.852	*B	1.689	-0.520	A	1.506	0.397	B	1.141
L-CV	0.004	A	0.042	-0.002	B	0.025	-0.011	A	0.039
P99/25	0.123	B	0.339	-0.013	B	0.062	-0.059	B	0.239
P99/50	0.015	A	0.047	-0.012	B	0.026	-0.023	A	0.088
P99/75	0.005	A	0.022	-0.002	B	0.011	0.002	A	0.041
P99/90	0.004	A	0.014	-0.004	B	0.005	0.015	*A	0.019
CV	0.002	A	0.073	-0.003	A	0.053	-0.020	A	0.067

Table 19. A summary of the differences (D) between selected diversity metrics calculated from the leaf-on and –off datasets. A positive 'D' indicates that leaf-on metrics were that amount of metres higher than leaf-off metrics. A negative 'D' indicates that leaf-on metrics were that amount of metres lower than leaf-off metrics. 'A' indicates normally distributed variables that underwent a paired t-test. B indicates non-normally distributed variables underwent the sign rank test. *=significantly different at the 95% CI **=significantly different at the 99% CI

Aside from comparing metrics between datasets it is also important to investigate the relationship between variables within each dataset. Clear relationships between diversity variables, such as that exhibited by the CV and L-CV or some of the percentile means (see Figure 32 page 87 and Figure 33 page 88), are important to note. This is because when creating the predictive models for forest diversity, variables displaying such relationships should not be utilised in the same models as they would add little additional predictive power. Many of the statistical relationships displayed are expected; Strong correlations between percentile means is anticipated as they are calculated in similar ways from ratios of specific quantiles in the data. As standard deviation is equal to the square root of the variance it is also expected that these would share a curvilinear relationship. The correlation of skewness with other variables seems to be much tighter in the leaf-off data than the leaf-on.

Any outliers easily identified in the correlations (Figure 32 page 87 and Figure 33 page 88) were investigated to ensure they were not the result of data entry errors or errors in calculation. As a result, all outliers still present in the dataset are verified results that, though they may not fit the general correlations shown between variables, would have no reason to be omitted and are a reflection of the diversity within the sample sites.

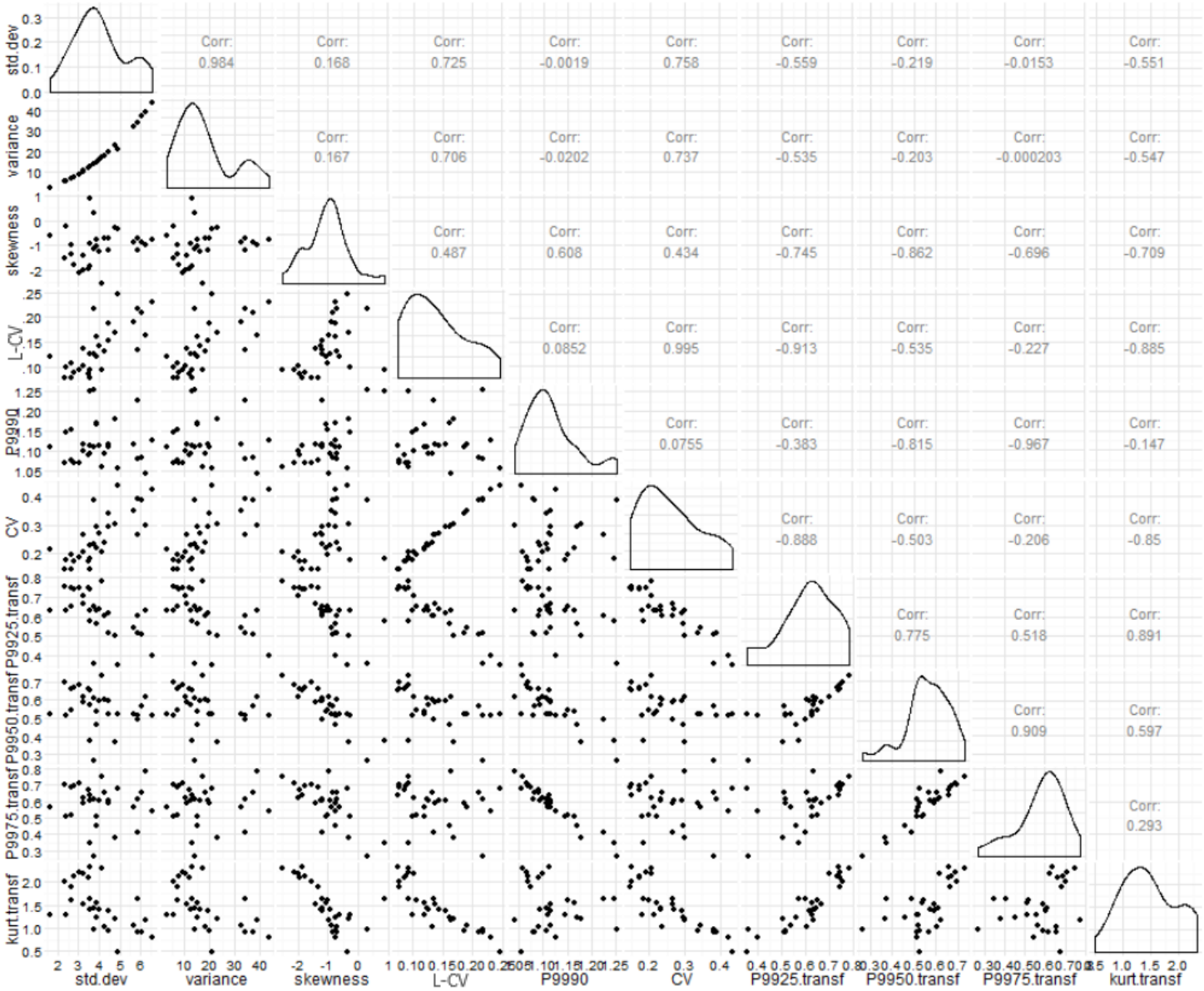

Figure 32. Graph matrix showing the correlation between the diversity variables calculated from the Leaf-on dataset.

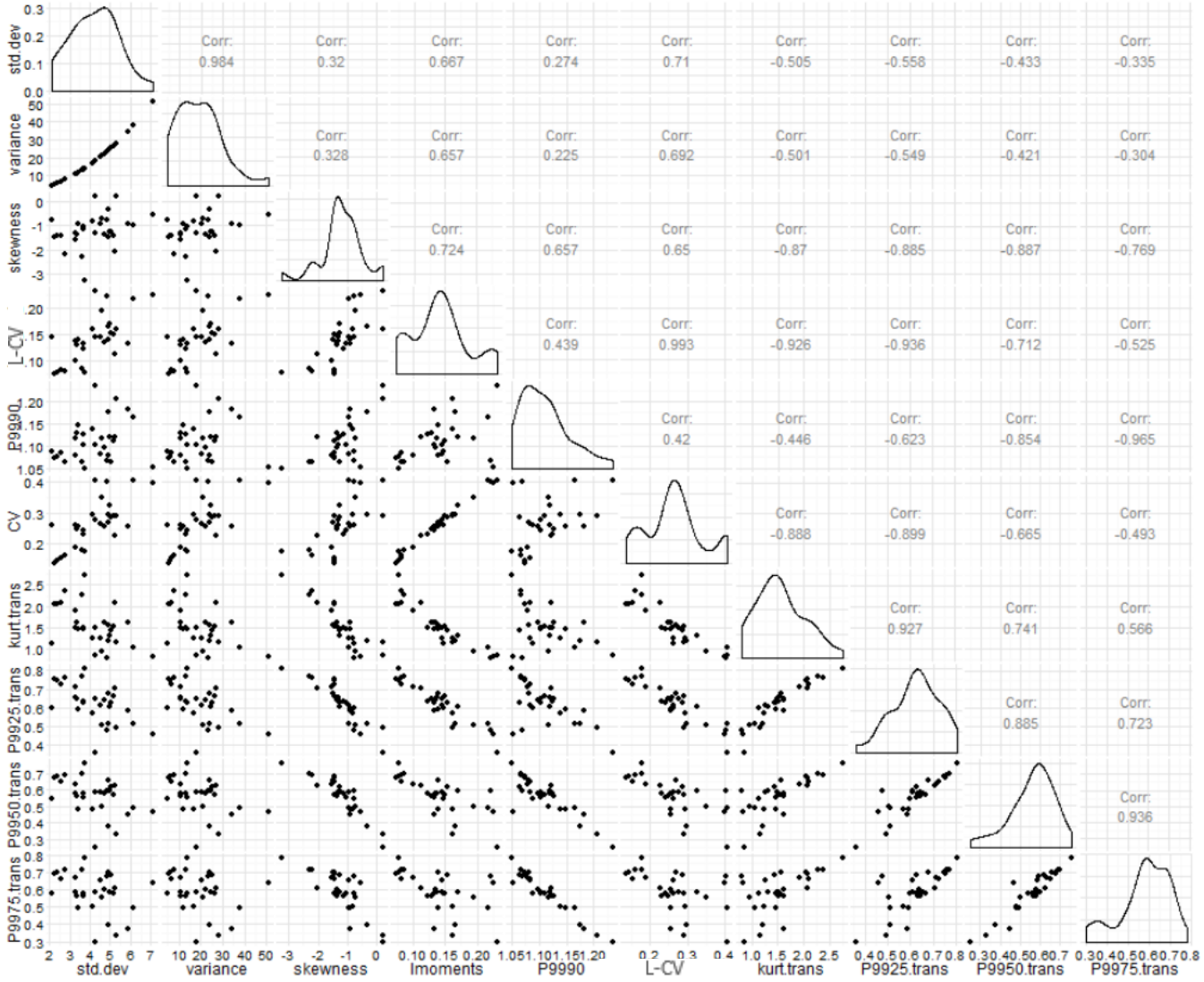

Figure 33. Graph matrix showing the correlation between the diversity variables calculated from the Leaf-off dataset

5.3 Investigating Tree Size Diversity

5.3.1 Diversity variable predictive power

It would be expected that due to the visual and statistical differences between the two LiDAR datasets there would be differences in the ability of models created from these to describe the field diversity variables. The calculated LiDAR metrics from each dataset were regressed against each field diversity measurements to assess the descriptive ability of each after normalisation of non-normal variables. With reference to Table 20 page 90, LiDAR diversity metrics calculated from the leaf-off dataset show a greater number of significant relationships (both at the 99 and 95% CI) to the field diversity measurements than those calculated from the leaf-on dataset. However, both datasets show statistically significant predictive power towards most of the diversity metrics. The THdiv and DBHdiv have the strongest relationship with the LiDAR datasets (R^2 of above 0.5 in both datasets). The Cldiv and CWdiv share significant relationship with the leaf-off CLdiv) but this is not the case with the THdiv or DBHdiv where the leaf-on dataset shows generally higher R^2 values.

The relationships for P99/25, skewness and kurtosis, the three variable that show statistically significant relationships with each of the field diversity variables, are shown in more detail in Figure 34, Figure 35 and Figure 36 pages 91 and 92. This again reflects the similarities in the predictability of both LiDAR datasets despite the visual and statistical differences.

LiDAR Variables	Field tree size diversity indices															
	Tree Height diversity				DBH diversity				CL Diversity				CW diversity			
	leaf-on		leaf-off		leaf-on		leaf-off		leaf-on		leaf-off		leaf-on		leaf-off	
	R^2	p-value	R^2	p-value	R^2	p-value	R^2	p-value	R^2	p-value	R^2	p-value	R^2	p-value	R^2	p-value
$P99/25^{-1}$	0.43	<0.001	0.45	<0.001	0.49	<0.001	0.54	<0.001	0.25	0.008	0.52	<0.001	0.14	0.043	0.24	0.006
$\frac{1}{P99/50^2}$	0.19	0.016	0.23	0.009	0.31	0.001	0.32	0.001	0.24	0.007	0.4	<0.001	0.07	0.166	0.12	0.062
$\frac{1}{P99/75^3}$	0.03	0.375	0.08	0.125	0.09	0.117	0.15	0.036	0.09	0.111	0.2	0.013	0.01	0.704	0.03	0.4
P99/90	0.02	0.491	0.02	0.413	0.06	0.205	0.07	0.151	0.1	0.098	0.07	0.07	0	0.742	0.01	0.574
CV	0.48	<0.001	0.5	<0.001	0.4	<0.001	0.49	<0.001	0.1	0.085	0.43	<0.001	0.07	0.153	0.21	0.012
skew	0.24	0.006	0.32	0.001	0.43	<0.001	0.42	<0.001	0.41	<0.001	0.39	<0.001	0.17	0.022	0.18	0.021
Log(kurt)	0.54	<0.001	0.52	<0.001	0.54	<0.001	0.53	<0.001	0.29	0.002	0.46	<0.001	0.19	0.017	0.26	0.004
L-CV	0.5	<0.001	0.52	<0.001	0.44	<0.001	0.52	<0.001	0.12	0.057	0.46	<0.001	0.09	0.104	0.23	0.008
var	0.46	<0.001	0.45	<0.001	0.34	0.001	0.42	<0.001	0.1	0.084	0.34	0.001	0.06	0.119	0.18	0.021
SD	0.46	<0.001	0.44	<0.001	0.37	<0.001	0.44	<0.001	0.1	0.084	0.33	0.001	0.07	0.145	0.19	0.017

Table 20. The R^2 and p-values from each individual linear regression the field diversity measurements and LiDAR metrics are summarised here. The LiDAR metrics were calculated from all returns above 2m to remove the effect of understorey and after normalisation (normalised variables are highlighted blue). R^2 values that are significant at a greater than 99% CI are highlighted in green, those at the 95% CI are highlighted in yellow

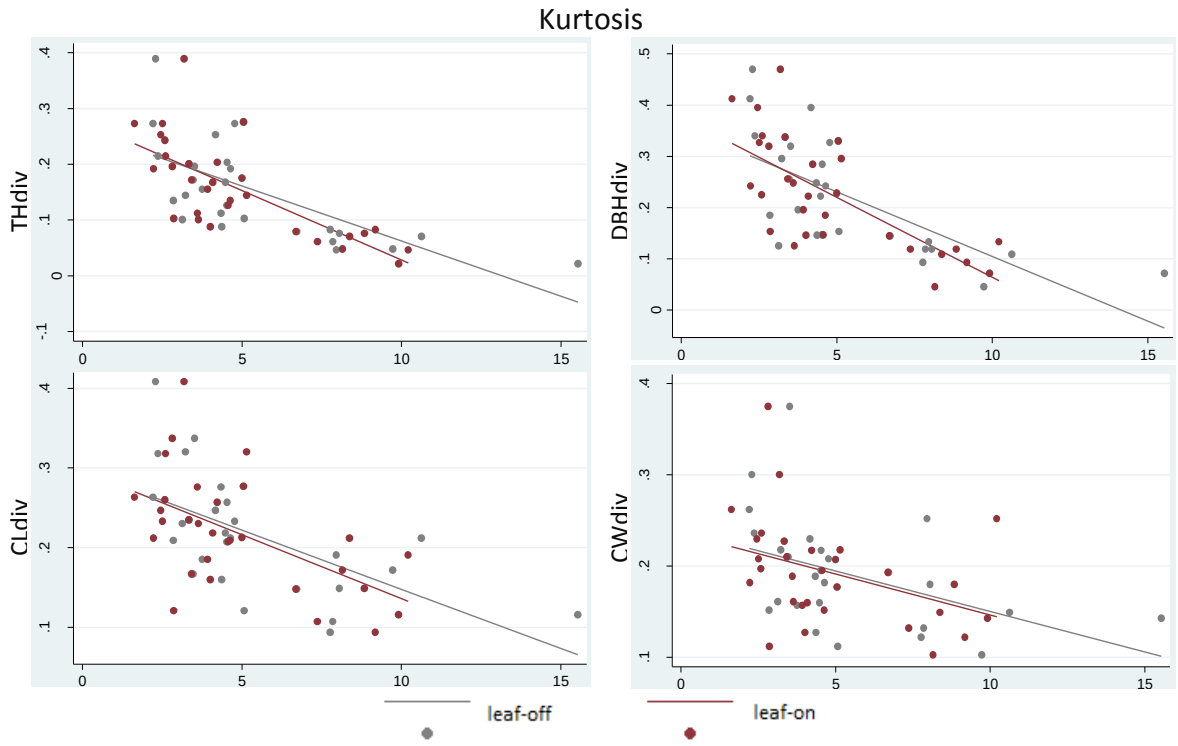

Figure 34. Scatter plots to demonstrate the relationship between the field diversity metrics and the kurtosis of each LiDAR derived diversity metric, leaf-on and –off

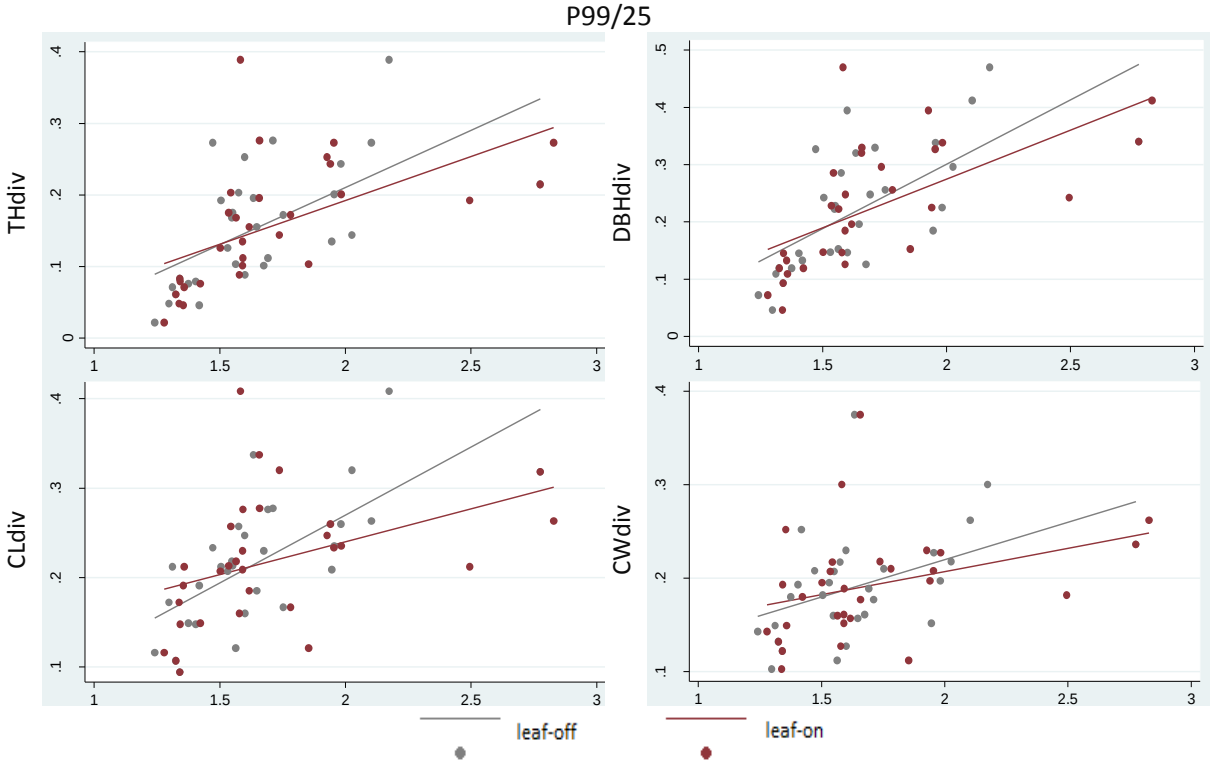

Figure 35. Scatter plots to demonstrate the relationship between the field diversity metrics and the means of the 99th and 25th percentile of each LiDAR derived diversity metric, leaf-on and –off.

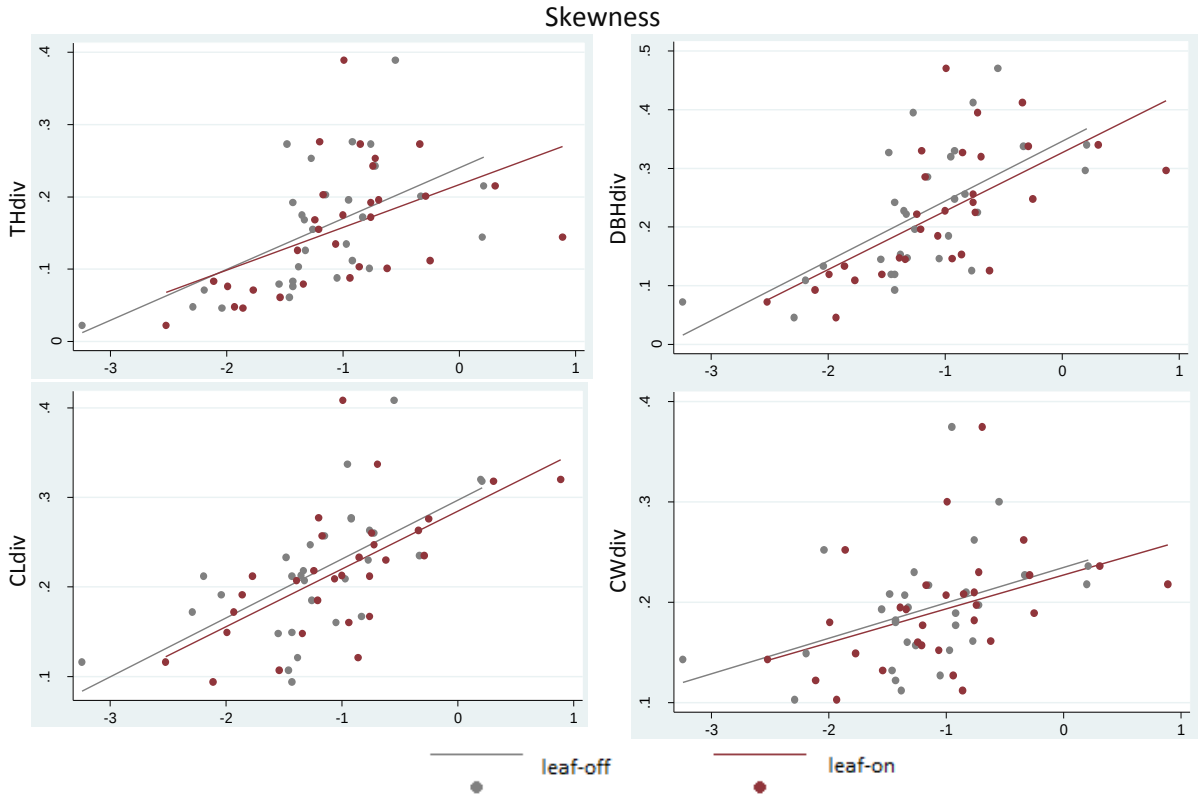

Figure 36 Scatter plots to demonstrate the relationship between the field diversity metrics and the Skewness of each LiDAR derived diversity metric, leaf-on and –off

5.3.2 Summary of Models

Models describing field measured tree size diversity metrics are summarised in Table 21 page 93 and further summary statistics are covered in Table 22 page 94. There are 10 models in total, 4 models constructed of leaf-on variables describing tree size diversity field metrics, 4 models constructed of leaf-off variables describing tree size diversity field metrics and 2 models where both leaf-on and leaf-off diversity metrics were combined to describe THdiv and DBHdiv. When constructing models for CLdiv and CWdiv no suitable combination of variables would produce a model describing field diversity with any significance and so these are not present.

Model	**Equation**
1	$THdiv = 0.234 - 0.090\log(Kurt_{lon}) + 0.003Var_{lon}$
2	$THdiv = 0.233 - 0.092\log(Kurt_{loff}) + 0.003Var_{loff}$
3	$THdiv = 0.245 - 0.104\log(Kurt_{loff}) + 0.004 \times Var_{lon}$
4	$DBHdiv = 0.139 + 0.087Skew_{lon} + 0.044SD_{lon}$
5	$DBHdiv = 0.791 + 0.103Skew_{loff} + 0.048SD_{loff} - 0.576P99/90_{loff}$
6	$DBHdiv = 0.115 + 0.004Var_{loff} + 0.064Skew_{loff} + 0.433CV_{lon}$
7	$CLdiv = 0.285 + 0.065Skew_{lon}$
8	$CLdiv = 0.35 + 0.568\frac{1}{P99/75_{loff}{}^3} - 0.892\frac{1}{P99/50_{loff}{}^2} + 0.002Var_{loff}$
9	$CWdiv = 0.267 - 0.051\log(Kurt_{lon})$
10	$CWdiv = 0.286 - 0.061\log(Kurt_{loff})$

Table 21. Models constructed for tree size diversity variables.

Throughout model construction various tests of collinearity, normality, model specification and homogeneity of residuals (described in Section 4.4.1) were undertaken and those that violated some of the assumptions required were undertaken with Robust Standard Errors as discussed. From Table 22 (page 94) it is apparent that models 1 and 2 similarly describe approximately 65% of the variability in THdiv. However when combining LiDAR derived diversity metrics from both datasets in model 3 this increases to 77%. The values for RMSE, signifying the accuracy of the models, seem very low. This would usually be an indicator of alarmingly high accuracy however considering RMSE depends on the unit of measurement, in this case the diversity metrics or L-CV of field variables, these low values are sensible.

Out of the further single survey models (4, 5 and 7-10) leaf-off LiDAR derived variables seem to consistently produce models which describe a greater proportion of the field diversity (71% versus 61% for DBHdiv, 62% versus 41% for CLdiv and 26% versus 19% for CWdiv). Again, the combined model describing DBHdiv (model 6) performs better than single survey models 4 and 5, but only slightly, accounting for 1-4% more DBH diversity. Models for CWdiv seem to perform poorly

compared to the models linked to the other field diversity variables accounting for only 19% and 26% of the CWdiv variability. As mentioned in Section 5.3.2 no models constructed with combined leaf-on and leaf-off diversity variables could describe the field diversity variables with any significance and so are omitted here.

	Model	Dataset	Independent Variables	*t*	P>|t|	RMSE	R^2	F	*p*	
THdiv	1	Leaf-on	Kurtosis	-4.97	0.000	0.05	0.65	29.12	0.0000	Robust standard errors
			Variance	1.85	0.075					
	2	Leaf-off	Kurtosis	-3.88	0.001	0.05	0.65	24.68	0.0000	
			Variance	3.12	0.004					
	3	Leaf-on & Leaf-off	Kurtosis (leaf-off)	-6.04	0.000	0.04	0.77	44.98	0.0000	
			Variance (leaf-on)	5.41	0.000					
DBHdiv	4	Leaf-on	Skewness	6.37	<0.001	0.06	0.68	30.76	0.0000	Robust standard errors
			SD	3.44	0.002					
	5	Leaf-off	Skewness	4.82	0.000	0.06	0.71	20.82	0.0000	
			SD	4.96	0.000					
			P99/90	-2.34	0.027					
	6	Leaf-on & Leaf-off	Variance (leaf-off)	3.18	0.004	0.06	0.72	22.00	0.0000	
			Skewness (leaf-off)	3.56	0.001					
			CV (leaf-on)	2.85	0.008					
CLdiv	7	Leaf-on	Skewness	4.36	<0.001	0.06	0.41	19.02	0.0002	Robust standard errors
	8	Leaf-off	P99/75	2.57	0.016	0.05	0.62	13.94	0.0000	
			P99/50	-3.63	0.001					
			Variance	2.05	0.050					
CWdiv	9	Leaf-on	Kurtosis	-2.47	0.020	0.05	0.19	3.95	0.0197	Robust standard errors
	10	Leaf-off	Kurtosis	-3.58	0.001	0.05	0.26	9.57	0.0013	Robust standard errors

Table 22. Summary of constructed diversity models. Each field diversity measurement has a corresponding model created from leaf-off LiDAR derived diversity metrics and leaf-on LiDAR derived diversity metrics. THdiv and DBHdiv also have a corresponding model created from a combination leaf-on and leaf-off LiDAR derived diversity metrics where this improved the accuracy of the regression. Similar models were not included for the CLdiv and CWdiv as the predictive ability of these compared to the single dataset model was lower.

6. DISCUSSION AND CONCLUSIONS

This section will discuss in more detail observations made in Chapter 5 and relate these to relevant studies in the literature to answer the following research questions:

1. How does the seasonal time of capture impact upon the LiDAR point distributions and structural diversity metrics generated from the LiDAR point cloud?
2. What is the relative accuracy of models describing tree size diversity metrics generated from leaf-on LiDAR derived diversity metrics, leaf-off LiDAR derived diversity metrics and models generated from a mix of the two?
3. Can this tell us anything about when is best to undertake airborne LiDAR survey when modelling forest structure diversity and assessing biodiversity?

The layout is outlined to reflect the objectives of the study. Objective 1 (to remove systematic bias between surveys) has been carried out within 4.3.1 Initial Filtering of the LiDAR Datasets and Assessment of Relative Accuracy and 4.3.2 and this section is organised as follows to realise the remaining objectives:

- 6.1 Comparing forest structure and structural diversity metrics calculated from leaf-off and –on LiDAR datasets

  As all relevant forest structure metrics and structural diversity metrics have been calculated (and displayed in Chapter 5 sections 5.1 and 5.2) this section will directly compare these between surveys whilst discussing the potential reasons for similarities and differences based around the influence of seasonal changes, growth between surveys and differences in survey parameters. This will provide the answer to research question 1.

- 6.2 Assessing the relative capacity of leaf-on and -off LiDAR derived structural diversity metrics to describe true structural diversity in Chopwell Woodland Park

  In this section the relative capacity of forest diversity metrics calculated from LiDAR datasets which have been correlated to the field metrics (section 5.3) will be discussed, assessing the individual metrics themselves and also the models derived from these. This will provide the answer to research question 2.

- 6.3 Assessing what the outcomes mean for LiDAR survey planning for forest biodiversity investigations in the UK

  This section will assess how applicable the results from this study are to forest sites across the UK and consider how use of either of the LiDAR datasets in isolation could potentially impact on outputs of biodiversity investigations. This will provide the answer to research question 3.

  To maintain continuity and clarity throughout each section will be concluded separately.

6.1 Comparing Forest Structure and Structural Diversity Metrics Calculated from Leaf-on and –off LiDAR Datasets

6.1.1 Comparing Leaf-on and –off LiDAR Point Distributions

6.1.1.1 Canopy return point distributions

As discussed in section 5.2.1 and shown in Figure 22, reproduced on page 98 for reference, the minimum and maximum of all LiDAR return heights between the leaf-on and leaf-off plot datasets

do not show very large differences. This could reflect the rigorous co-registration process undertaken (see Chapter 4 section 4.3.2) where datasets where corrected for absolute alignment over hard surfaces to make them directly comparable. However, the maximum heights across all plots are consistently larger under the 2011 leaf-off conditions by an average of approximately 57cm across all plots. In deciduous plots the increase is on average 41cm from leaf-on to –off but this rises to an average of 87cm in coniferous evergreen plots. It is accepted in this study that a proportion or all of this increase in maximum return height in evergreen plots between surveys is due to tree growth and/or changing survey parameters. Evergreen plots are of high interest as they allow the opportunity to isolate the growth and sensor/flight parameter variations between surveys for assessment. Using the average difference in maximum height between surveys over evergreen plots and negating this from the differences in return height in the remaining plot groups provides some indication of the influence of seasonal canopy change without further complication.

Using this principle results could suggest there would be a decrease in maximum return heights from leaf-on to –off datasets of around 7cm in mixed and 42cm in deciduous plots. It is likely that the correction to be applied from the evergreen plot return height differences is simplistic (as the number of useable plots is low and merchantable coniferous species in Chopwell Woodland Park have purposefully faster growth rates) but it is utilised to infer what the results could potentially have been had the survey parameters been identical and the surveys taken within months of one another.

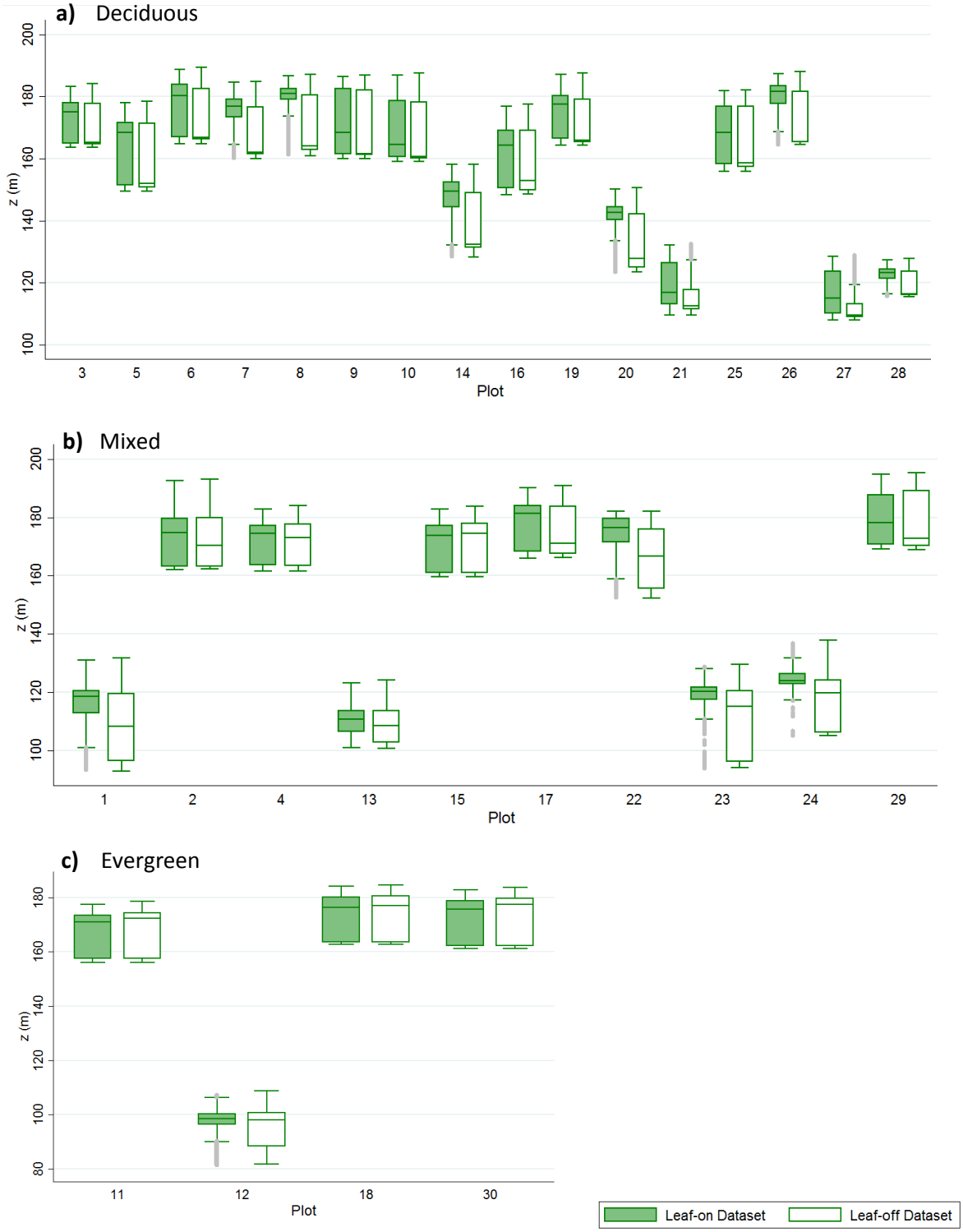

Figure 22. (Reproduced from section 5.2.1) Box plots of LiDAR return heights. The arms of the box plot represent all values within 1.5 x the interquartile range and grey markings on each graph represent returns outside of these boundaries. a: Deciduous plots. b:Mixed plots. c: Evergreen plots.

	Deciduous				Evergreen				Mixed		
	D		σ	Dcorr	D		σ	D		σ	Dcorr
P75	-0.25	A	0.526	0.45	-0.70	*A	0.25	-0.40	A	1.00	0.30
P90	-0.25	*B	0.462	0.46	-0.71	*A	0.28	-0.83	*A	0.94	-0.13
P99	-0.20	B	0.420	0.64	-0.84	**A	0.26	-0.66	*A	0.69	0.18

Table 23. A subset of Table 15 in section 5.2.1. A summary of the differences (D) between selected statistics calculated from the leaf-on and –off datasets. A positive 'D' indicates that leaf-on metrics were that amount of metres higher than leaf-off metrics. A negative 'D' indicates that leaf-on metrics were that amount of metres lower than leaf-off metrics. 'A' indicates normally distributed variables that underwent a paired t-test. B indicates non-normally distributed variables underwent the sign rank test. *=statistically significantly different at the 95% CI **=statistically significantly different at the 99% CI. Dcorr corresponds to the difference values corrected for the difference in the evergreen coniferous plots.

The upper percentiles of return height (P99, P90 and P75) originally show a negative difference from leaf-on to leaf-off (see Table 23) but after correction these change to positive values, the largest in the deciduous plots (an increase of up to 64cm in return height from leaf-off to leaf-on). These results show some increase in penetration through deciduous and mixed canopies under leaf-off conditions, with a much greater effect in deciduous plots. This indicates that the absence of deciduous leaves during winter months may present a more porous upper canopy, resulting in maximum LiDAR return heights reflecting from lower canopy layers than during leaf-on conditions. It could be possible that smaller differences between mixed plots from leaf-on to off could be due to laser pulses reflecting off the relatively abundant coniferous trees compared to the complete absence of coniferous trees in many of the deciduous plots. This pattern is also reflected in the maximum return heights of first returns after correction (see Table 17 page 100) where in deciduous plots maximum first return heights were around 42cm higher under leaf-on conditions. This is inconsistent with findings from Ørka et al. (2010) and Næsset (2005) where maximum return heights from first returns (which are reflected from the upper canopy layers) were not significantly different between leaf-on and –off acquisitions when accounting for changes due to growth and

survey characteristics. However, in the case of Ørka et al. (2010), these comparisons were made from ground height corrected datasets which could be influenced by ground classification accuracy.

First and Single Returns – difference leaf-on - leaf-off								
	hmean	σ		hmax	σ		Hmean-corr	Hmax-corr
Deciduous plots	-0.45	0.78	*	-0.22	0.27	*	-0.45	0.42
Mixed plots	-0.65	0.39	NS	-0.65	0.39	***	-0.65	-0.01
Evergreen plots	0.00	0.38	NS	-0.64	0.36	NS	0.00	0.00

Last Returns - difference leaf-on - leaf-off								
	hmean	σ		hmax	σ		Hmean-corr	Hmax-corr
Deciduous plots	7.41	4.91	**	0.94	1.05	**	7.71	0.91
Mixed plots	4.27	6.51	NS	-0.21	0.64	NS	4.57	-0.19
Evergreen plots	-0.30	3.72	NS	0.03	0.81	NS	0.00	0.00

Table 17. (Reproduced from section 5.2.3). A summary of the differences in mean and maximum return height of the first and single and last returns between the leaf-on and –off datasets. hmean = difference in average mean return height across plot type, hmax = difference in average maximum return height across plot type. σ = standard deviation of the differences. A positive hmax or hmean indicates that leaf-on metrics were that amount of metres higher than leaf-off metrics. A negative hmax or hmean indicates that leaf-on metrics were that amount of metres lower than leaf-off metrics. It also describes whether the leaf-on and leaf-off hmean and hmax are significantly different. NS=Not significant *=significant 0.05 **=significant 0.01 ***=significant 0.001. Hmean-corr and Hmax-corr correspond to values for Hmean and Hmax corrected for the differences in evergreen coniferous plots.

It is interesting to note that the mean of first return heights in mixed and deciduous plots (after correction) show a negative difference from leaf-on to –off (Table 17). This means on average first returns could have been 45-65cm higher in the canopy during leaf-off conditions. It is difficult to explain the reasoning behind this, it could be an indication of the imprecise nature of the correction applied to the means from the evergreen plots or a result of tree growth. What is more convincing is the large positive difference between surveys between the means of the last returns before and after correction (up to 7.71 metres in deciduous plots and 4.57 metres in mixed plots though only

the deciduous plot difference is significant). This is in agreement with Næsset (2005) where it was shown that last return pulse measurements are in general more affected by canopy conditions than the first return data. Comparing the mean and maximum return height differences from the two surveys in evergreen plots also suggests that last returns are influenced more by growth and survey characteristics than first returns. Last return mean and maximum height difference also show much greater variability (σ = 0.64-6.51) than that of the first returns (σ = 0.27-0.78). This is also again in agreement with Wasser et al. (2013) who found laser pulse penetration lower in the canopy appeared more variable compared to top of the canopy penetration between survey conditions. In support of the patterns shown in the LiDAR metrics the selected visual representations of LiDAR return height against easting (Figures 25-30 section 5.2.3) visually demonstrate the clear differences between the penetrability of last returns between the two surveys in mixed and deciduous plots. This is in agreement to the study by Ørka et al. (2010) where it was found that the 'last of many' return height category showed a larger difference in height distributions which were shifted ground-wards under leaf-off conditions. These visualisations also highlight differences in understorey conditions between the surveys with greater levels of understorey seemingly present under leaf-off conditions due to the point in the season when the leaf-off dataset was collected. The additional understorey does not seem to have affected the distribution of last returns penetrating through the canopy during leaf-off conditions.

The interquartile range in deciduous and mixed plots generally increases in leaf-on conditions and the mean is lower in the canopy compared to leaf-off conditions (see Figure 22 page 98). This is in agreement with the findings of Wasser et al. (2013) who found laser pulse penetration lower in the canopy appeared more variable compared to top of the canopy penetration between survey conditions under hardwood trees. In contrast differences in point distribution shapes through the evergreen plots (after exclusion of plot 12) are minimal (see Figure 22 page 98). The differences in

deciduous and mixed plot interquartile range and mean highlights the influence of seasonal canopy coverage on the point distributions.

6.1.1.2 Ground Return Point Distributions

As shown in Figure 22 page 98 the minimum return height appears lower during the leaf-off conditions, even without correction of growth and survey variables. This is in agreement with statistics in Table 24 showing leaf-on LiDAR generally overestimated the ground height in comparison to leaf-off (hence the many positive differences). Gatziolis et al. (2010) also found that DTMs derived from LiDAR datasets were affected by canopy conditions (leaf-on and –off) and that using leaf-on LiDAR generally overestimated the ground surface while using leaf-off led to less overestimation. However, it should be noted that though leaf-on datasets tended to overestimate the ground surface, often statistically significantly more than leaf-off, these differences generalised come to only sub-10cm.

		Mean z (m nearest cm)		
	Plot	leaf-on	leaf-off	Leaf-on-Leaf-off
Deciduous	**Average**	**147.36**	**147.28**	**0.08**
Mixed	**Average**	**137.76**	**137.74**	**0.03**
Evergreen	**Average**	**160.84**	**160.76**	**0.08**

Table 24. A summary of Table 16 from section 5.2.2 showing the mean height of the classified ground points in each plot group and the average difference..

There were, however, some exceptions to the leaf-on overestimation of ground classification, such as plots 22 and 6 which show negative differences converse to most other plots and the literature. However, these negative differences in average ground classified return heights between leaf-on and -off datasets are either insignificant or the number of ground returns per plot was so

incomparable it was likely this affected the significance of the distribution difference. A similar result was shown by Hollaus et al. (2006) as though the authors expected the summer DTM to be higher than the winter DTM they found positive and negative differences between the two were equally abundant. This was due to the comparatively low amount of ground classified returns in the leaf-on dataset leading to over and underestimation of the ground as it was interpolated across the gaps.

It is interesting to note that there is a significant difference between the ground models from some evergreen plots where the leaf-on DTM is around 11cm higher than the leaf-off. Both Hollaus et al. (2006) and Hadley and Smith (1986) have considered the fact that the coniferous tree crowns are more transparent for infra-red laser pulses in winter than in summer due to higher needle mortality during this time. Though these results are based on forests in the Rocky Mountains USA and changes in climate for Chopwell Woodland Park winter to summer will be less extreme it may play a small part in the increased evergreen coniferous penetration during this time.

6.1.2 Comparing Leaf-on and –off LiDAR Derived Structural Diversity Metrics

The LiDAR derived diversity metrics primarily provide information regarding forest structure diversity in each plot. However, these metrics, like the point height distributions, are also influenced by scanner/flight parameters and growth, which can be investigated by looking at the difference between diversity statistics derived from the leaf-on and –off LiDAR dataset over evergreen plots, similar to sections 6.1.1 and 6.1.2. As noted in section 6.1.1.1 there are differences in return height distributions in evergreen plots between surveys however there are no significant effects seen in the diversity metrics (see Table 19 page 104). Evergreen plots generally show small and non-significant differences in diversity metrics calculated between surveys. Mixed and deciduous plots are more variable, showing some larger and statistically significant differences between surveys,

indicating the influence of changing canopy conditions on the derived diversity metrics. Næsset (2005) found that the CV of LiDAR canopy height was significantly higher under leaf-off conditions and Wasser et al. (2013) found that the CV of all none ground returns differed significantly between surveys for all plot types aside from evergreen coniferous plots. Only small and insignificant differences are seen in this study however. The study by Wasser et al. (2013) appears less affected by vegetation growth (with surveys less than a year apart) and sees no significant differences between percentile heights over what they term 'deciduous simple' plots but some significant differences between surveys in what they term 'deciduous compound' plots. This study does not differentiate between the two.

	Deciduous			Evergreen			Mixed		
	D		σ	D		σ	D		σ
SD	-0.048	A	0.856	-0.085	A	0.705	-0.433	A	0.849
Variance	0.002	A	8.787	-0.558	A	4.023	-4.028	A	7.853
Skewness	0.248	**B	0.274	0.083	A	0.596	0.072	A	0.406
Kurtosis	-0.852	*B	1.689	-0.520	A	1.506	0.397	B	1.141
L-CV	0.004	A	0.042	-0.002	B	0.025	-0.011	A	0.039
P99/25	0.123	B	0.339	-0.013	B	0.062	-0.059	B	0.239
P99/50	0.015	A	0.047	-0.012	B	0.026	-0.023	A	0.088
P99/75	0.005	A	0.022	-0.002	B	0.011	0.002	A	0.041
P99/90	0.004	A	0.014	-0.004	B	0.005	0.015	*A	0.019
CV	0.002	A	0.073	-0.003	A	0.053	-0.020	A	0.067

Table 19. (Reproduced from section 5.2.4) A summary of the differences (D) between selected diversity metrics calculated from the leaf-on and –off datasets. A positive 'D' indicates that leaf-on metrics were that amount of metres higher than leaf-off metrics. A negative 'D' indicates that leaf-on metrics were that amount of metres lower than leaf-off metrics. 'A' indicates normally distributed variables that underwent a paired t-test. B indicates non-normally distributed variables underwent the sign rank test. *=significantly different at the 95% CI **=significantly different at the 99% CI

It is interesting to note that the diversity variables which show significant differences from leaf-on to -off (skewness and kurtosis) are also shown to be common variables chosen for inclusion in the regression models which highlights the sensitivity of these metrics to changes in forest structure.

6.1.3 Summary and Conclusions: How does the seasonal time of capture impact upon the LiDAR point distributions and structural diversity metrics generated from the LiDAR point cloud?

Leaf-off LiDAR metrics in all plots seem to be consistently affected by growth and change of survey parameters compared to the leaf-on dataset, making the isolation and assessment of the effects of seasonal change difficult. However, by assessing the change from leaf-on to –off in evergreen coniferous plots and negating the same scale of differences from the remaining plot types this study attempts to go some ways to diminish these influences. After corrections were applied it appeared returns from mixed and deciduous plots would likely have higher maximum heights under leaf-on conditions, likely due to the reduction of the tree crown size in deciduous species due to leaf loss. Ground classification though slightly overestimated under leaf-on conditions, was comparable between surveys and therefore was not found to be influenced by canopy cover in this study (potentially due to the high point densities). Last return heights are shifted downward penetrating further into leaf-off canopies. All of these conclusions match expectations regarding the relationship between canopy openness.

None of the structural diversity metrics seemed to be significantly different between leaf-on and –off datasets in the evergreen plots, though variance and kurtosis seemed to be most affected by growth and survey parameters showing the largest change between surveys. There were however significant differences between some of the deciduous and mixed variables: skewness and kurtosis in deciduous plots and P99/90 in mixed plots.

6.2 Assessing the relative capability of leaf-on and leaf-off LiDAR derived structural diversity metrics to describe actual structural diversity

6.2.1 Assessing the relative relationships between metrics calculated from leaf-on and –off LiDAR datasets and the field derived structural diversity variables

Both leaf-on and -off datasets appear to provide diversity variables which correlate significantly with the field structural diversity variables (see Table 25 page 109). Metrics calculated from the leaf-off LiDAR dataset show a greater number of significant relationships (p value < 0.05) to field diversity metrics than leaf-on derived metrics (see Table 25 page 109). Relationships between kurtosis and THdiv or DBHdiv display slightly stronger relationships under leaf-on conditions (R^2=0.54; 0.52 (leaf-off; leaf-on kurtosis and THdiv), R^2=0.54; 0.53 (leaf-on; leaf-off kurtosis and DBHdiv). Variance and standard deviation also display slightly stronger relationships with THdiv under leaf-on conditions however the remaining metrics generally share stronger and more significant relationships with tree size diversity variables under leaf-off conditions. Both Ørka et al. (2010) and Næsset (2005) found that estimation of biophysical properties under leaf-off conditions (in coniferous and mixed deciduous plots) was slightly improved compared to leaf-on. Gatziolis et al. (2010) and Wasser et al. (2013) found that under hardwood canopies (which describes the majority of the survey plots in this study) leaf-on LiDAR was less accurate at describing biophysical forest parameters due to the underestimation of tree heights. Despite the apparent greater descriptive abilities offered by the leaf-off LiDAR dataset in this study, the metrics derived from this share more collinearity (Figures 32 and 33 pages 87 and 88) with one another and so many are restricted from inclusion in the same models.

It might be expected that as the chosen LiDAR derived structure metrics are directly related to the height distribution of returns the predictive ability of these variables would be most effective for THdiv and CLdiv field variables – both directly related to the vertical heights of trees in each plot. Though THdiv is well described by many metrics, DBHdiv looks to be described slightly better in both leaf-on and -off datasets (table 25 page 109). There is a strong correlation between THdiv and DBHdiv (r=0.92 see Table 3 section 5.1 page 40). Strong relationships between tree height and DBH are well documented in the forestry literature and practice (Martin and Flewelling, 1998) but this relationship can get complicated when considering multiple species, stand densities and tree ages and so this unexpected result may be somehow related to the diverse field dataset. Conversely, though CWdiv is significantly correlated to a selection of LiDAR variables, the significance of these relationships is relatively low compared to others in the study. This is somewhat in agreement with regression analysis undertaken in Ozdemir and Donoghue (2013) where CWdiv could only be described statistically significantly by skewness and P99/25 at the 95% level of confidence.

The LiDAR metrics CV, skewness, kurtosis and L-CV of return height correlate to many field diversity variables well whilst mostly maintaining a relatively low correlation amongst one another (aside from CV and L-CV which are understandably highly related). Though Watt et al. (2013) did not assess LiDAR diversity metrics against the same specific tree size diversity variables used in this study, the authors found that many metrics such as CV, SD, skewness and kurtosis of the LiDAR return heights displayed significant correlations to structural variables such as volume, mean top height and stand density. Similarly, Simonson et al. (2012) found that skewness of last returns was highly correlated with foliage height density (or the proportion of foliage in the canopy layers), mean understorey height and vegetation volume (R^2 -0.69, -0.75 and -0.63 respectively p<0.01). Simonson et al. (2012) also investigated the relationship between standard deviation of first return heights and various forest structure metrics and could not identify any significant correlations. Conversely in this research standard deviation showed a significant relationships with all field structure variables

(though only the leaf-off versions of the metrics show a significant relationship to CLdiv and CWdiv). These differences could be due to the differences in point distributions analysed in this and the Simonson et al. (2012) study, the latter of which only considers standard deviation of first returns, and the differences in field metrics, this study focuses on diversity whereas the Simonson et al. (2012) study deals with direct biophysical measurements. Donoghue et al. (2007) found that the CV of LiDAR return height produced a negative relationship to proportion of Sitka Spruce (R^2 =0.914) and related this to the denser forest canopies that species provide inhibiting LiDAR pulse penetration creating lower CV.

Ozdemir and Donoghue (2013) found that P99/90 appeared sensitive to changes in diversity indices compared to the other point-based LiDAR variables (see Table 25 page 109), this is in contrast to the findings of this study where this metric shows few significant relationships with any of the field diversity metrics despite the fact that the field and leaf-on datasets in both studies were comprised of around two thirds of the same data.

Variables	Field tree size diversity indices											
	THdiv			DBHdiv			CLdiv			CWdiv		
	leaf-on R^2	leaf-off R^2	Ozdemir and Donoghue (2013) R^2	leaf-on R^2	leaf-off R^2	Ozdemir and Donoghue (2013) R^2	leaf-on R^2	leaf-off R^2	Ozdemir and Donoghue (2013) R^2	leaf-on R^2	leaf-off R^2	Ozdemir and Donoghue (2013) R^2
$P99/25^{-1}$	0.43	0.45	0.36	0.49	0.54	0.34	0.25	0.52	0.15	0.14	0.24	0.05
$\frac{1}{P99/50^2}$	0.19	0.23	0.35	0.31	0.32	0.42	0.24	0.4	0.26	0.07	0.12	0.12
$\frac{1}{P99/75^3}$	0.03	0.08	0.17	0.09	0.15	0.19	0.09	0.2	0.28	0.01	0.03	0.06
P99/90	0.02	0.02	0.41	0.06	0.07	0.43	0.1	0.07	0.35	0	0.01	0.1
CV	0.48	0.5	0.3	0.4	0.49	0.25	0.1	0.43	0.04	0.07	0.21	0.01
skew	0.24	0.32	0.31	0.43	0.42	0.35	0.41	0.39	0.31	0.17	0.18	0.15
Log(kurt)	0.54	0.52	0.34	0.54	0.53	0.3	0.29	0.46	0.19	0.19	0.26	0.08
L-CV	0.5	0.52	0.33	0.44	0.52	0.28	0.12	0.46	0.05	0.09	0.23	0.01
var	0.46	0.45		0.34	0.42		0.1	0.34		0.06	0.18	
SD	0.46	0.44		0.37	0.44		0.1	0.33		0.07	0.19	

Table 25. (Table 20 from section 5.3.1 altered to include corresponding results from Ozdemir and Donoghue (2013)) The R^2 values from each univariate linear regression between the field diversity measurements and LiDAR metrics are summarised here. The LiDAR metrics from both studies were calculated from all returns above 2m to remove the effect of understorey and the results from this study refer to the metrics after normalisation. R^2 values that are significant at a greater than 99% CI are highlighted in green, those at the 95% CI are highlighted in yellow

6.2.2 Assessing the Capacity for Models Constructed from Leaf-on and –off LiDAR Derived Metrics to Describe Tree Size Diversity Variables

I believe this research can be confident that, through validation involving statistical analysis and analysis of graphical representations shown in Section 4.4.1, the regression models constructed are valid and largely describe tree diversity variables to a significant degree. The models were kept as simple as possible in order to be easy to conceptualise whilst not sacrificing any substantial accuracy.

Model 3 describes up to 77% of THdiv utilising only leaf-off kurtosis and leaf-on variance (see Table 22 page 111). It is likely that the combination of metrics from the two separate datasets was able to offer some form of advantage, due to the high value of the Link test (Link test value of 1.68, the largest of all of the models) suggesting that these variables could describe the variability in the field data very well. However, Villikka et al. (2012) mention that utilising leaf-on and –off LiDAR data within the same model would often be impractical. When isolating each dataset to construct models 1 and 2 these were able to describe 65% of the variability in THdiv.

	Model	Dataset	Independent Variables	*t*	P>|t|	RMSE	R^2	F	*p*	
THdiv	1	Leaf-on	Kurtosis	-4.97	0.000	0.05	0.65	29.12	0.0000	Robust standard errors
			Variance	1.85	0.075					
	2	Leaf-off	Kurtosis	-3.88	0.001	0.05	0.65	24.68	0.0000	
			Variance	3.12	0.004					
	3	Leaf-on & -off	Kurtosis (leaf-off)	-6.04	0.000	0.04	0.77	44.98	0.0000	
			Variance (leaf-on)	5.41	0.000					
DBHdiv	4	Leaf-on	Skewness	6.37	<0.001	0.06	0.68	30.76	0.0000	Robust standard errors
			SD	3.44	0.002					
	5	Leaf-off	Skewness	4.82	0.000	0.06	0.71	20.82	0.0000	
			SD	4.96	0.000					
			P99/90	-2.34	0.027					
	6	Leaf-on & -off	Variance (leaf-off)	3.18	0.004	0.06	0.72	22.00	0.0000	
			Skewness (leaf-off)	3.56	0.001					
			CV (leaf-on)	2.85	0.008					
CLdiv	7	Leaf-on	Skewness	4.36	<0.001	0.06	0.41	19.02	0.0002	Robust standard errors
	8	Leaf-off	P99/75	2.57	0.016	0.05	0.62	13.94	0.0000	
			P99/50	-3.63	0.001					
			Variance	2.05	0.050					
CWdiv	9	Leaf-on	Kurtosis	-2.47	0.020	0.05	0.19	3.95	0.0197	Robust standard errors
	10	Leaf-off	Kurtosis	-3.58	0.001	0.05	0.26	9.57	0.0013	Robust standard errors

Table 22. (Reproduced from section 5.3.2). Each field diversity measurement has a corresponding model created from leaf-off LiDAR derived diversity metrics and leaf-on LiDAR derived diversity metrics. THdiv and DBHdiv also have a corresponding model created from a combination leaf-on and leaf-off LiDAR derived diversity metrics where this improved the accuracy of the regression. Similar models were not included for the CLdiv and CWdiv as the predictive ability of these compared to the single dataset model was lower.

Converse to expectations that regression models of THdiv would describe the most variability of all of the tree size diversity variables, it seems that single dataset models of DBHdiv (R^2= 0.68, 0.71 leaf –on and –off) surpass THdiv (R^2= 0.65 for both leaf-on and –off). This mirrors what was shown in Table 25 (page 109) in the correlation of LiDAR diversity metrics and tree size diversity variables and is in agreement with Mura et al. (2015) who modelled DBHdiv and THdiv (or standard deviation of DBH and tree height respectively) from various height summary statistics and found the best to

describe DBHdiv (with an R^2=0.63 utilising minimum, CV, skewness and 20th percentile of return height). This surpassed that describing THdiv (R^2 0.52 utilising minimum, CV and 20th percentile of return height). The large descriptive ability displayed by the THdiv and DBHdiv models is consistent with natural forest dynamics. Greater DBHdiv is linked to variability in tree size and shape, greater THdiv is more indicative of complex vertical forest structures and can be an excellent indicator of trees of different ages and species (Mura et al., 2015).

Considering how the significance and strength of relationships between LiDAR return height metrics and field derived diversity variables differed between this research and the study conducted by Ozdemir and Donoghue (2013) (see section 6.2.1) it is not surprising that when constructing their own models to describe forest structural diversity the authors chose different point based metrics to be incorporated (such as P99/90, CV and P99/25). Often these variables are included together in the models which would not have been possible in this study due to the high correlation between them in both LiDAR datasets. When comparing models constructed in this study to models constructed by Ozdemir and Donoghue (2013) it is clear that their inclusion of gridded texture measures greatly improved the descriptive ability (for example describing THdiv they achieved an R^2 0.85 and 0.75 compared to 0.65 in this study using a single dataset). Ozdemir and Donoghue (2013) found that texture measures were in fact superior to point based LiDAR metrics in explaining tree size diversity. Despite this, many additional authors have found point based metrics still of use to describe forest structure variables. Clawges et al. (2008) found that a LiDAR derived index of tree vegetation volume was highly correlated with the field-based tree vegetation density index (r^2= 0.68, r= 0.822, p<0.001, n= 204).

Models describing CLdiv under leaf-on conditions and CWdiv under both survey conditions (7, 9 and 10) show comparably lower and less significant descriptive abilities compared to models describing THdiv and DBHdiv. It is likely that the wide species diversity in the field dataset and the inability of

field methods to accurately constrain the whole crown footprint may have contributed to the models' low descriptive power. Crown width and length can be highly related to variables such as tree spacing (Smith and Reukema, 1986; Khan and Chaudhry, 2007) which were not utilised as dependant variables in the models.

Across the board leaf-off models seem to describe the variability in the field derived diversity variables to the same level as leaf-on models if not better. Villikka et al. (2012) also found that leaf-off LiDAR derived variables created more accurate regression models of stand volume and could distinguish between coniferous and deciduous trees. However regression models created to estimate above ground biomass and species richness using leaf-on and –off LiDAR datasets in a study by Hernández‐Stefanoni et al. (2015) showed that a larger percentage of both was described by leaf-on data though the differences between the two were insignificant and use of either would be comparably accurate.

Despite the differences identified between regression models constructed between the two LiDAR datasets, the metrics chosen for inclusion in all models were a consistently small group: kurtosis, variance, skewness and SD. Though L-CV and CV also displayed consistently high R^2 values when regressed against the independent diversity variables (0.46 – 0.53 for THdiv for example) these variables showed high levels of collinearity with many other variables and so could not be included alongside these.

6.2.3 Summary and Conclusions: What is the relative accuracy of models describing tree size diversity metrics generated from the LiDAR datasets?

Both leaf-on and -off datasets appear to provide diversity variables which correlate significantly with the field data. These are generally at a comparable level of correlation though selected leaf-

on or –off survey derived variables may be higher when regressed against specific field diversity variables. Leaf-off variables generally more significantly account for greater proportions of tree size diversity than leaf-on, especially with CLdiv and CWdiv. Variables which described tree size diversity well and were compatible for inclusion into multivariate models included kurtosis, variance, skewness and SD.

The regression models constructed from both datasets largely describe tree diversity variables to a significant degree. Leaf-off models tend to account for the same or greater amounts of variability in the field metrics than leaf-on, especially when considering crown shape diversity indices such as CLdiv and CWdiv. When the datasets are combined the regression model is able to describe over 10% more of the variance in THdiv than the leaf-on or –off datasets alone, though the practicality of creating such regression models is called into question due to the low cost effectiveness of multiple LiDAR surveys over the same area for research purposes alone.

6.3 Understanding What the Outcomes of Sections 6.1 and 6.2 Mean for LiDAR Survey Planning for Forest Biodiversity Investigations in the UK

6.3.1 Assessing how widely the applicability of observations obtained from this study could extend across the UK

Though a purposive strategy for choosing additional sample plots that would increase structural diversity was utilised (see section 4.1.1.2) this was limited by the coverage of both datasets and recent management activity at Chopwell Woodland Park. This meant that a very small selection of primarily evergreen coniferous plots could be included representing only a small selection of

evergreen coniferous species, limiting the applicability of the summary statistics describing these regression models to be applicable across the UK. Inclusion of more evergreen coniferous plots may have increased the accuracy of growth and sensor parameter corrections, enabling clearer assessments of the seasonal changes in tree biophysical parameters. Despite this it is questionable whether inclusion of more evergreen coniferous plots would have significantly improved the assessments of tree size diversity in this study. This is because the evergreen forested areas covered by both LiDAR campaigns over Chopwell Woodland Park do not incorporate more diverse age and species mixes than those already included due to their commercial management. Therefore it is unlikely that addition of further evergreen plots within the capture area would enhance the structural variability of the field dataset or the robustness of the regression models. The range of structural diversity in the field sites could still be seen as relatively large (THdiv range 0.156) in comparison to the Ozdemir and Donoghue (2013) where the range of variables such as THdiv was smaller (0.136).

Despite the apparent range of structural variability in the field dataset it would be naïve to assume that the selection of test sites within Chopwell Woodland Park is fully representative of all UK woodland. There are numerous environments which are not represented in the field data such as upland or wet woodlands comprising of species absent from this study. However, when considering low lying woodland comprised of common UK species, this dataset provides a satisfactory representation encompassing a range of management levels and additionally some stands of relatively rare ancient woodland.

6.3.2 Understanding How Differences Between Leaf-on and –off LiDAR Derived Forest Structure Metrics can Affect Estimates of Forest Biodiversity

In this study, after a basic correction for the effects of survey parameters and growth, leaf-on LiDAR data appear to better realise the upper canopy layers than leaf-off returns which penetrate further into the canopy layers of deciduous and mixed forest types during the leaf-off months. This led to maximum return heights from the leaf-on LiDAR dataset being higher than the leaf-off (by an average of 42cm in deciduous plots as discussed in section 6.1.1.1) and with comparable ground classifications between surveys indications are that leaf-on LiDAR datasets could provide better estimations of canopy height. Direct measurements of canopy height have been correlated to the suitability of habitat for birds and mammals (North et al., 1999; Nelson et al., 2005) and can be used as an important indicator of forest successional stage (Morgan and Freedman, 1986).

For modelling tree size diversity leaf-off LiDAR data appear to have an equal or better capacity to describe tree size diversity indices providing an important advantage. Vertical forest structure can in itself be used as a conceptual framework for habitat structure (McCoy and Bell, 1991) and so accurate LiDAR representations of this can be incredibly important. Clawges et al. (2008) and Goetz et al. (2010) found that LiDAR derived vegetation structure diversity data were positively and significantly correlated with indices of bird species diversity. Low diversity in overstorey structure has been linked to low understorey diversity in temperate forests by Lenière and Houle (2006)]. Greater tree height variability indicates trees of different ages and species that are more suitable to host multiple species of animals (Sullivan et al., 2001; Svensson and Jeglum, 2001; Zenner and Hibbs, 2000). Conversely, DBH diversity is a measure of the variability in tree size, and is considered indicative for the presence and for the diversity of micro-habitats within a forest (Acker et al., 1998; Van Den Meersschaut and Vandekerkhove, 2000).

6.3.3 Summary and Conclusions: When is best to undertake airborne LiDAR survey when modelling forest structure diversity?

The results suggest strongly that both leaf-on and off airborne LiDAR datasets provide the capacity to describe the structural diversity of comparative lowland woodland across the UK. The results (see Table 22 page 111) and discussion in section 6.3.2 also should provide guidance into when may be most appropriate to undertake LiDAR acquisition flights for biodiversity analysis depending on the forest structural diversity metrics of interest. If diversity in tree height or DBH across a stand is used to facilitate mapping of habitat suitability for example (Sullivan et al., 2001; Svensson and Jeglum, 2001; Zenner and Hibbs, 2000) then it is unlikely that any significant improvements in LiDAR diversity estimations would be gained by undertaking a LiDAR survey at a particular time of year. However, some advantage may be gained in such a scenario when combining multi-seasonal LiDAR datasets as demonstrated by the greater ability of models to describe height and DBH diversity where leaf-on and –off diversity variables are combined. This would only be appropriate after careful co-registration of the multiple LiDAR datasets to avoid incorporating bias. Additionally, the advantages provided by combining datasets should be weighed up against the increased costs of additional surveys and time and effort taken to process additional datasets.

This is not the case for crown shape diversity indices, better estimates of crown shape diversity (CLdiv and CWdiv) can be obtained from LiDAR data collected over deciduous and mixed deciduous/evergreen coniferous plots during leaf-off periods (see Table 25 page 109 and Table 22 page 111). As discussed combining crown shape diversity metrics obtained from multi-season LiDAR datasets in models does not appear to provide an advantage.

7. EVALUATION AND FURTHER WORK

7.1 Evaluation of methodology

7.1.1 Potential Sources of Error

7.1.1.1 *Field Data*

The two field data collection campaigns utilised in this research were undertaken with the gap between spanning just under two years. The first field data collection period collected by Ozdemir and Donoghue (2013) spanned the period May-July 2011 and additional data collection to facilitate this study was undertaken in February and March 2013. Between field data collections and LiDAR surveys tree growth will have inevitably made the accuracy of representation of vegetation during LiDAR surveys variable. However, though analysis of tree size indices from the LiDAR were made and compared to the field data the main focus of the study was on diversity measures. It is demonstrated in Table 19 pages 85 and 104 that in plots with the fastest growing tree species (coniferous evergreen) the growth between surveys did not make a significant difference to the diversity metrics.

The earlier field data collection took place under leaf-on conditions (May, June and July 2011) and could have affected the ability of the Vertex hypsometer to reach the very top of the tree crown through the occlusive canopy. This could result in underestimation of tree heights though it was endeavoured during fieldwork that the very top of the tree was visible to minimise these issues. Additionally as the Vertex hypsometer has the ability to travel around some small occlusive branches and leaves this further minimises this issue.

Finally, tree death, disease or tree fall could have occurred between field surveys or LiDAR surveys again reducing the relevance to the representations of the plots in the LiDAR surveys. However communication with the Forestry Commission indicated that it was unlikely any harvesting or management had taken place since the first round of field data collection this was independently assessed in the field and also checked in the LiDAR data (see section 5.2.3) and as a result plot 12 was removed from analysis.

7.1.1.2 *LiDAR Data*

A large amount of effort was made to reduce both the systematic error between LiDAR datasets through co-registration, and random error through manual check of the point clouds for each plot. The only remaining potential source of error from the LiDAR dataset was the classification of the ground returns and correcting the corresponding point clouds to height above ground. Due to the differing levels of canopy openness it could be possible that one or both of the LiDAR datasets did not hold a true representation of the LiDAR ground surface. This was taken into account by this study and added an additional factor to the performance assessment of each dataset.

Though not necessarily an error, the time between surveys and change in survey parameters has shown to have greatly influenced the LiDAR derived metrics as discussed in detail in section 6. Though an immediately obvious significant influence on the tree size diversity metrics is not seen, this influence may have weakened the strength of the regression models in this study.

7.1.1.3 *Contextual Data*

Due to the low precision in the Forestry Commission sub-compartment database delineating additional sample plots which encompassed the required tree size diversity was difficult in the field but will not have introduced error as no measurements came directly from this database. Though some contextual data such as plantation dates were incorporated into the study to aid the selection of new survey sites, again these were not directly used in analysis.

7.1.2 Improvements

If presented with the same LiDAR and field dataset again an improvement on the current methods could include resurvey of a large range of the field data plots after a set amount of time had passed (for example two years). This could provide vital growth information for the entire range of species present in the field plots and would allow for correction of growth between field data collections and between LiDAR surveys. This however would have required a significantly longer amount of time in the field which was unlikely to be accommodated during a master's degree program timescale.

An additional interesting task could have included isolation of the regression models by plot type, to see if seasonality influenced deciduous and mixed plots more than evergreen coniferous. However, this would have produced just under twice as many regression models to analyse and with ten models constructed within the study already allowing for a wealth of observations to be discussed this could be considered instead for future work.

Despite the valuable conclusions drawn within this study there are further avenues that could be explored to reinforce or potentially challenge these. It would be incredibly useful to undertake a

similar study but with a much shorter time gap between LiDAR data and field data acquisitions to dramatically reduce the influence of tree growth. LiDAR surveys taken a matter of months apart still allowing for leaf-on and –off data acquisition would be ideal though these scenarios are likely to be incredibly rare due to the lack of cost effectiveness. In addition, if field data collection took place in one campaign this would remove the uncertainty introduced by a prolonged time period between field mobilisations.

Ideally further research would aim to include a larger proportion of evergreen coniferous plots, to better understand the effects of growth and survey parameters if these cannot be controlled, and also field sites from further UK woodland environments, in order to extend the applicability of conclusions across the UK.

Investigation of the comparable effects of seasonal canopy closure on point based metrics (as in this study) and grid based and raster based metrics of diversity would allow a full understanding of the effects of canopy closure on all diversity metrics and aid survey planning decisions.

7.2 Further Work

This study has explored the effect of seasonal changes in canopy conditions on aerial LiDAR derived forest structure diversity metrics, ground classification and direct LiDAR measurements of tree biophysical parameters. It would be interesting to extend this research to consider the terrestrial LiDAR perspective to see if these systems are similarly effected by canopy conditions. Additionally extending this research to consider technologies such as multi-spectral, full-waveform LiDAR systems and SAR systems would be incredibly interesting as systems of this nature are increasing in use and capability. Furthermore, assessing the seasonal differences in the intensity of returning

discrete pulses or waveforms or multi-spectral data collected from advanced LiDAR systems could aid assessments of vegetation health or species classification.

8. REFERENCES

Acker, S., Sabin, T., Ganio, L. & McKee, W. (1998). Development of old-growth structure and timber volume growth trends in maturing Douglas-fir stands. *Forest Ecology and Management,* **104**, 265-280.

Ahokas, E., Kaasalainen, S., Hyyppä, J. & Suomalainen, J. (2006). Calibration of the Optech ALTM 3100 laser scanner intensity data using brightness targets. *International Archives of Photogrammetry, Remote Sensing and Spatial Information Sciences,* **36**, 1Á6.

Amable, G., Devereux, B., Cockerell, T. & Renshaw, G. (2004). Analysis of interaction patterns between vegetation canopies and small footprint, high-density, airborne LiDAR. *In:* Proceedings of the 20th International Society for Photogrammetry and Remote Sensing Congress, Istanbul, 2004.

Axelsson, P. (1999). Processing of laser scanner data—algorithms and applications. *ISPRS Journal of Photogrammetry and Remote Sensing,* **54**, 138-147.

Axelsson, P. (2000). DEM generation from laser scanner data using adaptive TIN models. *International Archives of Photogrammetry and Remote Sensing,* **33**, 111-118.

Baltsavias, E. P. (1999). Airborne laser scanning: basic relations and formulas. *ISPRS Journal of Photogrammetry and Remote Sensing,* **54**, 199-214.

Beier, P. & Drennan, J. E. (1997). Forest structure and prey abundance in foraging areas of northern goshawks. *Ecological Applications,* **7**, 564-571.

Bergen, K., Goetz, S., Dubayah, R., Henebry, G., Hunsaker, C., Imhoff, M., Nelson, R., Parker, G. & Radeloff, V. (2009). Remote sensing of vegetation 3-D structure for biodiversity and habitat: Review and implications for lidar and radar spaceborne missions. *Journal of geophysical research,* **114**, G00E06.

Berger, A. L. & Puettmann, K. J. (2000). Overstory composition and stand structure influence herbaceous plant diversity in the mixed aspen forest of northern Minnesota. *The American Midland Naturalist,* **143**, 111-125.

Bolton, D., Coops, N. & Wulder, M. (2013). Measuring forest structure along productivity gradients in the Canadian boreal with small-footprint Lidar. *Environmental monitoring and assessment*.

Božić, M., Čavlović, J., Lukić, N., Teslak, K. & Kos, D. (2005). Efficiency of ultrasonic Vertex III hypsometer compared to the most commonly used hypsometers in Croatian forestry. *Croatian Journal of Forest Engineering,* **26**, 91-99.

Bradbury, R. B., Hill, R. A., Mason, D. C., Hinsley, S. A., Wilson, J. D., Balzter, H., Anderson, G. Q., Whittingham, M. J., Davenport, I. J. & Bellamy, P. E. (2005). Modelling relationships between birds and vegetation structure using airborne LiDAR data: a review with case studies from agricultural and woodland environments. *Ibis,* **147**, 443-452.

Brandtberg, T., Warner, T. A., Landenberger, R. E. & McGraw, J. B. (2003). Detection and analysis of individual leaf-off tree crowns in small footprint, high sampling density lidar data from the eastern deciduous forest in North America. *Remote sensing of Environment,* **85**, 290-303.

Breusch, T. S. & Pagan, A. R. (1979). A simple test for heteroscedasticity and random coefficient variation. *Econometrica: Journal of the Econometric Society*, 1287-1294.

Brodmann, P. A., Reyer, H.-U., Bollmann, K., Schläpfer, A. R. & Rauter, C. (1997). The importance of food quantity and quality for reproductive performance in alpine water pipits (Anthus spinoletta). *Oecologia,* **109**, 200-208.

Brokaw, N. V. L. & Lent, R. A. (1999). Vertical Structure. *In:* Hunter, M. L. (ed.) *Maintaining Biodiversity in Forest Ecosystems.* University of Maine, Orono: Cambridge University Press.

Broughton, R. K., Hinsley, S. A., Bellamy, P. E., Hill, R. A. & Rothery, P. (2006). Marsh Tit Poecile palustris territories in a British broad‐leaved wood. *Ibis,* **148**, 744-752.

Butchart, S. H. M., Walpole, M., Collen, B., van Strien, A., Scharlemann, J. P. W., Almond, R. E. A., Baillie, J. E. M., Bomhard, B., Brown, C. & Bruno, J. (2010). Global biodiversity: indicators of recent declines. *Science,* **328**, 1164-1168.

Cameron, A. C. & Trivedi, P. K. (1990). Regression-based tests for overdispersion in the Poisson model. *Journal of econometrics,* **46**, 347-364.

Chasmer, L., Hopkinson, C., Smith, B. & Treitz, P. (2006). Examining the influence of changing laser pulse repetition frequencies on conifer forest canopy returns. *Photogrammetric Engineering & Remote Sensing,* **72**, 1359-1367.

Clawges, R., Vierling, K., Vierling, L. & Rowell, E. (2008). The use of airborne lidar to assess avian species diversity, density, and occurrence in a pine/aspen forest. *Remote Sensing of Environment,* **112**, 2064-2073.

Coops, N. C., Hilker, T., Wulder, M. A., St-Onge, B., Newnham, G., Siggins, A. & Trofymow, J. A. (2007). Estimating canopy structure of Douglas-fir forest stands from discrete-return LiDAR. *Trees,* **21**, 295-310.

Donoghue, D. N., Watt, P. J., Cox, N. J. & Wilson, J. (2007). Remote sensing of species mixtures in conifer plantations using LiDAR height and intensity data. *Remote Sensing of Environment,* **110**, 509-522.

Duong, V., Lindenbergh, R., Pfeifer, N. & Vosselman, G. (2008). Single and two epoch analysis of ICESat full waveform data over forested areas. *International Journal of Remote Sensing,* **29**, 1453-1473.

EDINA (2013). Digimap. Edina.

Forestry-Commission. (2009). *Wildlife at Chopwell Woodland Park*. URL: http://www.forestry.gov.uk/website/wildwoods.nsf/LUWebDocsByKey/EnglandTyneandWearNoForestChopwellWoodlandPark.

Forestry-Commission (2013). NATIONAL_FOREST_INVENTORY_ENGLAND_2013. *In:* GeoData, M. (ed.).

Forestry-Commission. (2015). *Sitka spruce - picea sitchensis*. URL: http://www.forestry.gov.uk/forestry/INFD-5NLEJ6 [5th November].

Frazer, G., Magnussen, S., Wulder, M. & Niemann, K. (2011). Simulated impact of sample plot size and co-registration error on the accuracy and uncertainty of LiDAR-derived estimates of forest stand biomass. *Remote Sensing of Environment,* **115**, 636-649.

Gatziolis, D., Fried, J. S. & Monleon, V. S. (2010). Challenges to estimating tree height via LiDAR in closed-canopy forests: A parable from western Oregon. *Forest Science,* **56**, 139-155.

Gobakken, T. & Næsset, E. (2008). Assessing effects of laser point density, ground sampling intensity, and field sample plot size on biophysical stand properties derived from airborne laser scanner data. *Canadian Journal of Forest Research,* **38**, 1095-1109.

Gobakken, T. G. T. & Næsset, E. N. E. (2009). Assessing effects of positioning errors and sample plot size on biophysical stand properties derived from airborne laser scanner data. *Canadian Journal of Forest Research,* **39**, 1036-1052.

Goetz, S., Steinberg, D., Dubayah, R. & Blair, B. (2007). Laser remote sensing of canopy habitat heterogeneity as a predictor of bird species richness in an eastern temperate forest, USA. *Remote Sensing of Environment,* **108**, 254-263.

Goetz, S. J., Steinberg, D., Betts, M. G., Holmes, R. T., Doran, P. J., Dubayah, R. & Hofton, M. (2010). Lidar remote sensing variables predict breeding habitat of a Neotropical migrant bird. *Ecology,* **91**, 1569-1576.

Goodwin, N. R., Coops, N. C. & Culvenor, D. S. (2006). Assessment of forest structure with airborne LiDAR and the effects of platform altitude. *Remote Sensing of Environment,* **103**, 140-152.

Hadley, J. L. & Smith, W. K. (1986). Wind effects on needles of timberline conifers: seasonal influence on mortality. *Ecology*, 12-19.

Hall, F. G., Bergen, K., Blair, J. B., Dubayah, R., Houghton, R., Hurtt, G., Kellndorfer, J., Lefsky, M., Ranson, J. & Saatchi, S. (2011). Characterizing 3D vegetation structure from space: Mission requirements. *Remote Sensing of Environment,* **115**, 2753-2775.

Hall, S., Burke, I., Box, D., Kaufmann, M. & Stoker, J. (2005). Estimating stand structure using discrete-return lidar: an example from low density, fire prone ponderosa pine forests. *Forest Ecology and Management,* **208**, 189-209.

He, Q. S. & Li, N. (2012). Estimation of individual tree parameters using small-footprint LiDAR with Different density in a coniferous forest. *Advanced Materials Research,* **518**, 5320-5323.

Hernández‐Stefanoni, J. L., Johnson, K. D., Cook, B. D., Dupuy, J. M., Birdsey, R., Peduzzi, A. & Tun‐Dzul, F. (2015). Estimating species richness and biomass of tropical dry forests using LIDAR during leaf‐on and leaf‐off canopy conditions. *Applied Vegetation Science,* **18**, 724-732.

Hill, R. & Broughton, R. K. (2009). Mapping the understorey of deciduous woodland from leaf-on and leaf-off airborne LiDAR data: A case study in lowland Britain. *ISPRS Journal of Photogrammetry and Remote Sensing,* **64**, 223-233.

Hill, R., Hinsley, S., Gaveau, D. L. & Bellamy, P. E. (2004). Cover: Predicting habitat quality for Great Tits (Parus major) with airborne laser scanning data.

Hinsley, S., Hill, R., Fuller, R., Bellamy, P. E. & Rothery, P. (2009). Bird species distributions across woodland canopy structure gradients. *Community Ecology,* **10**, 99-110.

Hinsley, S., Hill, R., Gaveau, D. L. & Bellamy, P. E. (2002). Quantifying woodland structure and habitat quality for birds using airborne laser scanning. *Functional Ecology,* **16**, 851-857.

Höfle, B. & Pfeifer, N. (2007). Correction of laser scanning intensity data: Data and model-driven approaches. *ISPRS Journal of Photogrammetry and Remote Sensing,* **62**, 415-433.

Hollaus, M., Wagner, W., Eberhöfer, C. & Karel, W. (2006). Accuracy of large-scale canopy heights derived from LiDAR data under operational constraints in a complex alpine environment. *ISPRS Journal of Photogrammetry and Remote Sensing,* **60**, 323-338.

Hopkinson, C. (2007). The influence of flying altitude, beam divergence, and pulse repetition frequency on laser pulse return intensity and canopy frequency distribution. *Canadian Journal of Remote Sensing,* **33**, 312-324.

Hudak, A. T., Crookston, N. L., Evans, J. S., Hall, D. E. & Falkowski, M. J. (2008). Nearest neighbor imputation of species-level, plot-scale forest structure attributes from LiDAR data. *Remote Sensing of Environment,* **112**, 2232-2245.

Hyde, P., Dubayah, R., Peterson, B., Blair, J., Hofton, M., Hunsaker, C., Knox, R. & Walker, W. (2005). Mapping forest structure for wildlife habitat analysis using waveform lidar: Validation of montane ecosystems. *Remote sensing of environment,* **96**, 427-437.

Hyde, P., Dubayah, R., Walker, W., Blair, J. B., Hofton, M. & Hunsaker, C. (2006). Mapping forest structure for wildlife habitat analysis using multi-sensor (LiDAR, SAR/InSAR, ETM+, Quickbird) synergy. *Remote Sensing of Environment,* **102**, 63-73.

Hyyppä, H., Yu, X., Hyyppä, J., Kaartinen, H., Kaasalainen, S., Honkavaara, E. & Rönnholm, P. (2005). Factors affecting the quality of DTM generation in forested areas. *International Archives of Photogrammetry, Remote Sensing and Spatial Information Sciences,* **36**, 85-90.

Jakubowski, M. K., Guo, Q. & Kelly, M. (2013). Tradeoffs between lidar pulse density and forest measurement accuracy. *Remote Sensing of Environment,* **130**, 245-253.

Jansson, G. & Andrén, H. (2003). Habitat composition and bird diversity in managed boreal forests. *Scandinavian Journal of Forest Research,* **18**, 225-236.

Jenkins, T. (2009). Growth and yield models for improved Sitka spruce. *In:* Commission, F. (ed.).

Jones, T. G., Coops, N. C. & Sharma, T. (2012). Assessing the utility of LiDAR to differentiate among vegetation structural classes. *Remote Sensing Letters,* **3**, 231-238.

Jutzi, B. & Stilla, U. (2006). Range determination with waveform recording. *Journal of Phorogrammetry and Remote Sensing,* **61**, 95-107.

Khan, G. & Chaudhry, A. K. (2007). Effect of spacing and plant density on the growth of poplar (Populus deltoides) trees under agro-forestry system. *Pak J Agric Sci,* **44**, 321-327.

Kim, S., McGaughey, R. J., Andersen, H.-E. & Schreuder, G. (2009). Tree species differentiation using intensity data derived from leaf-on and leaf-off airborne laser scanner data. *Remote Sensing of Environment,* **113**, 1575-1586.

Kimmins, J. (1997). Biodiversity and its relationship to ecosystem health and integrity. *The Forestry Chronicle,* **73**, 229-232.

Kraus, K. & Pfeifer, N. (1998). Determination of terrain models in wooded areas with airborne laser scanner data. *ISPRS Journal of Photogrammetry and remote Sensing,* **53**, 193-203.

Landy, J. (2011). *Sub-canopy terrain modelling for archaeological prospecting in forested areas through multiple-echo discrete-pulse laser ranging: a case study from Chopwell Wood, Tyne & Wear.* Durham University.

Lefsky, M. A., Cohen, W. B., Acker, S. A., Parker, G. G., Spies, T. A. & Harding, D. (1999a). Lidar Remote Sensing of the Canopy Structure and Biophysical Properties of Douglas-Fir Western Hemlock Forests. *Remote Sensing of Environment,* **70**, 339–361.

Lefsky, M. A., Cohen, W. B., Parker, G. G. & Harding, D. J. (2002). Lidar Remote Sensing for Ecosystem Studies. *BioScience,* **52**, 19-30.

Lefsky, M. A., Harding, D., Cohen, W. B., Parker, G. & Shugart, H. H. (1999b). Surface Lidar Remote Sensing of Basal Area and Biomass in Deciduous Forests of Eastern Maryland, USA. *Remote Sensing of Environment,* **67**, 83–98.

Lei, X., Wang, W. & Peng, C. (2009). Relationships between stand growth and structural diversity in spruce-dominated forests in New Brunswick, Canada. *Canadian journal of forest research,* **39**, 1835-1847.

Lenière, A. & Houle, G. (2006). Response of herbaceous plant diversity to reduced structural diversity in maple-dominated (Acer saccharum Marsh.) forests managed for sap extraction. *Forest Ecology and Management,* **231**, 94-104.

Li, J., Hu, B. & Noland, T. L. (2013). Classification of tree species based on structural features derived from high density LiDAR data. *Agricultural and Forest Meteorology,* **171**, 104-114.

Lillesand, T., Kiefer, R. W. & Chipman, J. (2014). *Remote sensing and image interpretation.* John Wiley & Sons.

Lim, K., Treitz, P., Wulder, M., St-Onge, B. & Flood, M. (2003). LiDAR remote sensing of forest structure. *Progress in Physical Geography,* **27**, 88-106.

Lindberg, E., Olofsson, K., Holmgren, J. & Olsson, H. (2012). Estimation o f 3D vegetation structure from waveform and discrete return airborne laser scanning data. *Remote Sensing of Environment,* **118**, 151-161.

Lovell, J., Jupp, D., Newnham, G., Coops, N. & Culvenor, D. (2005). Simulation study for finding optimal lidar acquisition parameters for forest height retrieval. *Forest Ecology and Management,* **214**, 398-412.

Ma, H., Song, J., Wang, J., Xiao, Z. & Fu, Z. (2014). Improvement of spatially continuous forest LAI retrieval by integration of discrete airborne LiDAR and remote sensing multi-angle optical data. *Agricultural and Forest Meteorology,* **189**, 60-70.

Mackie, E. D. & Matthews, R. W. (2008). *Timber measurement: field guide.* Forestry Commission.

Mallet, C. & Bretar, F. (2009). Full-waveform topographic lidar: State-of-the-art. *ISPRS Journal of photogrammetry and remote sensing,* **64**, 1-16.

Mallows, C. L. (1986). Augmented partial residuals. *Technometrics,* **28**, 313-319.

Martin, F. C. & Flewelling, J. W. (1998). Evaluation of tree height prediction models for stand inventory. *Western Journal of Applied Forestry,* **13**, 109-119.

Martinuzzi, S., Vierling, L. A., Gould, W. A. & Vierling, K. T. (2009). Improving the characterization and mapping of wildlife habitats with lidar data: Measurement priorities for the inland northwest, USA. *The Gap Analysis Program... in Brief,* **1**, 1.

McCoy, E. D. & Bell, S. S. (1991). Habitat structure: the evolution and diversification of a complex topic. *Habitat structure.* Springer.

Morgan, K. & Freedman, B. (1986). Breeding Bird Communities in a Hardwood Forest Succession in Nova-Scotia. *Canadian Field-Naturalist*.

Morsdorf, F., Meier, E., Ko¨tz, B., Itten, K. I., Dobbertin, M. & Allgo¨wer, B. (2004). LIDAR-based geometric reconstruction of boreal type forest stands at single tree level for forest and wildland fire management. *Remote Sensing of Environment,* **92**, 353–362.

Mura, M., McRoberts, R. E., Chirici, G. & Marchetti, M. (2015). Estimating and mapping forest structural diversity using airborne laser scanning data. *Remote Sensing of Environment,* **170**, 133-142.

Næsset, E. (2002). Predicting forest stand characteristics with airborne scanning laser using a practical two-stage procedure and field data. *Remote Sensing of Environment,* **80**, 88-99.

Næsset, E. (2004). Effects of different flying altitudes on biophysical stand properties estimated from canopy height and density measured with a small-footprint airborne scanning laser. *Remote Sensing of Environment,* **91**, 243-255.

Næsset, E. (2005). Assessing sensor effects and effects of leaf-off and leaf-on canopy conditions on biophysical stand properties derived from small-footprint airborne laser data. *Remote Sensing of Environment,* **98**, 356-370.

Næsset, E. & Bjerknes, K.-O. (2001). Estimating tree heights and number of stems in young forest stands using airborne laser scanner data. *Remote Sensing of Environment,* **78**, 328-340.

Næsset, E., Gobakken, T. & Nelson, R. (Year). Sampling and mapping forest volume and biomass using airborne LIDARs. *In:* Proceedings of the eight annual forest inventory and analysis symposium, 2006. 297-301.

Nelson, R., Keller, C. & Ratnaswamy, M. (2005). Locating and estimating the extent of Delmarva fox squirrel habitat using an airborne LiDAR profiler. *Remote Sensing of Environment,* **96**, 292-301.

North, M. P., Franklin, J. F., Carey, A. B., Forsman, E. D. & Hamer, T. (1999). Forest stand structure of the northern spotted owl's foraging habitat. *Forest Science,* **45**, 520-527.

O'brien, R. M. (2007). A caution regarding rules of thumb for variance inflation factors. *Quality & Quantity,* **41**, 673-690.

Oliver, C. D. & Larson, B. C. (1990). *Forest stand dynamics.* McGraw-Hill, Inc.

Ørka, H. O., Næsset, E. & Bollandsås, O. M. (2010). Effects of different sensors and leaf-on and leaf-off canopy conditions on echo distributions and individual tree properties derived from airborne laser scanning. *Remote Sensing of Environment,* **114**, 1445-1461.

Ozdemir, I. & Donoghue, D. N. (2013). Modelling tree size diversity from airborne laser scanning using canopy height models with image texture measures. *Forest Ecology and Management,* **295**, 28-37.

Peck, J. E., Zenner, E. K., Brang, P. & Zingg, A. (2014). Tree size distribution and abundance explain structural complexity differentially within stands of even-aged and uneven-aged structure types. *European journal of forest research,* **133**, 335-346.

Persson, A., Holmgren, J. & Söderman, U. (2002). Detecting and measuring individual trees using an airborne laser scanner. *Photogrammetric Engineering and Remote Sensing,* **68**, 925-932.

Popescu, S. C. & Zhao, K. (2008). A voxel-based lidar method for estimating crown base height for deciduous and pine trees. *Remote Sensing of Environment,* **112**, 767-781.

Pregibon, D. (1979). *Data analytic methods for generalized linear models.* c1979.

Proulx, R. & Parrott, L. (2009). Structural complexity in digital images as an ecological indicator for monitoring forest dynamics across scale, space and time. *Ecological Indicators,* **9**, 1248–1256.

Recher, H., Majer, J. & Ganesh, S. (1996). Eucalypts, arthropods and birds: on the relation between foliar nutrients and species richness. *Forest Ecology and Management,* **85**, 177-195.

Reitberger, J., Krzystek, P. & Stilla, U. (2008). Analysis of full waveform LIDAR data for the classification of deciduous and coniferous trees. *International journal of remote sensing,* **29**, 1407-1431.

Royston, P. (1992). Which measures of skewness and kurtosis are best? *Statistics in Medicine,* **11**, 333-343.

Saatchi, S., Halligan, K., Despain, D. G. & Crabtree, R. L. (2007). Estimation of forest fuel load from radar remote sensing. *Geoscience and Remote Sensing, IEEE Transactions on,* **45**, 1726-1740.

Searle, L. (2000). Chopwell Wood, past and present. *Friends of Chopwell Wood*.

Shi, J.-q. & Shi, Z.-L. (Year). Study of matching the lidar data set on overlapping flightstrips. *In:* International Symposium on Lidar and Radar Mapping Technologies, 2011. International Society for Optics and Photonics, 82860W-82860W-7.

Simonson, W. D., Allen, H. D. & Coomes, D. A. (2012). Use of an airborne lidar system to model plant species composition and diversity of Mediterranean oak forests. *Conservation Biology,* **26**, 840-850.

Smith, J. H. G. & Reukema, D. L. (1986). Effects of plantation and juvenile spacing on tree and stand development.

Soininen, A. (2015). Terrasolid. 014.013 ed.

Soininen, A. (2016). Terrascan User's Guide. Terrasolid.

Solberg, S., Naesset, E. & Bollandsas, O. M. (2006). Single Tree Segmentation Using Airborne Laser Scanner Data in a Structurally Heterogeneous Spruce Forest. *Photogrammetric Engineering & Remote Sensing,* **72**, 1369–1378.

StataCorp. (2013). *Stata 13 Base Reference Manual.* College Station: TX: Stata Press.

Sullivan, T. P., Sullivan, D. S. & Lindgren, P. M. (2001). Stand structure and small mammals in young lodgepole pine forest: 10-year results after thinning. *Ecological Applications,* **11**, 1151-1173.

Svensson, J. S. & Jeglum, J. K. (2001). Structure and dynamics of an undisturbed old-growth Norway spruce forest on the rising Bothnian coastline. *Forest Ecology and Management,* **151**, 67-79.

Swatantran, A., Dubayah, R., Hofton, M., Blair, J. & Handley, L. (Year). Mapping Potential Ivory Billed Woodpecker Habitat using Lidar and Hyperspectral Data Fusion. *In:* AGU Fall Meeting Abstracts, 2008. 04.

Takahashi, T., Awaya, Y., Hirata, Y., Furuya, N., Sakai, T. & Sakai, A. (2010). Stand volume estimation by combining low laser-sampling density LiDAR data with QuickBird panchromatic imagery in closed-canopy Japanese cedar (Cryptomeria japonica) plantations. *International Journal of Remote Sensing,* **31**, 1281-1301.

Tesfamichael, S., Van Aardt, J. & Ahmed, F. (2010). Estimating plot-level tree height and volume of Eucalyptus grandis plantations using small-footprint, discrete return lidar data. *Progress in Physical Geography,* **34**, 515-540.

Thiel, K. & Wehr, A. (2004). Performance Capabilities of Laser-Scanners-An Overview and Measurement Principle Analysis. *International Archives of Photogrammetry, Remote Sensing and Spatial Information Sciences,* **36**, W2.

Townsend Peterson, A. & Kluza, D. A. (2003). New distributional modelling approaches for gap analysis. *Animal Conservation,* **6**, 47-54.

Treitz, P., Lim, K., Woods, M., Pitt, D., Nesbitt, D. & Etheridge, D. (2012). LiDAR sampling density for forest resource inventories in Ontario, Canada. *Remote Sensing,* **4**, 830-848.

Ussyshkin, V. & Theriault, L. (2011). Airborne lidar: advances in discrete return technology for 3D vegetation mapping. *Remote Sensing,* **3**, 416-434.

Van Den Meersschaut, D. & Vandekerkhove, K. (2000). Development of a stand-scale forest biodiversity index based on the State Forest Inventory.

Vepakomma, U., St-Onge, B. & Kneeshaw, D. (2008). Spatially explicit characterization of boreal forest gap dynamics using multi-temporal lidar data. *Remote Sensing of Environment,* **112**, 2326-2340.

Villikka, M., Packalén, P. & Maltamo, M. (2012). The suitability of leaf-off airborne laser scanning data in an area-based forest inventory of coniferous and deciduous trees. *Silva Fenn,* **46**, 99-110.

Wagner, W., Ullrich, A., Melzer, T., Briese, C. & Kraus, K. (2004). From single-pulse to full-waveform airborne laser scanners: potential and practical challenges.

Waring, R. H., Way, J., Hunt, E. R., Morrissey, L., Ranson, K. J., Weishampel, J. F., Oren, R. & Franklin, S. E. (1995). Imaging radar for ecosystem studies. *BioScience,* **45**, 715-723.

Wasser, L., Day, R., Chasmer, L. & Taylor, A. (2013). Influence of vegetation structure on lidar-derived canopy height and fractional cover in forested riparian buffers during leaf-off and leaf-on conditions. *PloS one,* **8**, e54776.

Watt, M., Meredith, A., Watt, P. & Gunn, A. (2013). Use of LiDAR to estimate stand characteristics for thinning operations in young Douglas-fir plantations. *NZJ For. Sci,* **43**.

Watt, P. J. (2005). *An evaluation of LiDAR and optical satellite data for the measurement of structural attributes in British upland conifer plantation forestry.* Durham University.

Wehr, A. & Lohr, u. (1999). Airborne laser scanning-an introduction and overview. *Journal of Phorogrammetry and Remote Sensing,* **54**, 68-82.

Weisberg, S. (2005). *Applied linear regression.* John Wiley & Sons.

Whittingham, M. & Markland, H. (2002). The influence of substrate on the functional response of an avian granivore and its implications for farmland bird conservation. *Oecologia,* **130**, 637-644.

Wulder, M. & Franklin, S. E. (2003). *Remote sensing of forest environments: concepts and case studies.* Springer Science & Business Media.

Yu, X., Hyyppä, J., Hyyppä, H. & Maltamo, M. (2004a). Effects of flight altitude on tree height estimation using airborne laser scanning. *Proceedings of the Laser Scanners for Forest and Landscape Assessment–Instruments, Processing Methods and Applications*, 02-06.

Yu, X., Hyyppä, J., Kaartinen, H. & Maltamo, M. (2004b). Automatic detection of harvested trees and determination of forest growth using airborne laser scanning. *Remote Sensing of Environment,* **90**, 451-462.

Zakšek, K., Pfeifer, N. & IAPŠ, Z. S. (2006). An improved morphological filter for selecting relief points from a LIDAR point cloud in steep areas with dense vegetation. *Luubljana, Slovenia and Innsbruck, Austria: Institute of Anthropological and Spatial Studies, Scientific Research Centre of the Slovenian Academy of Sciences and Arts, and Institute of Geography, Innsbruck University*.

Zenner, E. K. & Hibbs, D. E. (2000). A new method for modeling the heterogeneity of forest structure. *Forest ecology and management,* **129**, 75-87.

Zimble, D. A., Evans, D. L., Carlson, G. C., Parker, R. C., Grado, S. C. & Gerard, P. D. (2003). Characterizing vertical forest structure using small-footprint airborne LiDAR. *Remote Sensing of Environment,* **87**, 171–182.

APPENDICES

Appendix 1

Summaries of each of the LiDAR derived diversity variables which were transformed to increase the normality of the distribution.

Leaf-on variables

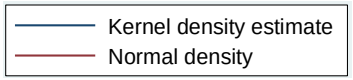

Variable	Transf.	Min	Max	Mean	pre-transform	post-transform
Kurtosis	Log	0.49	2.32	1.46	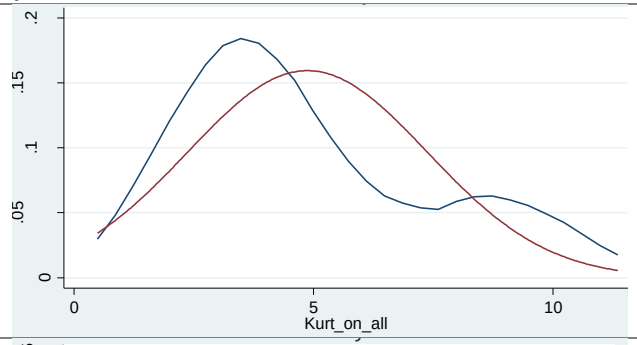	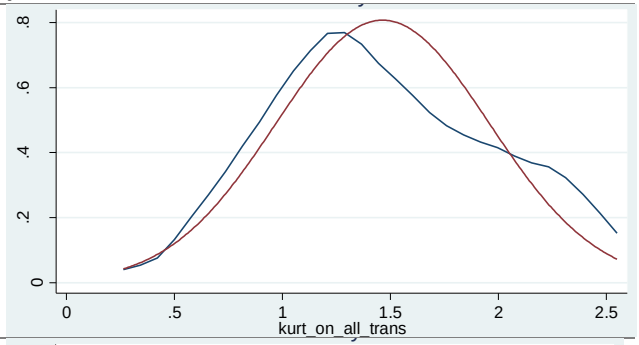
P99/25	inverse	0.35	0.78	0.61	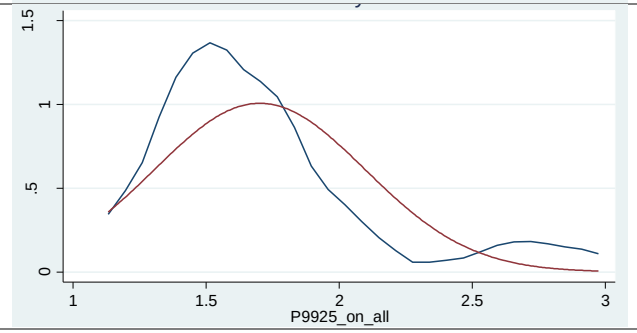	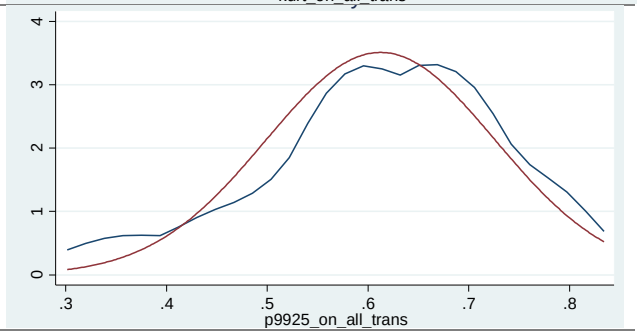

Variable	Transf.	Min	Max	Mean	pre-transform	post-transform
P99/50	1/square	0.27	0.73	0.56	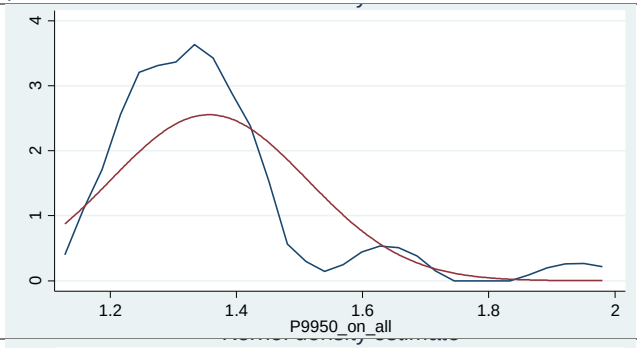	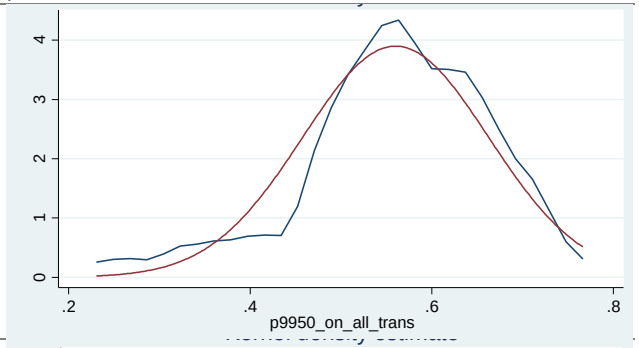
P99/75	1/cubic	0.27	0.78	0.58	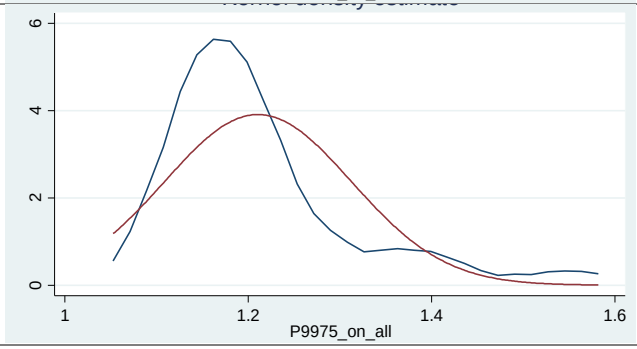	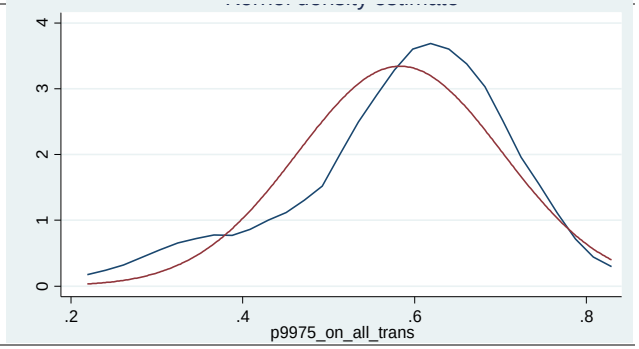

Leaf-off variables

Variable	Transf.	Min	Max	Mean	pre-transform	post-transform
Kurtosis	Log	0.79	2.74	1.54	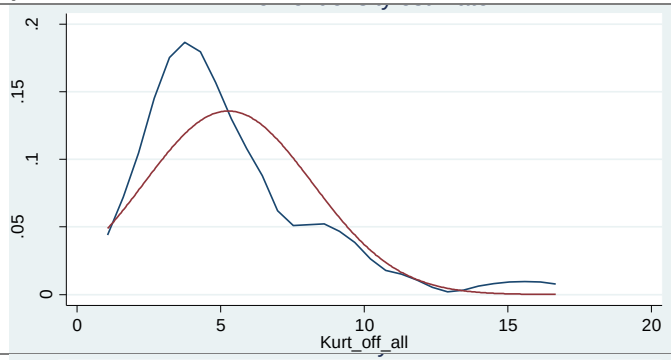	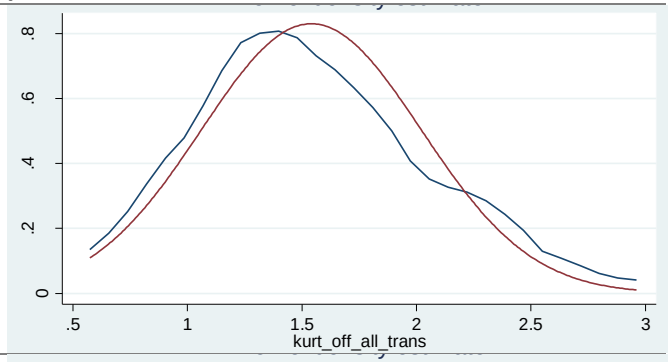
P99/25	inverse	0.36	0.81	0.62	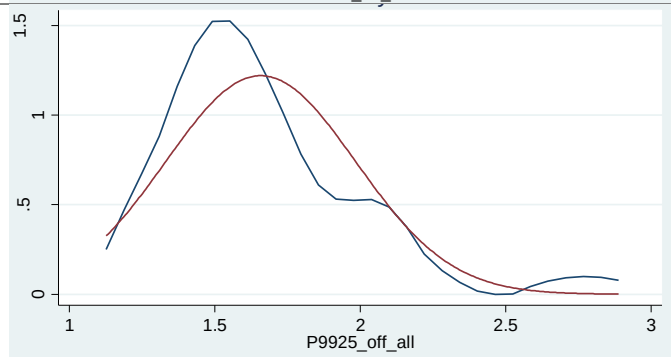	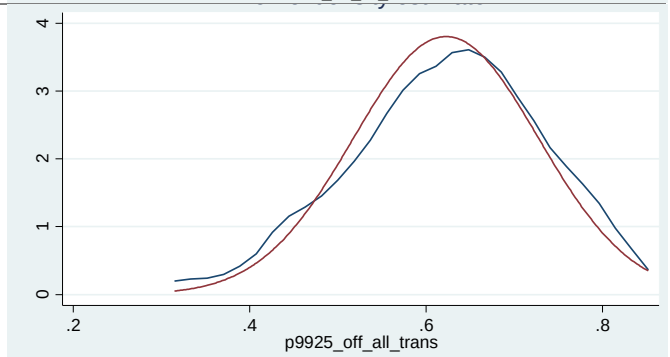

Variable	Transf.	Min	Max	Mean	pre-transform	post-transform
P99/50	1/square	0.25	0.76	0.56	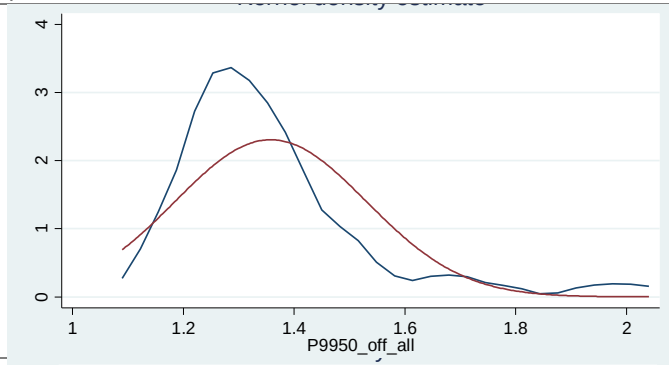	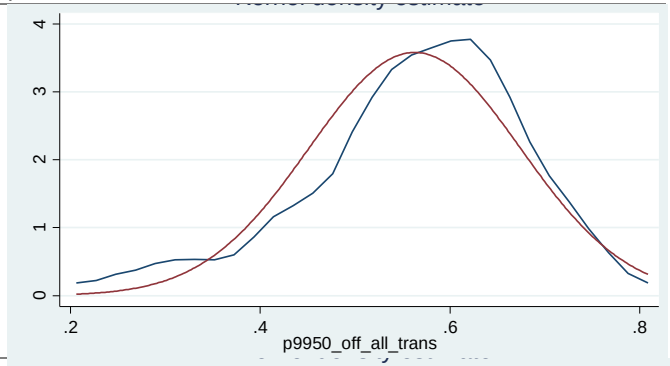
P99/75	1/cubic	0.30	0.78	0.59	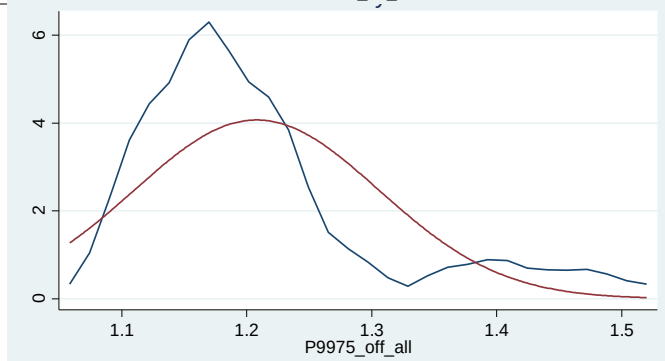	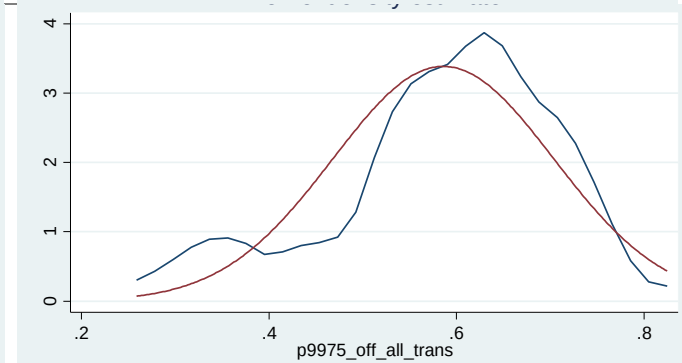

Appendix 2

Graphical and statistical indicators of normality of residuals from each constructed regression model.

The kernel density and quantile plots display graphically whether the distribution of residuals differs from normal. Significant values of 0.05 or greater associated with skewness and kurtosis statistical tests rejects the null hypothesis of normality.

Model	Distribution	Quantile Plot with CI (95%)	Skewness and Kurtosis
1	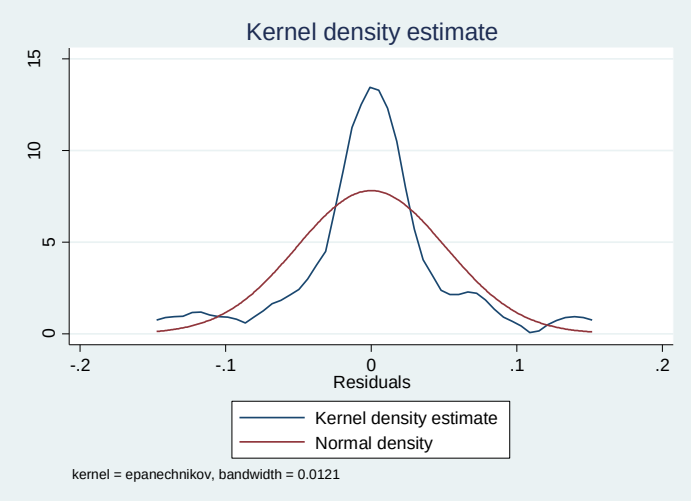	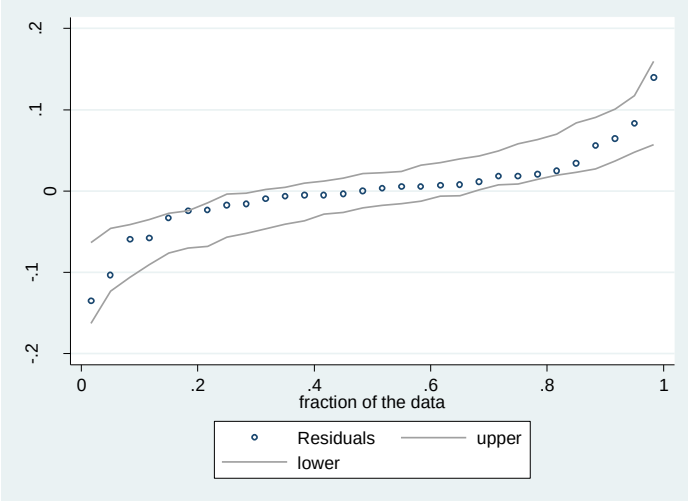	Skewness: 0.87 Kurtosis: 0.03 Evidence for non-normality in kurtosis of distribution and statistical analysis. Distribution also strays outside the quantile confidence.

Model	Distribution	Quantile Plot with CI (95%)	Skewness and Kurtosis
2	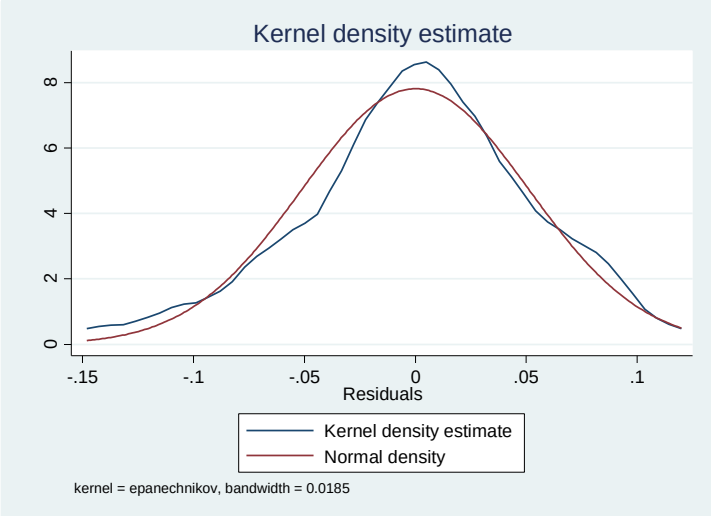	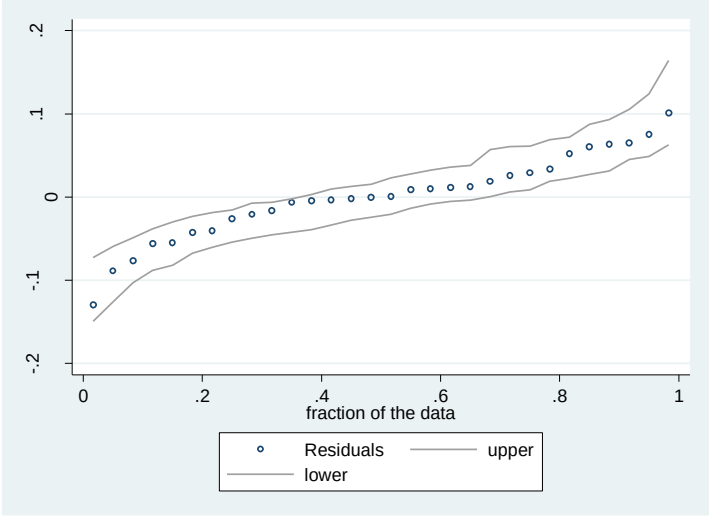	Skewness: 0.35 Kurtosis: 0.49 No significant evidence of none normality.
3	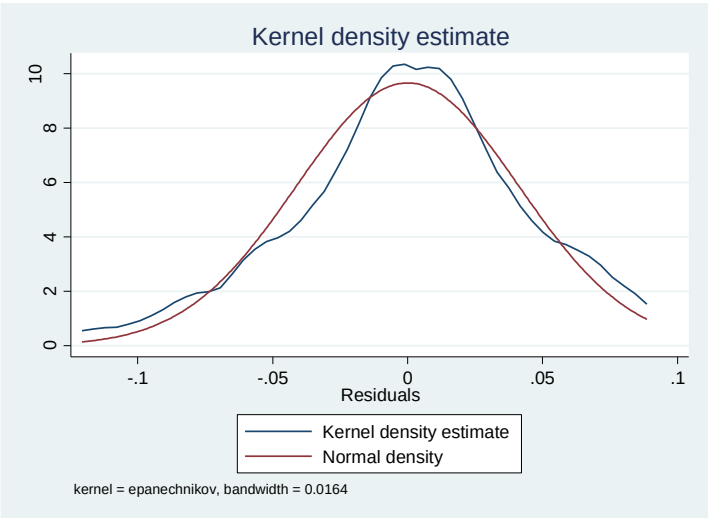	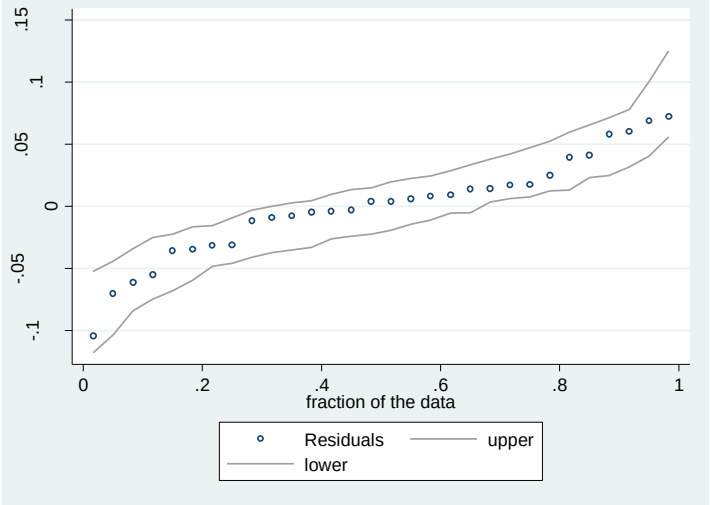	Skewness: 0.35 Kurtosis: 0.53 No significant evidence of none normality.

Model	Distribution	Quantile Plot with CI (95%)	Skewness and Kurtosis
4	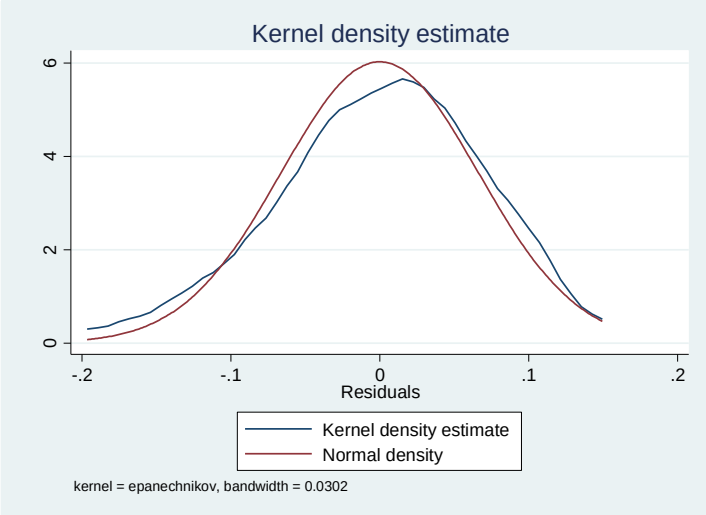	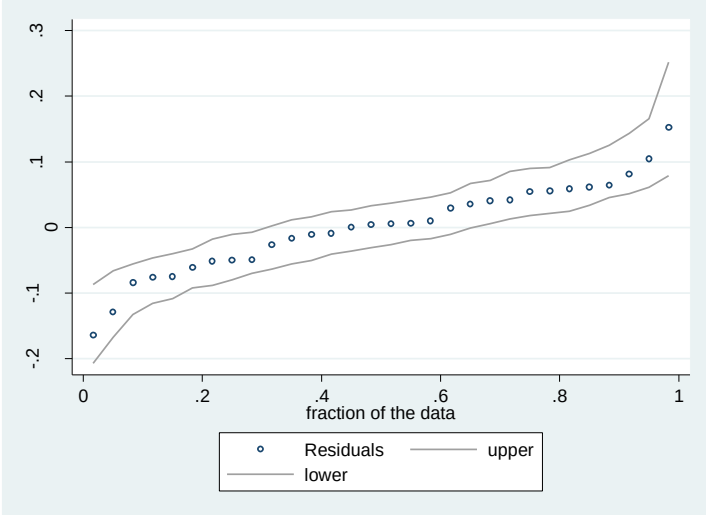	Skewness: 0.28 Kurtosis: 0.69 No significant evidence of none normality.
5	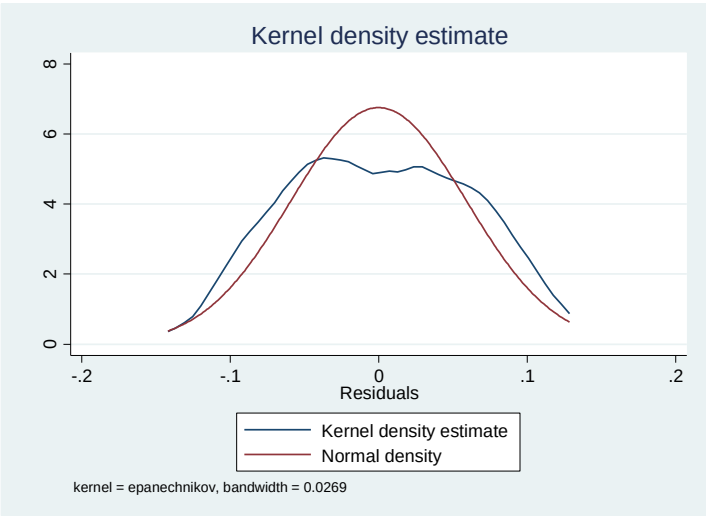	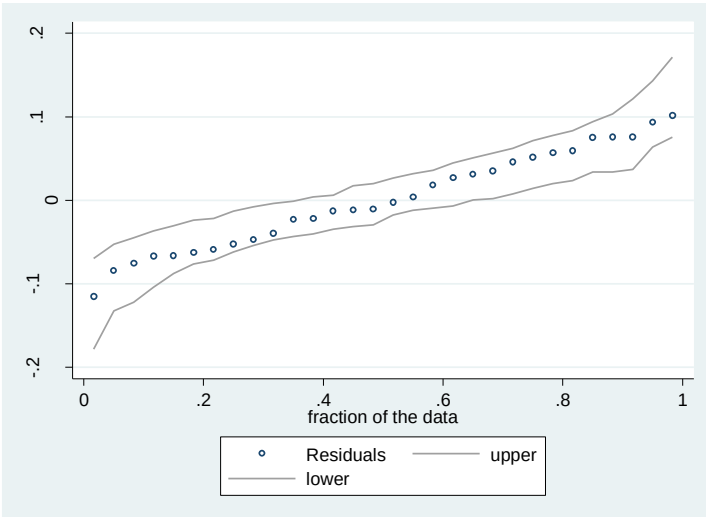	Skewness: 0.98 Kurtosis: 0.07 Though the kernel density graph displays the residuals having a more reduced kurtosis than the normal the quantile plot and statistical analysis indicate this is not a significant deviation from normal

Model	Distribution	Quantile Plot with CI (95%)	Skewness and Kurtosis
6	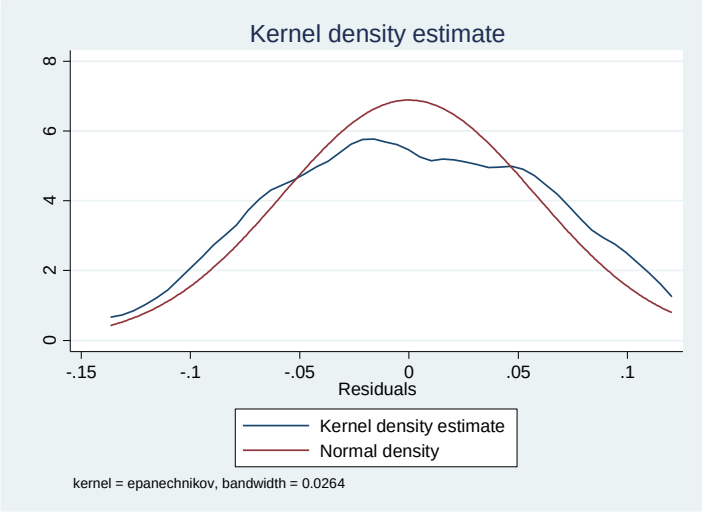	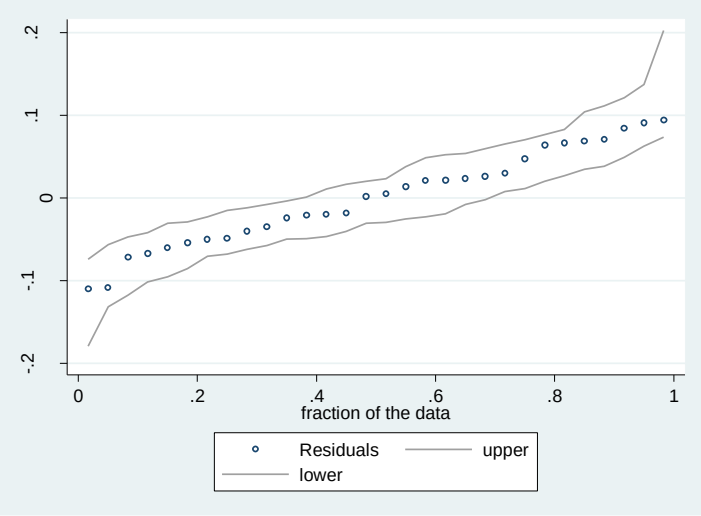	Skewness: 0.83 Kurtosis: 0.19 No significant evidence of none normality.
7	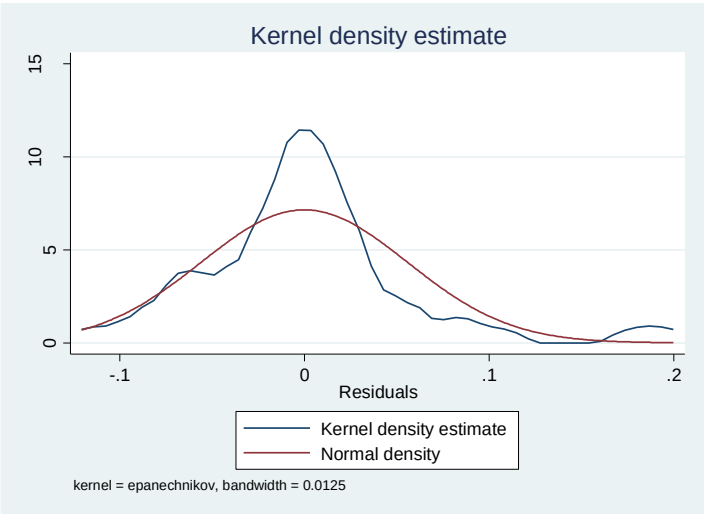	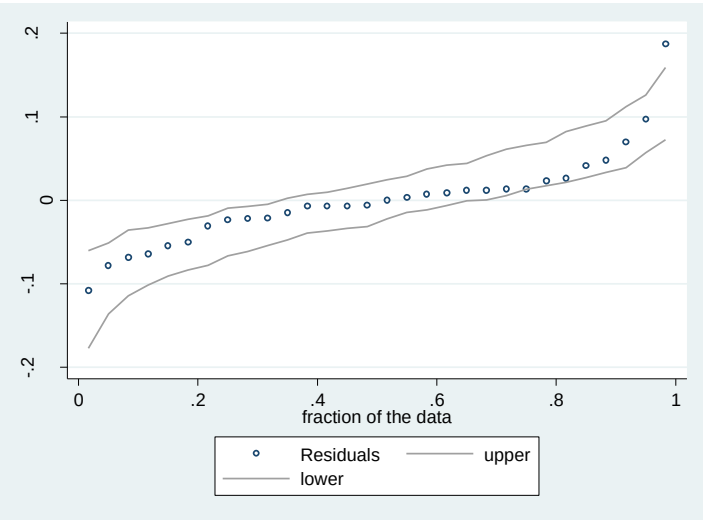	Skewness: 0.01 Kurtosis: 0.01 There is every indication of a significantly none normal distribution

Model	Distribution	Quantile Plot with CI (95%)	Skewness and Kurtosis
8	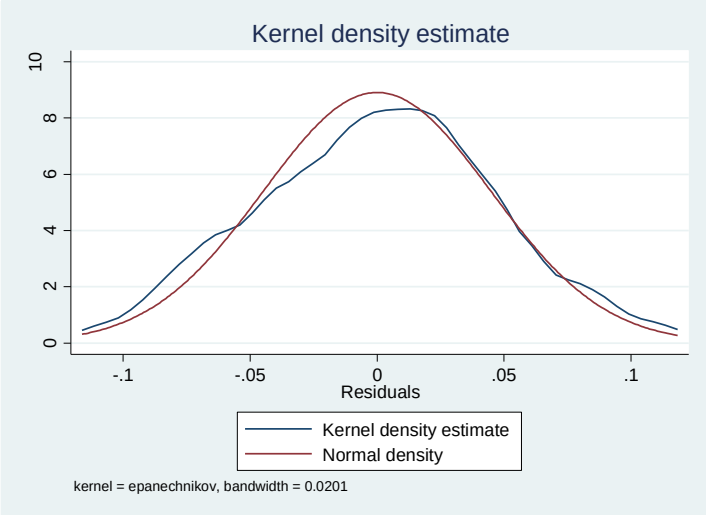	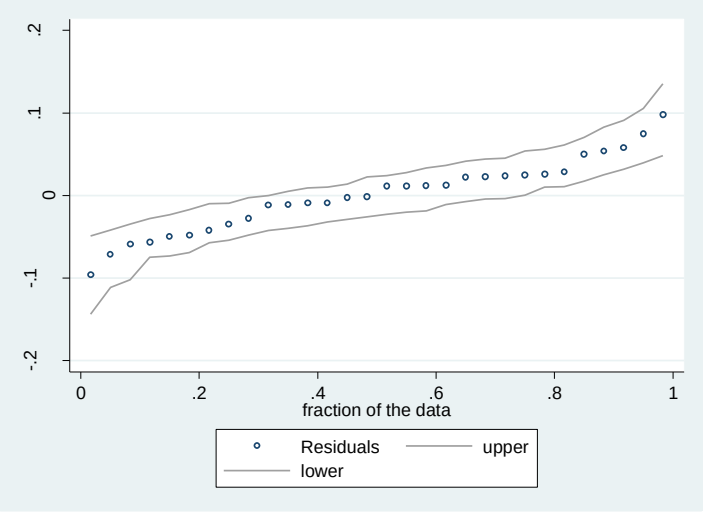	Skewness: 0.94 Kurtosis: 0.98 No significant evidence of none normality.
9	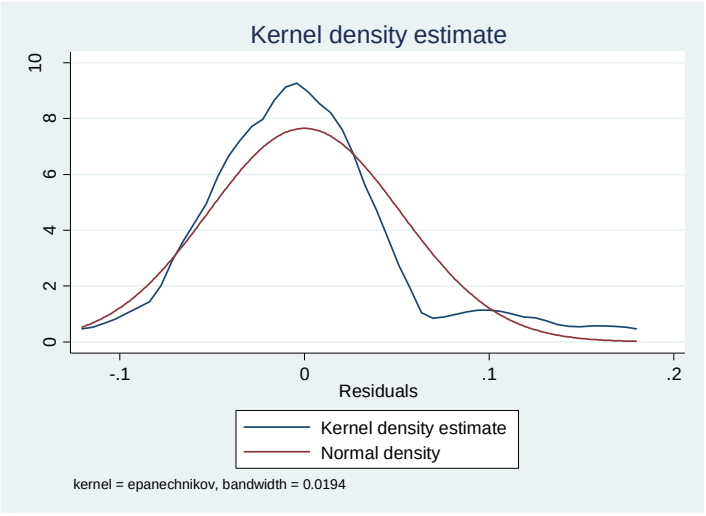	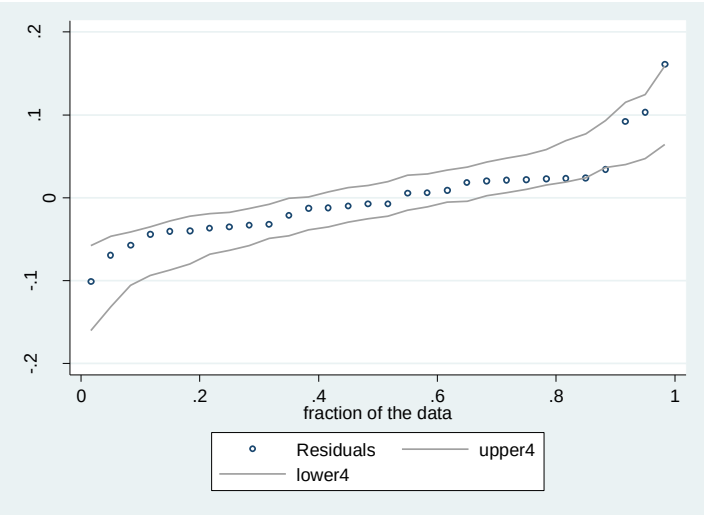	Skewness: 0.02 Kurtosis: 0.03 Though the kernel density distribution shows a generally normal shape there is significant evidence for both none normal skewness and kurtosis

Model	Distribution	Quantile Plot with CI (95%)	Skewness and Kurtosis
10	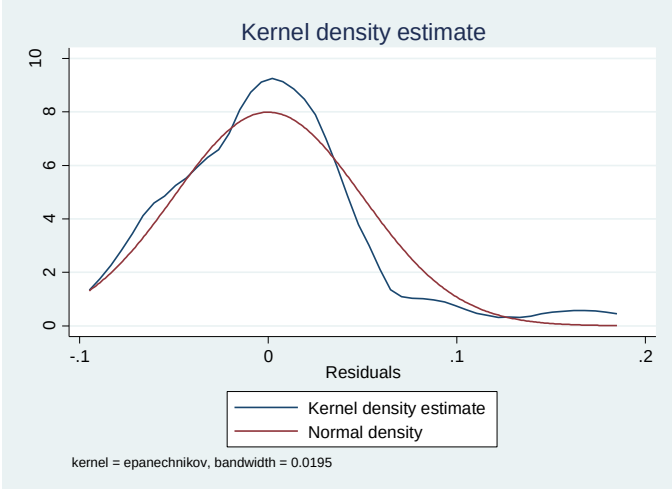	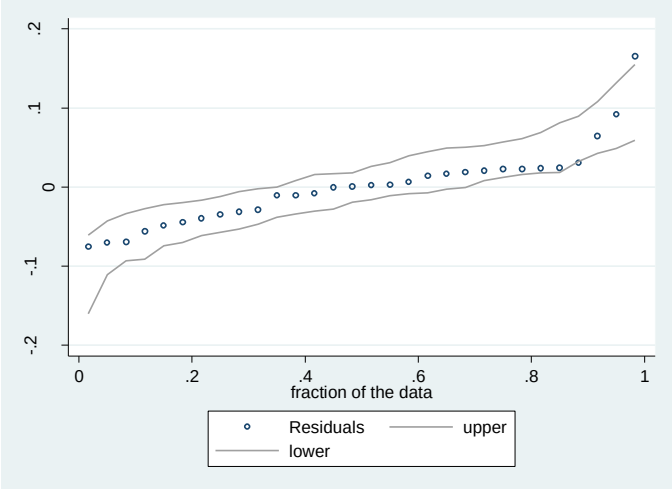	Skewness:0.01 Kurtosis:0.02 Again, though the kernel density distribution shows a generally normal shape there is significant evidence for both none normal skewness and kurtosis

Appendix 3

Summary of tests of homogeneity of residuals.

Residuals plotted against the fitted values in each model should be randomly distributed around the reference line as any patterns seen in the data, such as a narrowing to either side, towards the centre or a curvilinearity would indicate heteroscedasticity or none homogeneity of residuals. In the Breusch-Pagan (1979) and the Cameron and Trivedi (1990) White's test a p value <=0.05 indicates a rejection of the null hypothesis that the variance of the residuals is homogenous and accepting the alternative hypothesis that the variance is not homogenous.

	Residuals verses fitted values	**Breusch -Pagan test *p***	**White's test *p***	**Comments**
1	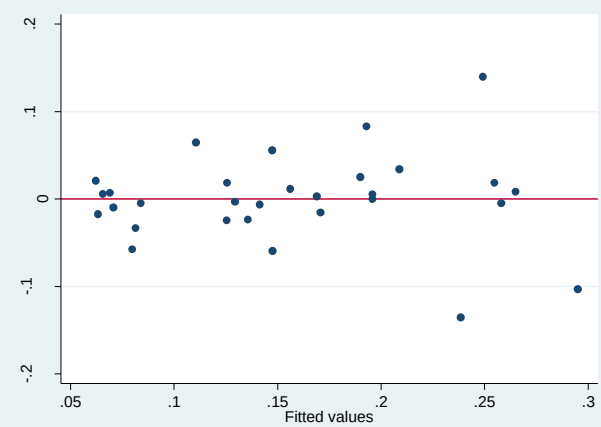	<0.001	0.001	Residuals display narrowing to the left of the plot and both tests display very low *p*-values. There is significant evidence for non-homogenous variance in the residuals for this model.
2	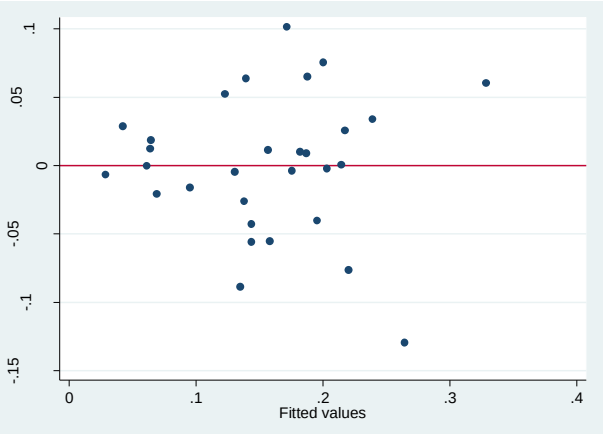	0.04	0.05	Though the statistical tests show some evidence of non-homogeneity the graph does not.

	Residuals verses fitted values	Breusch-Pagan test *p*	White's test *p*	Comments
3	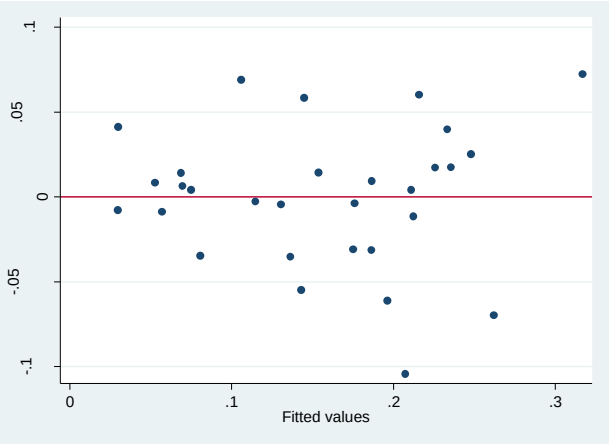	0.05	0.09	No evidence for non-homogeneity of residuals.
4	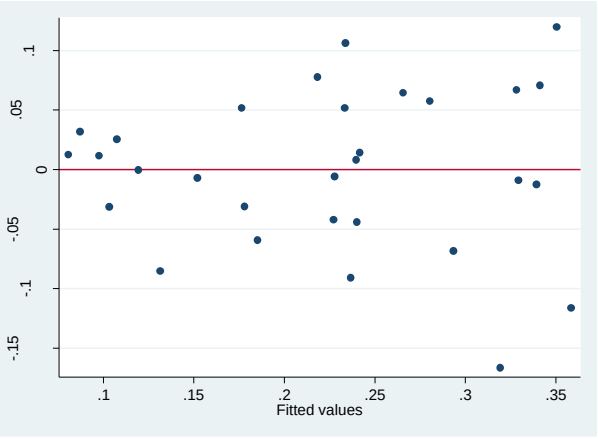	0.01	0.38	Though the Breusch-Pagan test *p-value* is very low, there is less of a clear pattern of non-homogeneity of residuals in the graph.
5	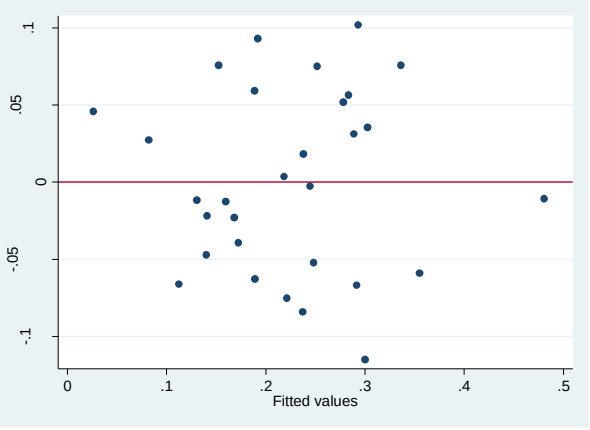	0.49	0.54	No evidence for non-homogeneity of residuals.
6	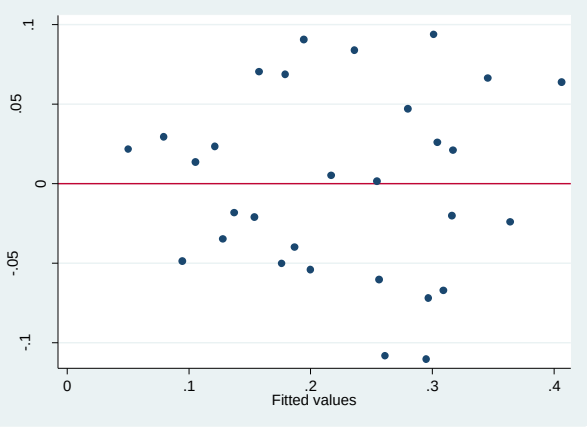	0.23	0.36	No evidence for non-homogeneity of residuals.

	Residuals verses fitted values	Breusch -Pagan test *p*	White's test *p*	Comments
7	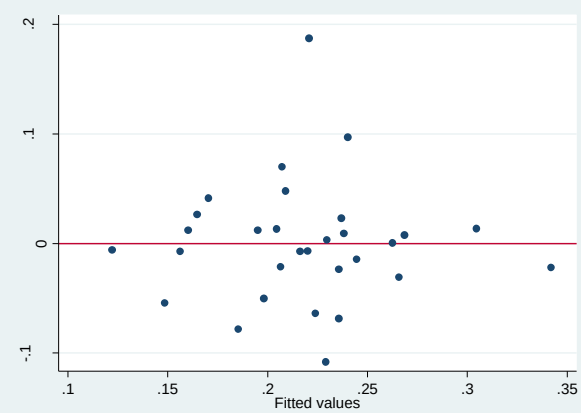	0.99	0.42	No evidence for non-homogeneity of residuals.
8	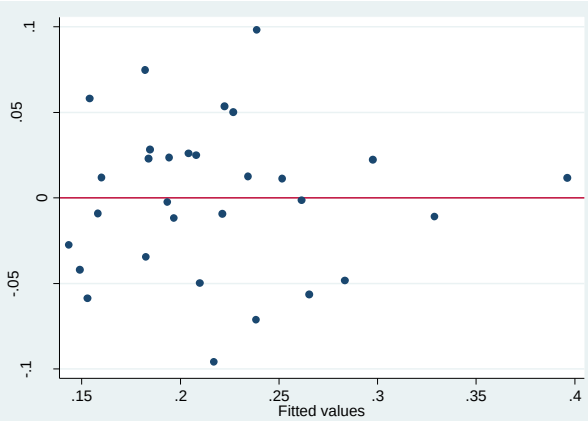	0.76	0.97	There is a thinning towards the right of the plot but little statistical evidence of heteroscedasticity.
9	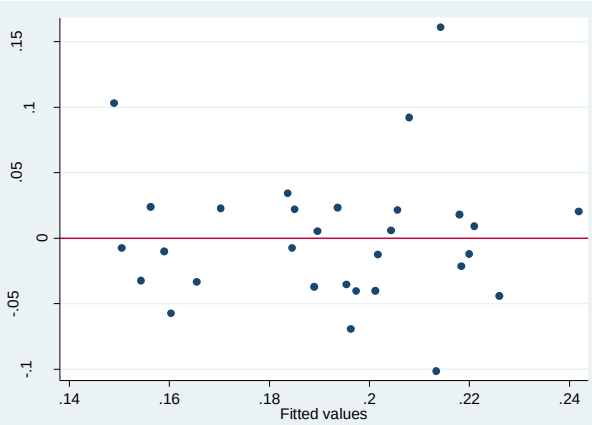	0.45	0.38	No evidence for none homogeneity of residuals.
10	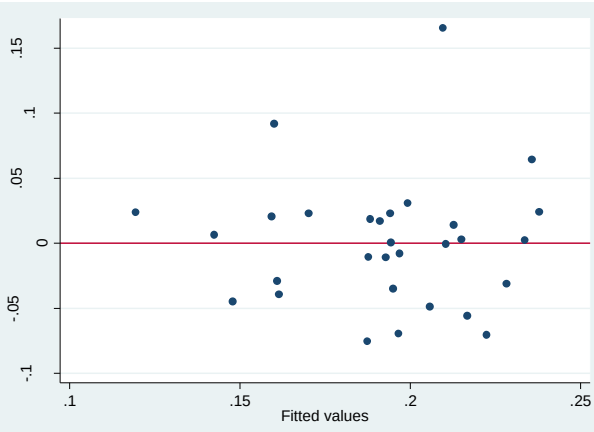	0.39	0.51	No evidence for none homogeneity of residuals.

Appendix 4

Summary of the linearity of relationships between dependant and independent variables for each regression model.

The augmented component-plus-residual plot (a.k.a. augmented partial residual plots) include a line of best fit and a locally weighted smoothing to aid in the reader's interpretation. If the smoothed line differed substantially from the line of best fit it would indicate non-linearities between dependant and independent variables.

Model 1 LiDAR variables			
Field variable	**Kurtosis (leaf-on)**	**Variance (leaf-on)**	**N/A**
THdiv	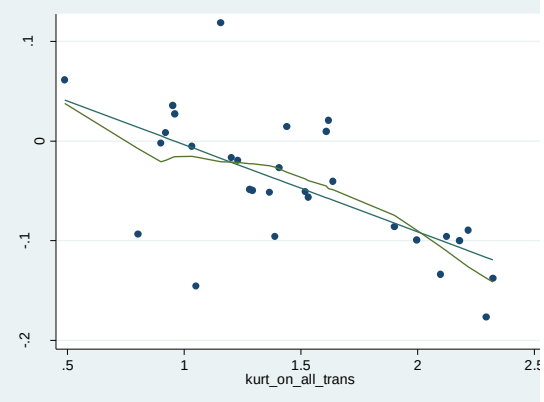	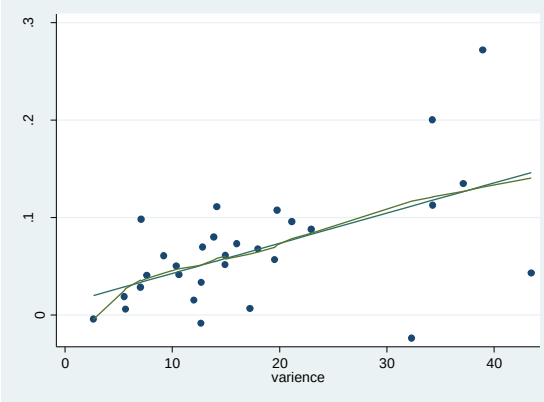	

Model 2 LiDAR variables			
Field variable	**Kurtosis (leaf-off)**	**Variance (leaf-off)**	**N/A**
THdiv	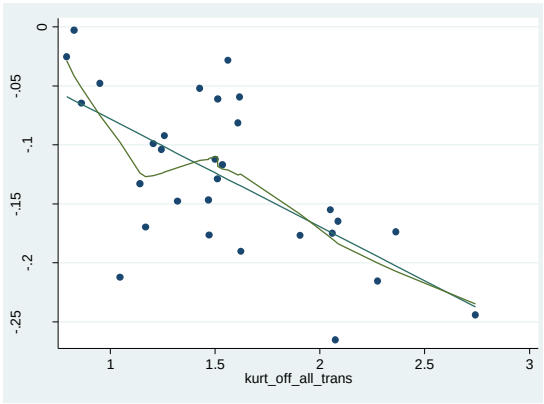	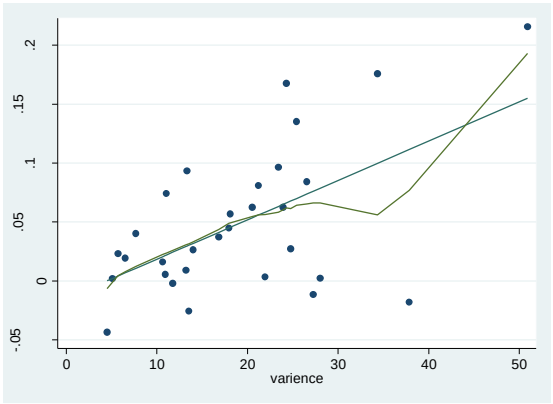	

Model 3 LiDAR variables			
Field variable	**Kurtosis (leaf-off)**	**Variance (leaf-on)**	**N/A**
THdiv	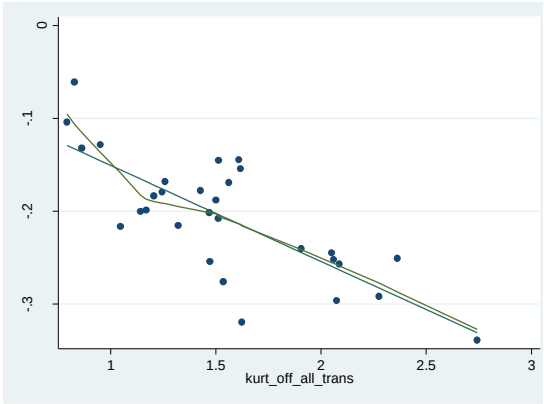	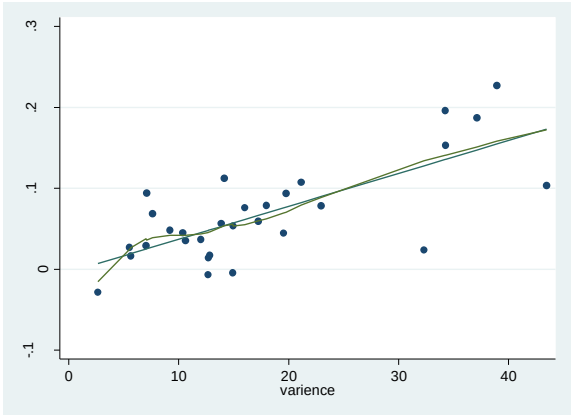	

Model 4 LiDAR variables			
Field variable	**SD (leaf-on)**	**Skewness (leaf-on)**	**N/A**
DBHdiv	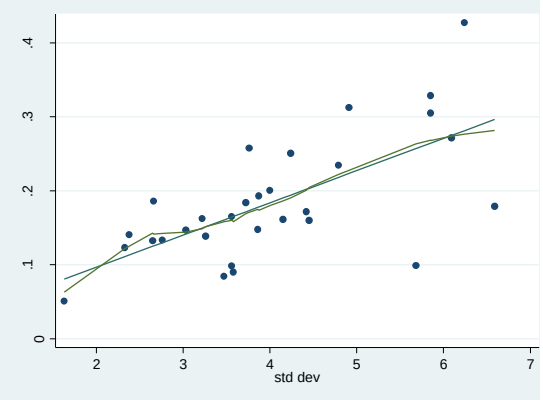	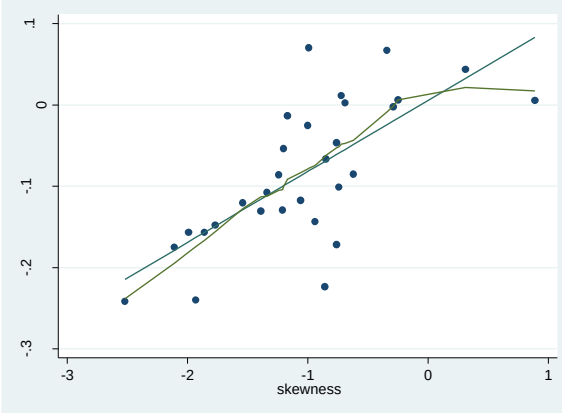	

Model 5 LiDAR variables			
Field variable	**SD (leaf-off)**	**Skewness (leaf-off)**	**P99/90 (leaf-off)**
DBHdiv	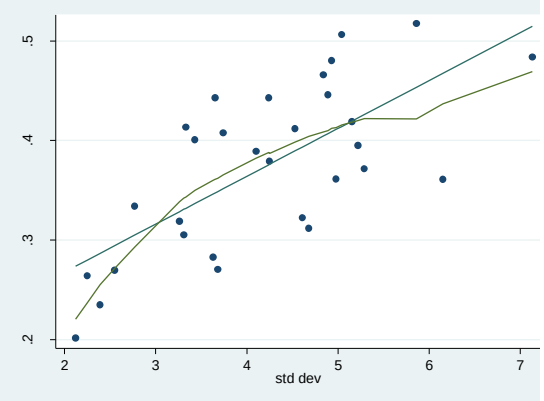	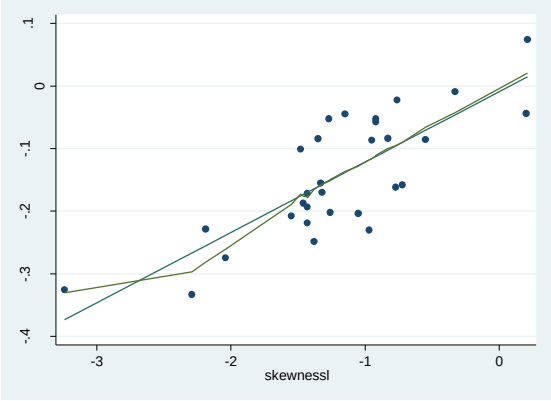	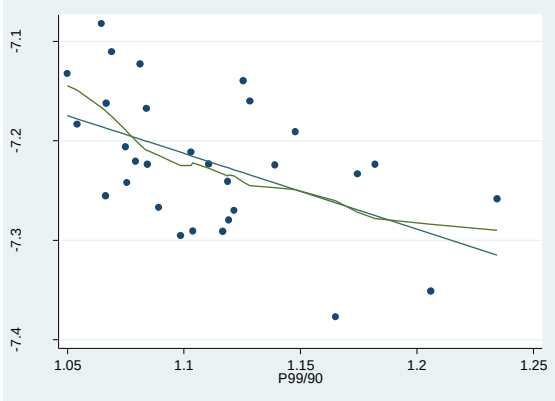

Model 6 LiDAR variables			
Field variable	**Variance (leaf-off)**	**Skewness (leaf-off)**	**CV (leaf-on)**
DBHdiv	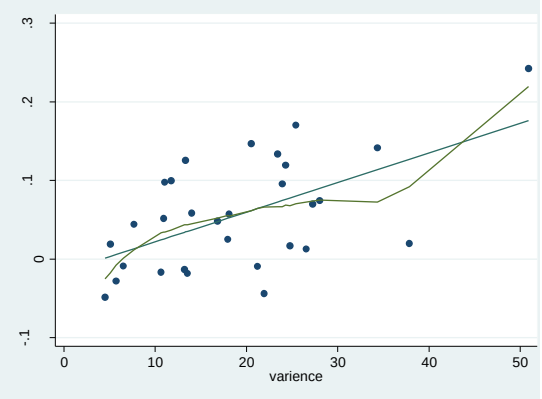	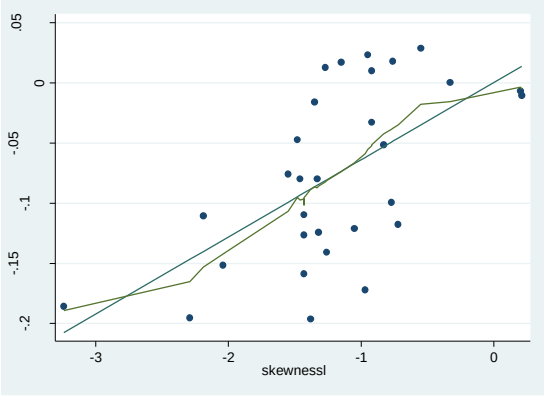	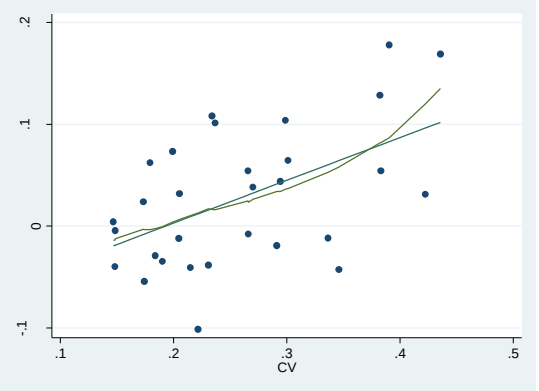
Model 7 LiDAR variables			
Field variable	**Skewness (leaf-on**	**N/A**	**N/A**
CLdiv	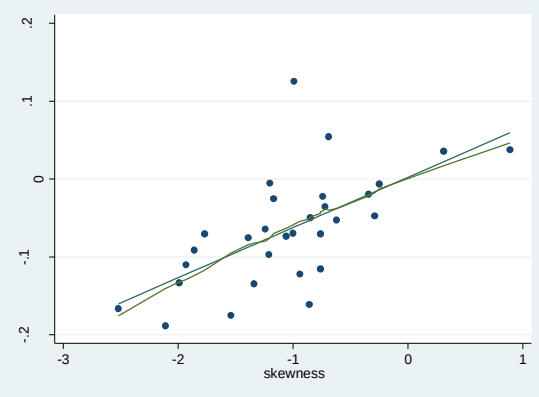		

Model 8 LiDAR variables			
Field variable	**P99/75 (leaf-off)**	**P99/50 (leaf-off)**	**Variance (leaf-off)**
CLdiv	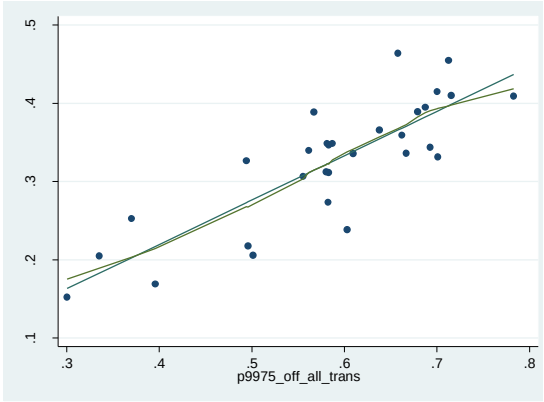	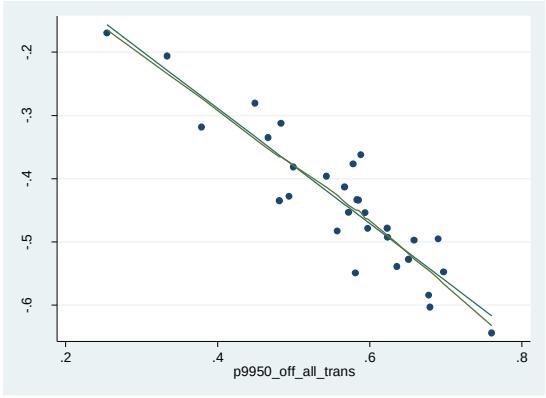	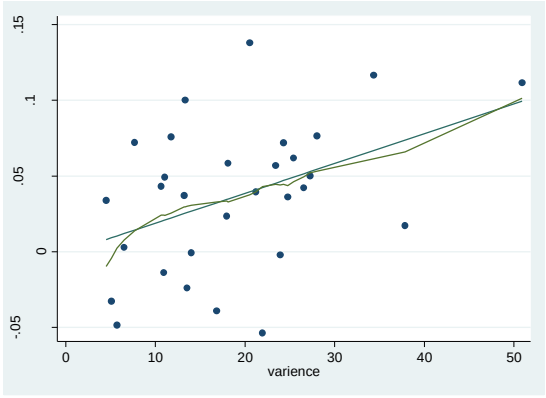
Model 9 LiDAR variables			
Field variable	**Kurtosis (leaf-on)**	**N/A**	**N/A**
CWdiv	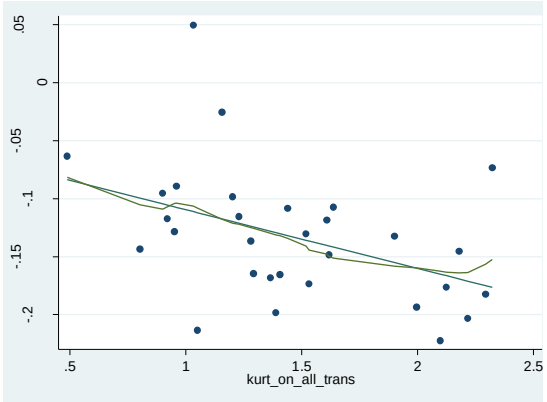		

		Model 10 LiDAR variables	
Field variable	**Kurtosis (leaf-off)**	**N/A**	**N/A**
CWdiv